KINETIC STUDIES OF THE NITROLYSIS OF HEXAMINE IN ACETIC ACID AND IN CHLOROFORM

and

THE DETONATION VELOCITY OF AXIALLY CAVITATED CYLINDERS OF CAST DINA

Milton Kirsch B.Sc.

A Thesis

Submitted to

The Faculty of Graduate Studies and Research
of McGill University
in partial fulfilment of the
requirements for the Degree of
Doctor of Philosophy

from the
Physical Chemistry Laboratory
of McGill University
under the supervision of
Dr. C.A. Winkler.

McGill University April 1945.

ACKNOWLEDGMENT

Acknowledgment is due to the National Research Council for the award of a studentship (1943-1944) and to Canadian Industries Limited for the award of a fellowship (1944-1945).

TABLE OF CONTENTS

SECTION I

KINETIC STUDIES OF THE NITROLYSIS OF HEXAMINE IN ACETIC ACID AND IN CHLOROFORM

SECTION II

THE DETONATION VELOCITY OF AXIALLY CAVITATED CYLINDERS OF CAST DINA

ABSTRACT

Ph. D. Physical Chemistry

Milton Kirsch

KINETIC STUDIES OF THE NITROLYSIS OF HEXAMINE IN ACETIC ACID AND IN CHLOROFORM

Kinetic studies at 1°C and at 30°C show that both solvents have a harmful effect on the reaction rate and on the yield of RDX for a given nitric acid:hexamine ratio below a certain optimum value. At the optimum, however, the maximum yield of 80% is obtained with both solvents at both temperatures.

The deleterious effect of acetic acid is of a larger order of magnitude than that of chloroform, and may be explained on the assumptions that the active nitrolyzing agent is nitracidium ion and that acetic acid and nitric acid form a complex which is more highly dissociated at the higher temperature.

--o--

THE DETONATION VELOCITY OF AXIALLY CAVITATED CYLINDERS OF CAST DINA

The equipment necessary for the optical study of detonation has been installed at the National Research Council laboratories in Ottawa. A method is described, involving the use of the Jones and Lamson Comparator, for estimating velocities of detonation from the photographic record of a detonation obtained on a rapidly moving film.

The increase in detonation velocity in cavitated charges is accompanied by the appearance of a luminous effect which moves down the cavity at a velocity of approximately 1.65 times the detonation velocity. Both the luminous effect and the increase in detonation velocity disappear when the cavity is filled with either water or solid rods.

The numerical and qualitative results obtained may be explained by assuming that the shock wave, which causes the luminosity in an air-filled cavity, or the hot gases which follow it, may sensitize the explosive along the walls of the cavity.

SECTION I

KINETIC STUDIES OF THE NITROLYSIS OF HEXAMINE IN ACETIC ACID AND IN CHLOROFORM

INTRODUCTION

The nitrolysis reaction between hexamethylenetetramine (hexamine) and fuming nitric acid has long been known to produce the powerful explosive, cyclo-trimethylenetrinitramine, (RDX) (1). The preparation is made simply by addition of hexamine to the fuming nitric acid with external cooling, followed by dilution with water to precipitate the RDX formed. The overall reaction has been written (2):

$$C_6H_{12}N_4 + 3HNO_3 \longrightarrow C_3H_6O_6N_6 + 3CH_2O + NH_3 \quad (1)$$

but much more nitric acid is required than indicated stoichiometrically. Hale (3) found that eleven parts by weight of 100% nitric acid per part of hexamine were necessary to obtain the maximum yield of RDX.

Since the start of the present war there has been great interest in the reaction, but relatively few of the investigations have been along kinetic lines, and all have been made in the absence of solvent. Brief mention may be made, however, of two studies of the nitrolysis in pure nitric acid which bear directly on the results of the present study.

The Research Department, Woolwich (4) controlled the temperature by adding hexamine and solid carbon dioxide alternately to the precooled 98% nitric acid, and were thus able to investigate the effect of temperature on the yield of RDX. They found that the yield decreased gradually from 82% at -25°C to 80% at 30°C, and then fell off sharply to about 51% as the temperature was raised to 70°C.

Vroom and Winkler (5) eliminated the difficulty of uncontrollable temperature rise accompanying the addition of large quantities of hexamine to nitric acid by using hexamine dinitrate as the starting material. In this way they were able to study thoroughly the effect of nitric acid strength and of nitric acid:hexamine ratio on the reaction rate and on the final yield of RDX produced. They found that at 0°C the maximum yield of RDX was obtained only if the molar ratio of 97% nitric acid:hexamine was at least 26:1. With decreasing amounts of nitric acid the yield fell off sharply. Good yields were obtained with nitric acid as dilute as 88% if enough nitric acid were used. The rate curve for the nitrolysis in 22 moles of 97% nitric acid per mole of hexamine was almost exactly superimposable on those for 45 moles of 91% nitric acid and 110 moles of 88% nitric acid.

Some study has been made of the effect of chloroform and of acetic acid on the reaction (6, 7). With 0.56

mole of chloroform and 32.5 moles of 90-93% nitric acid per mole of hexamine RDX in 72% yield was obtained in 75 minutes at -20°C to -25°C by adding hexamine to the mixed liquids, but only in 56% yield by adding a chloroform solution of hexamine to the nitric acid (6). No RDX whatever was isolated in 140 minutes at the same temperature from a nitrolysis mixture containing 25 moles of acetic acid and 32.5 moles of 90-93% nitric acid.

Springall and Woodbury (7) investigated the possibility of replacing the fuming nitric acid, essential for the successful conversion of hexamine to RDX, by aqueous 70% nitric acid and sufficient acetic anhydride to combine with the water and increase the acid strength to 98.5%. After 30 minutes at 20°C, the insoluble product that precipitated was hexamine dinitrate. No RDX was obtained. The equivalent system of 98.5% nitric acid and the appropriate quantity of acetic acid led to the same result.

Because of the very definite harmful effect of the solvents it is necessary to examine their role in the nitrolysis mixture. The behaviour of nitric acid appears to depend to a large extent on the nature of the nitrating medium. According to the electronic picture of aromatic substitution, nitration occurs by attachment of nitrogen, positively polarized relative to nuclear carbon, with

elimination of a proton (8). It might be expected, therefore, that the best nitration solvents should be those which increase the concentration of this positively polarized nitrogen. Various investigators (5, 9, 10) have assumed that the active nitrating agent was a positive ion formed by the dissociation of nitric acid:

$$2HNO_3 \rightleftharpoons NO(OH)_2^+ + NO_3^- \quad \ldots\ldots\ldots\ldots (2)$$

There is considerable evidence from various sources for the existence in nitric acid of the positive nitracidium ion. Crystalline nitracidium perchlorates have been isolated (11), while a characteristic Raman shift of 1,400 $cm.^{-1}$ has been observed (12) in nitric acid containing nitrogen pentoxide and in sulfuric acid - nitric acid mixtures in which the nitration of nitrobenzene has been found (13) to proceed readily at 35°C. Migration experiments (14) with smooth platinum electrodes in sulfuric acid - nitric acid mixtures provide direct evidence that a nitric acid cation migrates toward the cathode, and that it has a transport number two to four times that of the barium ion.

Kinetic data indicate that nitracidium ion is the effective nitrating agent. Lauer and Oda (9) studied the nitration of anthraquinone with nitric acid and potassium nitrate in aqueous and absolute sulfuric acid. The

activation energy was 22 kcal. in 87-95.6% sulfuric acid, while in 100% sulfuric acid it was only 13 kcal. They concluded that nitration in aqueous sulfuric acid was due to pseudo-nitric acid, $HONO_2$, but that in concentrated sulfuric acid, the active nitrating agent was nitracidium ion. This latter assumption, together with the hypothesis that completion of the nitration requires removal of a proton by some agent such as bisulfate ion, permits the calculation of kinetic expressions for the nitration in mixed acid of 2,4-dinitrotoluene in agreement with experiment (15).

The effect of the nitrating medium on the simplicity and rate of nitration has been discussed by Bennett and Williams (8). They observed that among the common solvents nitration is fastest and the kinetics of nitration are simplest in sulfuric acid. Perchloric acid, a stronger acid, constitutes an even faster nitration solvent than sulfuric acid (16), while acetic acid is a particularly slow solvent. A kinetic study of the nitration of benzene in acetic anhydride permitted rate constants to be calculated (17), but in glacial acetic acid the nitration did not proceed at all. Benford and Ingold (18) in their extensive investigation of the kinetics of aromatic nitration classified acetic acid among the slow solvents.

In the nitration of toluene, it appears that the

nitration of the aromatic nucleus is due to the nitracidium cation, while that of the methyl group is due to the nitrate ion (10). In strongly acid media such as sulfuric acid and trichloracetic acid, nitration occurs only in the ring. In the inert solvents, dichloracetic acid and ethyl nitrate, the yields of nitrotoluene and of phenyl nitromethane decrease proportionately with increasing dilution of the nitric acid as a result of the decreasing concentration of both cations and anions of nitric acid. In acetic acid and nitrobenzene media, however, the relative yields of phenyl nitromethane increase and those of nitrotoluene decrease with dilution of the nitric acid by the solvent. These results indicate that the latter two solvents increase the relative concentration of nitrate ion at the expense of nitracidium ion.

No kinetic data for the nitrolysis of hexamine in the presence of solvents are available. The present investigation was undertaken with the view that useful information about the mechanism of hexamine nitrolysis might be obtained by studying the reaction in various solvents.

EXPERIMENTAL

Stock solutions of hexamine of desired compositions were prepared in acetic acid and in chloroform. The amount of water in these solutions, determined by the Karl Fischer reagent, was found to be negligible. The amount of hexamine was determined from time to time by titration with a solution of sulfuric acid in acetic acid. During the titration hexamine disulfate precipitated and the end-point was determined with an acetic acid solution of methyl violet as indicator which changed from violet to green. In this way it was found that the concentration of the stock solutions remained constant with time. The weight of solvent was determined directly by difference.

In making an experiment, the appropriate volume of hexamine solution was pipetted into a measured volume of solid 97% nitric acid, contained in a 250-ml. Erlemeyer flask, cooled in an acetone-dry-ice bath. The length of time for the addition of the hexamine varied with the solution, depending on its viscosity, but it never exceeded two minutes. Since the temperature never rose above -25°C during the addition there was no appreciable reaction (4). The flask was then shaken in the thermostat at 1°C or at 30°C, the initial time being taken as one minute after thermostating, since it required approximately one minute for the

reaction mixture to attain the temperature of the thermostat. After shaking for a definite time, the reaction mixture was diluted to about 200 ml. with water and allowed to stand overnight at room temperature to ensure complete precipitation of the RDX. The solid was filtered into tared sintered glass crucibles, dried at 100-110°C for four hours and weighed.

Final yields were obtained by allowing the reaction to proceed for a week at 1°C and for 24 hours at 30°C. No further increases in yield were noted after these times.

Attempts to thermostat the reaction mixture at the reaction temperature during the addition of the hexamine were unsuccessful, since the addition is then necessarily slow, and the uncertainty in the initial time is greater than with the technique adopted.

The solubility of RDX in the diluted liquors was found to be negligible in all cases.

In all the experiments, solid (presumably hexamine dinitrate) precipitated as soon as the hexamine solution was added to the nitric acid, but dissolved as the reaction mixture warmed up to the reaction temperature. In the experiments with chloroform the reaction mixture was heterogeneous, two liquid phases being formed soon after the start of the reaction.

RESULTS and DISCUSSION

Experiments were made at both 1°C and at 30°C using molar ratios of acetic acid:hexamine between 4.3:1 and 10.5:1 and varying the nitric acid:hexamine ratio between 81:1 and 26:1, and with molar ratios of chloroform: hexamine between 15.7:1 and 42.0:1, the molar ratio of nitric acid:hexamine was varied between 32:1 and 18:1.

The results with acetic acid are given in Tables I-IV, and Figs. 1-6; those with chloroform in Tables V-VIII and Figs. 7-12.

As a basis for comparison a set of experiments was made at 30°C using no solvent and hexamine dinitrate as starting material.

The results appear in Table IX and Fig. 13. Fig. 14, taken from a previous report (5), is included for comparison at 1°C.

A comparison of Figs. 1-12 with 13 and 14 shows that both acetic acid and chloroform may have a harmful

TABLE I

Rate of Nitrolysis of Hexamine in Acetic Acid.

2.00 ml. of solution containing 400 gm./l. of hexamine was used.
Weight of acetic acid = 1.45 gm.
Weight of hexamine = 0.80 gm.
Molar Ratio of AcOH:Hexamine = 4.3:1

Molar Ratio		Temperature - 1°C.			Temperature - 30°C.		
HNO_3:Hexamine	HNO_3:AcOH	Expt. No.	Reaction Time Mins.	RDX Yield %	Expt. No.	Reaction Time Mins.	RDX Yield %
48.5	11.3	1	2	49	6	4	75
			7	55		15	76
			10	56		40	77
			30	71		70	77
			60	73		120	77
			90	75		180	76
			120	78			
40	9.3	2	3	26			
			7	43			
			10	55			
			30	66			
			60	73			
			90	74			
			120	76			
32	7.4	3	3	17	7	5	65
			10	38		20	67
			20	49		30	69
			47	62		90	70
			60	64			
			90	69			
			120	71			
26	6.0	4	10	20	8	3	31
			20	25		10	53
			40	35		30	61
			60	44		60	65
			90	49		120	69
			120	48			
20	4.6	5	30	10	9	3	22
			60	14		10	28
			90	16		30	40
			120	16		60	45
			153	15		120	50
						167	52

TABLE II

Rate of Nitrolysis of Hexamine in Acetic Acid.

5.00 ml. of solution containing 300 gm./l. of hexamine was used.
Weight of acetic acid = 4.1$_1$ gm.
Weight of hexamine = 1.5$_0$ gm.
Molar Ratio of AcOH:Hexamine = 6.4:1

Molar Ratio		Temperature - 1°C.			Temperature - 30°C.		
HNO_3:Hexamine	HNO_3:AcOH	Expt. No.	Reaction Time Mins.	RDX Yield %	Expt. No.	Reaction Time Mins.	RDX Yield %
81	12.5	10	3 5 10 20 30 61 120	48 64 68 74 77 80 79			
48.5	7.6	11	3 10 30 60 91 120	27 46 68 74 77 76	16	3 10 30 60 120	62 76 77 77 76
40	6.3	12	5 10 30 60 90 120	15 36 60 73 76 76			
32	5.0	13	10 30 61 91 120	16 39 54 58 59	17	2 10 30 60 90 120	35 57 63 66 68 68
26	4.1	14	15 30 60 90 120	9 15 17 21 23	18	2 10 30 61 90 120	21 35 49 54 57 59
20	3.1	15	10 30 60 90 120	2 4 4 4 4	19	5 20 50 92 120	9 17 23 27 29

TABLE III

Rate of Nitrolysis of Hexamine in Acetic Acid.

5.00 ml. of solution containing 200 gm./l. of hexamine was used.
Weight of acetic acid = 4.5_1 gm.
Weight of hexamine = 1.0_0 gm.
Molar Ratio of AcOH:Hexamine = 10.5:1

Molar Ratio		Temperature - 1°C.			Temperature - 30°C.		
HNO_3:Hexamine	HNO_3:AcOH	Expt. No.	Reaction Time Mins.	RDX Yield %	Expt. No.	Reaction Time Mins.	RDX Yield %
81	7.7	20	2 10 20 30 60 120	40 60 68 73 80 83			
48.5	4.6	21	2 15 20 35 50 75 120 148	3 44 50 61 69 73 74 77	25	3 10 30 60 90 120	47 70 72 72 72 72
40	3.8	22	3 10 30 50 91 120	3 16 32 44 54 57	26	3 10 30 60 90 120	33 58 60 63 64 67
32	3.0	23	29 70 90 120 150	11 19 18 21 24	27	3 10 31 60 90 120	18 37 45 53 56 61
26	2.4_5	24	10 30 60 90 120	2 3 6 7 8	28	10 30 60 120	18 33 40 45

TABLE IV

Final Yields of RDX in the Presence of Acetic Acid

Molar Ratio			RDX Yield Per cent	
AcOH:Hexamine	HNO_3:Hexamine	HNO_3:AcOH	1°C.	30°C.
4.3	82	19.1	77	74
	48.5	11.3	83	77
	40	9.3	78	-
	32	7.4	70	71
	26	6.0	49	70
	20	4.6	32	52
6.4	81	12.5	83	-
	48.5	7.6	81	80
	40	6.3	79	-
	32	5.0	60	72
	26	4.1	45	65
	20	3.1	21	42
10.5	81	7.7	82	-
	48.5	4.6	78	73
	40	3.8	67	69
	32	3.0	45	66
	26	2.5	33	52

TABLE V

Rate of Nitrolysis of Hexamine in Chloroform

10.00 ml. of solution containing 100 gm./l. of hexamine was used.
Weight of chloroform = 13.4_2 gm.
Weight of hexamine = 1.0_0 gm.
Molar Ratio of $CHCl_3$:Hexamine = 15.7:1

Molar Ratio		Temperature - 1°C.			Temperature - 30°C.		
HNO_3:Hexamine	HNO_3:$CHCl_3$	Expt. No.	Reaction Time Mins.	RDX Yield %	Expt. No.	Reaction Time Mins.	RDX Yield %
40	2.54	29	3 5 10 15 30 120	40 52 63 70 75 77	35	3 5 15 30 60 120	80 82 80 79 80 81
32	2.02	30	5 10 20 60 120	43 58 67 72 77	36	3 5 15 60 120	77 76 75 77 78
26	1.59	31	5 10 30 60 90 120	27 44 64 70 73 73	37	5 15 70 93 120	66 72 75 73 76
22	1.40	32	5 20 60 90 120	13 46 60 63 64	38	5 15 40 70 120	56 62 67 71 73
20	1.27	33	10 20 30 60 119	12 21 27 37 45	39	5 9 30 60 120	45 49 59 68 68
18	1.15	34	15 30 62 91 113	6 12 21 25 27	40	5 10 30 60 120	32 36 46 53 60

TABLE VI

Rate of Nitrolysis of Hexamine in Chloroform

15.00 ml. of solution containing 75 gm./l. of hexamine was used.
Weight of chloroform = 20.7_0 gm.
Weight of hexamine = 1.1_2 gm.
Molar Ratio of $CHCl_3$:Hexamine = 21.6:1

Molar Ratio		Temperature - 1°C.			Temperature - 30°C.		
HNO_3:Hexamine	HNO_3:$CHCl_3$	Expt. No.	Reaction Time Mins.	RDX Yield %	Expt. No.	Reaction Time Mins.	RDX Yield %
32	1.48	41	5 15 40 80 120	43 66 77 81 81	45	5 10 30 60 120	77 78 77 79 78
26	1.20	42	5 15 40 80 120	28 51 67 69 73	46	5 10 30 60 120	64 67 70 73 75
22	1.02	43	5 30 60 90 120	10 43 54 57 60	47	5 19 50 80 120	50 58 63 68 69
18	0.83	44	10 30 60 90 121	3 12 20 24 26	48	5 20 50 80 120	23 33 43 47 52

TABLE VII

Rate of Nitrolysis of Hexamine in Chloroform

25.0 ml. of solution containing 40 gm./l. of hexamine was used.
Weight of chloroform = 35.7 gm.
Weight of hexamine = 0.9_9 gm.
Molar Ratio of $CHCl_3$:Hexamine = 42.0:1

Molar Ratio		Temperature - 1°C.			Temperature - 30°C.		
HNO_3:Hexamine	HNO_3:$CHCl_3$	Expt. No.	Reaction Time Mins.	RDX Yield %	Expt. No.	Reaction Time Mins.	RDX Yield %
32	0.76	49	5 10 20 30 61 90 120	22 37 44 60 68 72 72	53	3 20 40 80 120	59 62 66 69 72
26	0.62	50	5 10 20 30 63 90 120	5 16 26 38 46 51 53	54	3 20 40 81 111	37 47 52 56 58
22	0.52	51	15 25 40 80 120	9 15 21 31 33	55	4 10 20 60 120	22 28 35 45 49
18	0.43	52	15 40 60 80 120	2 3 3 4 6	56	10 20 60 120	9 11 13 20

TABLE VIII

Final Yields of RDX in the Presence of Chloroform

Molar Ratio			RDX Yield Per cent	
$CHCl_3$:Hexamine	HNO_3:Hexamine	HNO_3:$CHCl_3$	1°C.	30°C.
15.7	40	2.54	80	81
	32	2.02	80	78
	26	1.59	73	77
	22	1.40	63	73
	20	1.27	50	69
	18	1.15	33	60
21.6	32	1.48	80	78
	26	1.20	72	74
	22	1.02	60	68
	18	0.83	26	52
42.0	32	0.76	74	74
	26	0.62	60	71
	22	0.52	37	63
	18	0.43	11	41

TABLE IX

Rate of Nitrolysis of Hexamine Dinitrate at 30°C. in the Absence of Solvent.

Experiment No.	HNO_3:Hexamine Molar Ratio	Reaction Time Mins.	RDX Yield %
57	32	2	78
		5	80
		10	81
		30	81
		112	81
58	26	2	72
		5	74
		10	76
		30	77
		114	78
59	22	2	65
		5	67
		10	69
		30	72
		116	74
60	18	2	47
		6	49
		15	56
		40	63
		119	66

FIGURE 1

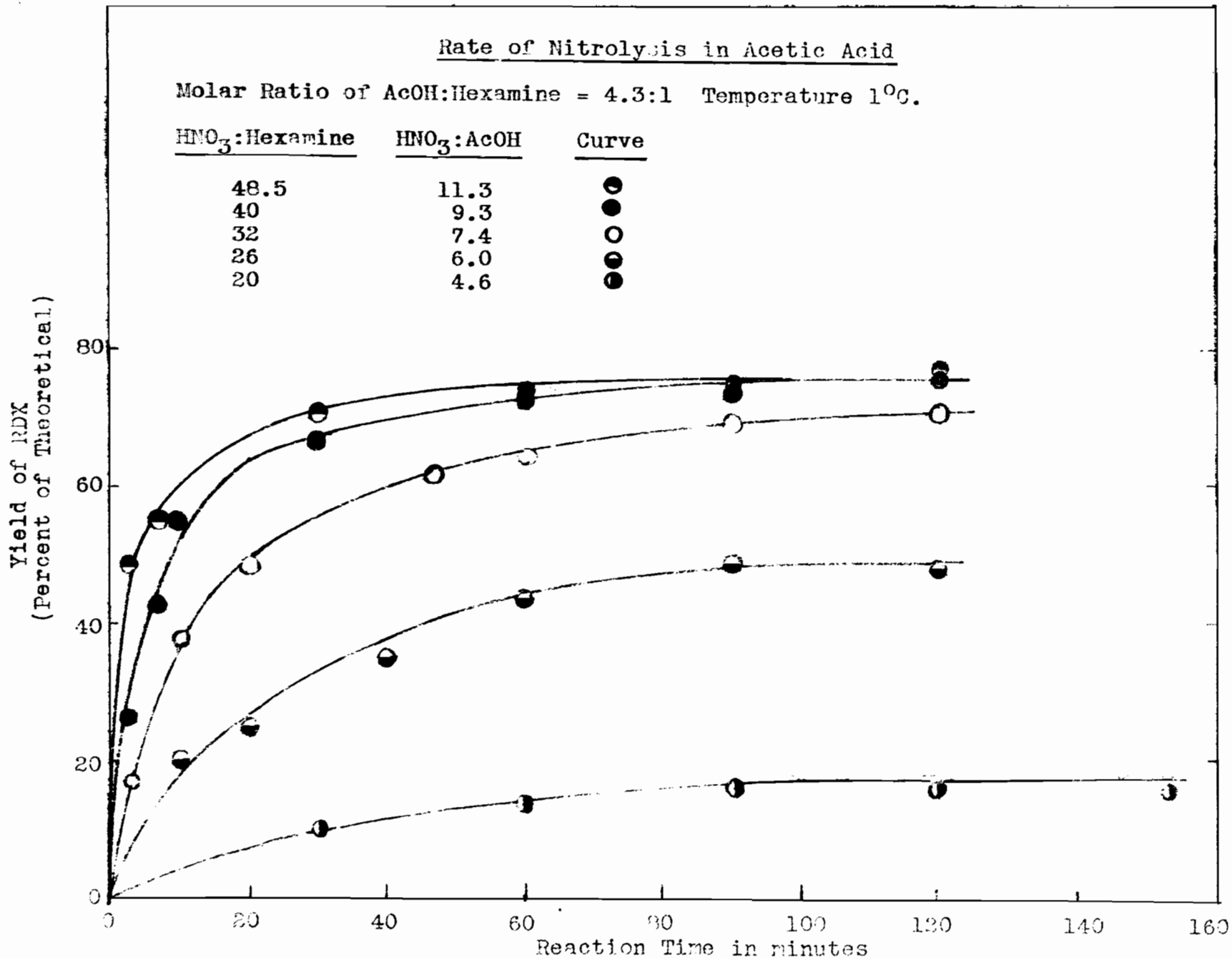
Rate of Nitrolysis in Acetic Acid
Molar Ratio of AcOH:Hexamine = 4.3:1 Temperature 1°C.
HNO3:Hexamine
HNO3:AcOH
Curve
48.5 11.3
40 9.3
32 7.4
26 6.0
20 4.6
Yield of RDX (Percent of Theoretical)
0
20
40
60
80
0
20
40
60
80
100
120
140
160
Reaction Time in minutes

FIGURE 2

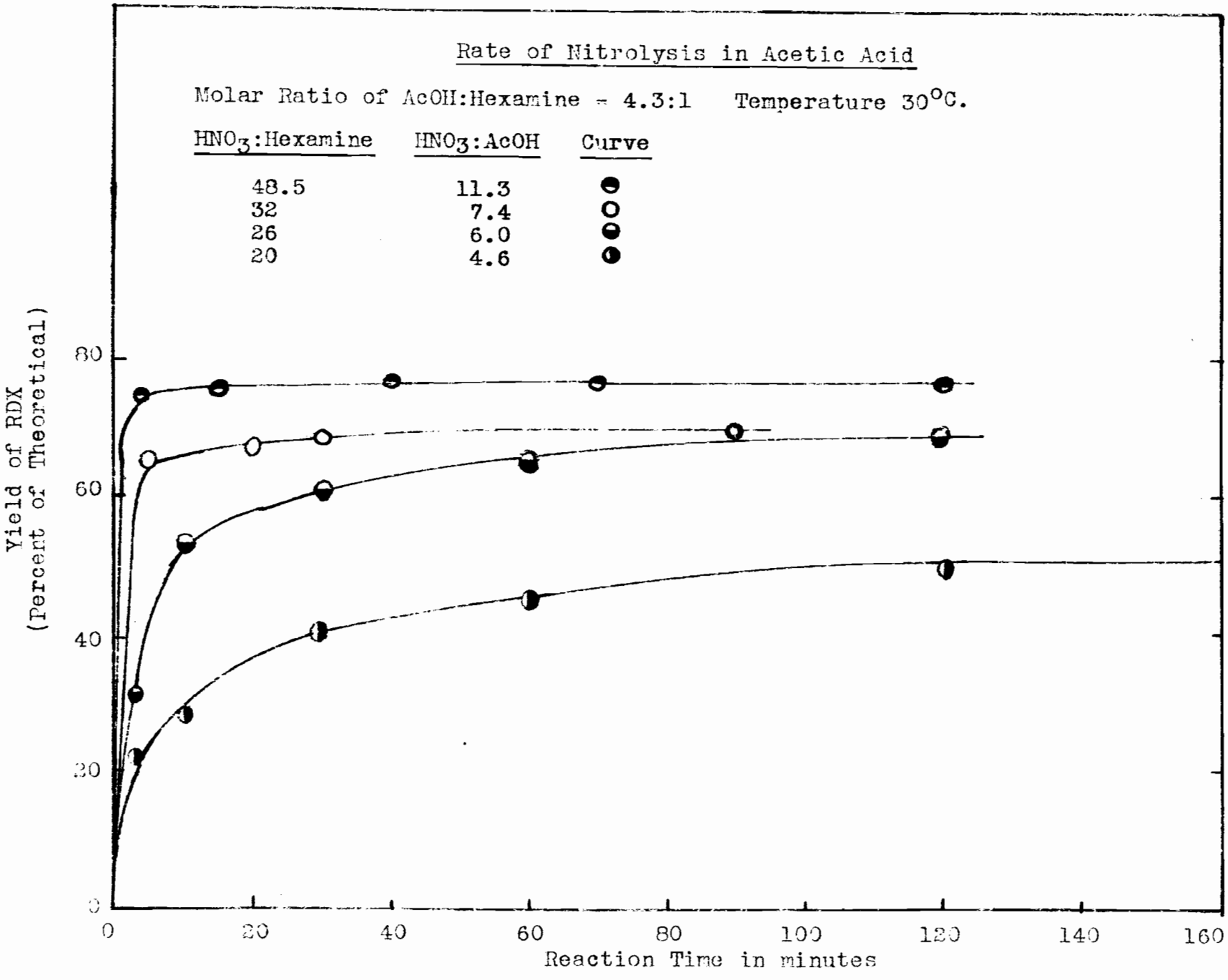
Rate of Nitrolysis in Acetic Acid
Molar Ratio of AcOH:Hexamine = 4.3:1 Temperature 30°C.
HNO3:Hexamine
HNO3:AcOH
Curve
48.5
11.3
32
7.4
26
6.0
20
4.6
Yield of RDX
(Percent of Theoretical)
0
20
40
60
80
100
120
140
160
Reaction Time in minutes

FIGURE 3

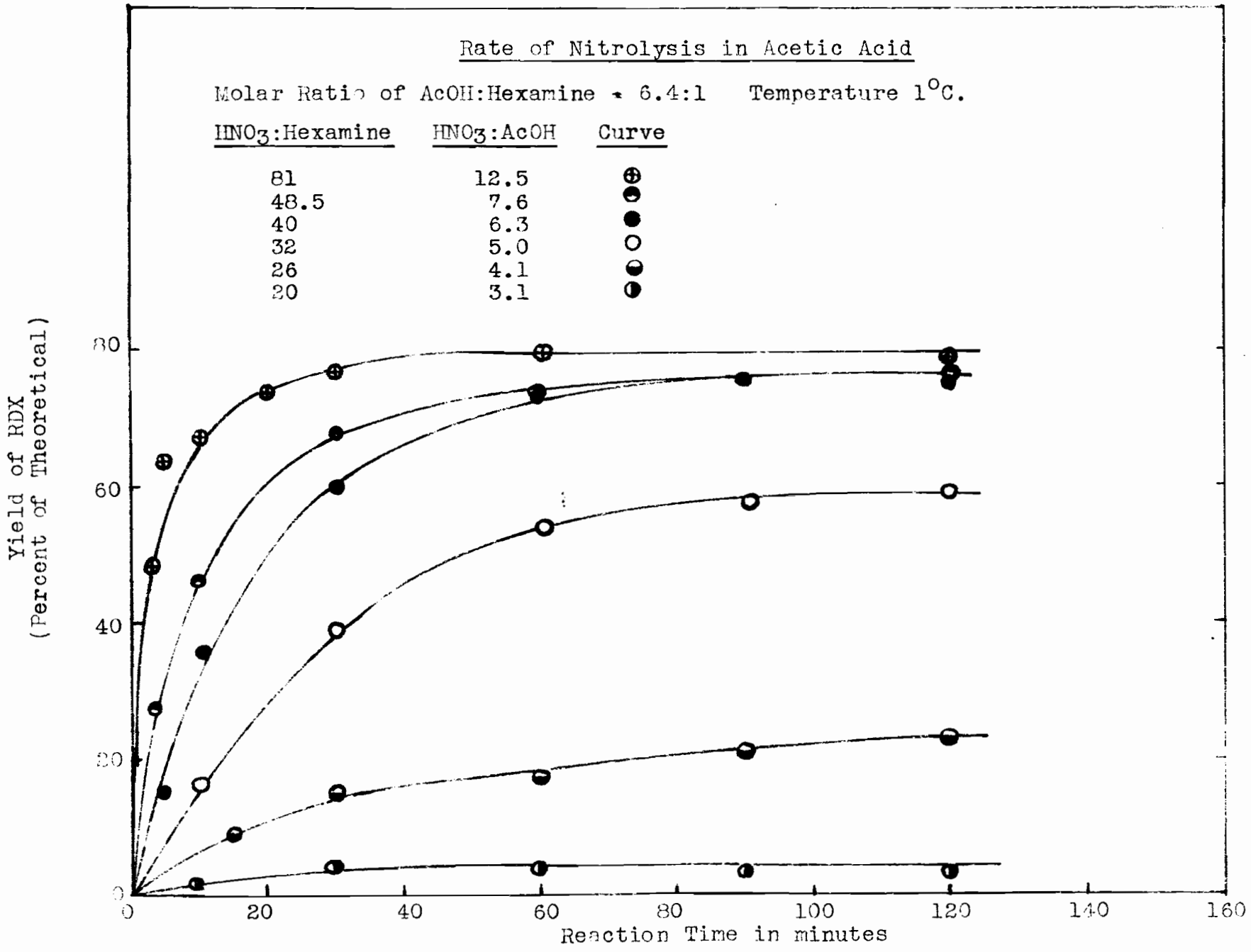
Rate of Nitrolysis in Acetic Acid
Molar Ratio of AcOH:Hexamine = 6.4:1 Temperature 1°C.
HNO3:Hexamine HNO3:AcOH Curve
81 12.5
48.5 7.6
40 6.3
32 5.0
26 4.1
20 3.1
Yield of RDX (Percent of Theoretical)
0
20
40
60
80
100
120
140
160
Reaction Time in minutes

FIGURE 4

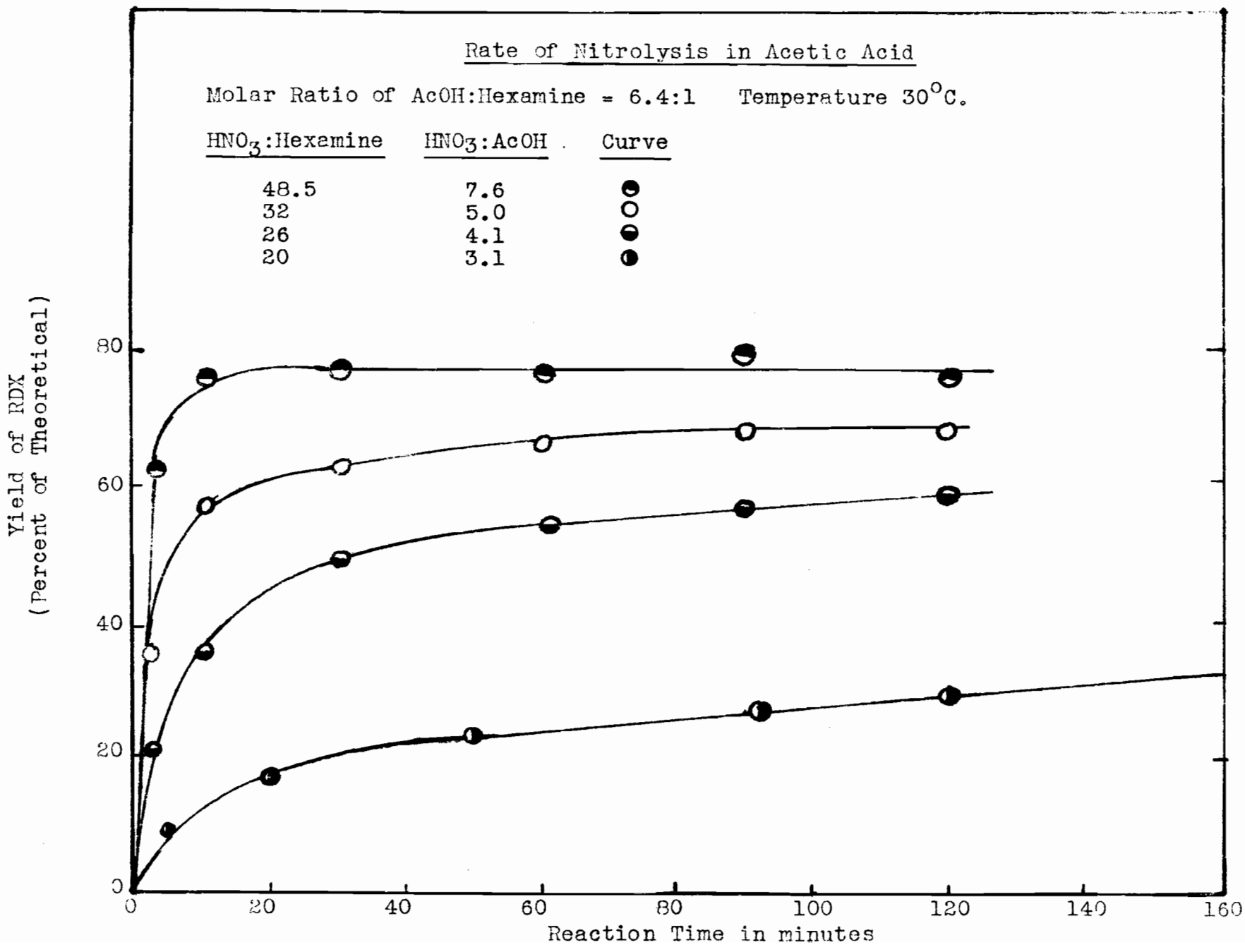
Rate of Nitrolysis in Acetic Acid
Molar Ratio of AcOH:Hexamine = 6.4:1 Temperature 30°C.
HNO3:Hexamine
HNO3:AcOH
Curve
48.5
7.6
32
5.0
26
4.1
20
3.1
Yield of RDX
(Percent of Theoretical)
0
20
40
60
80
100
120
140
160
Reaction Time in minutes

FIGURE 5

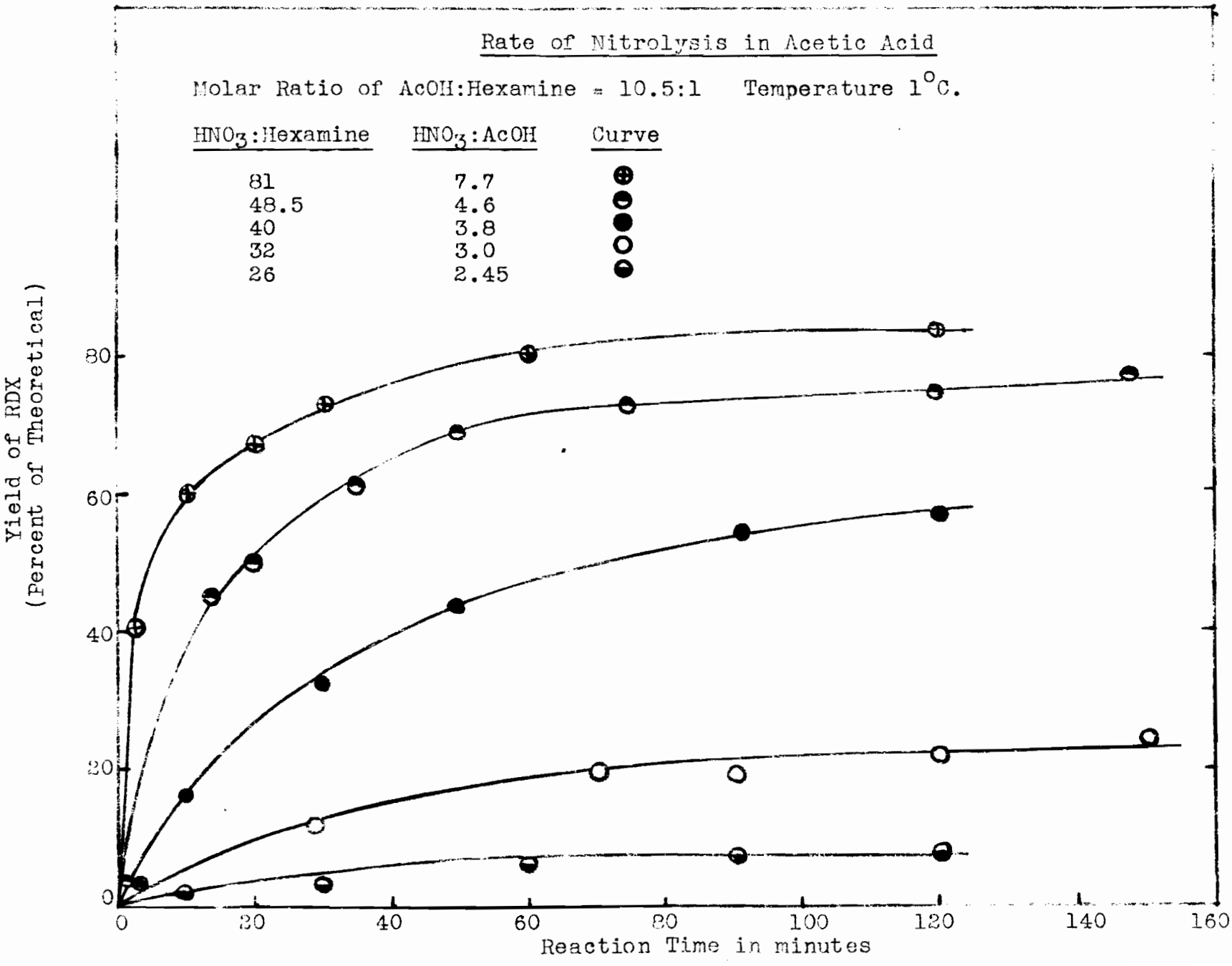
Rate of Nitrolysis in Acetic Acid
Molar Ratio of AcOH:Hexamine = 10.5:1 Temperature 1°C.
HNO3:Hexamine
HNO3:AcOH
Curve
81 7.7
48.5 4.6
40 3.8
32 3.0
26 2.45
Yield of RDX (Percent of Theoretical)
0
20
40
60
80
0
20
40
60
80
100
120
140
160
Reaction Time in minutes

FIGURE 6

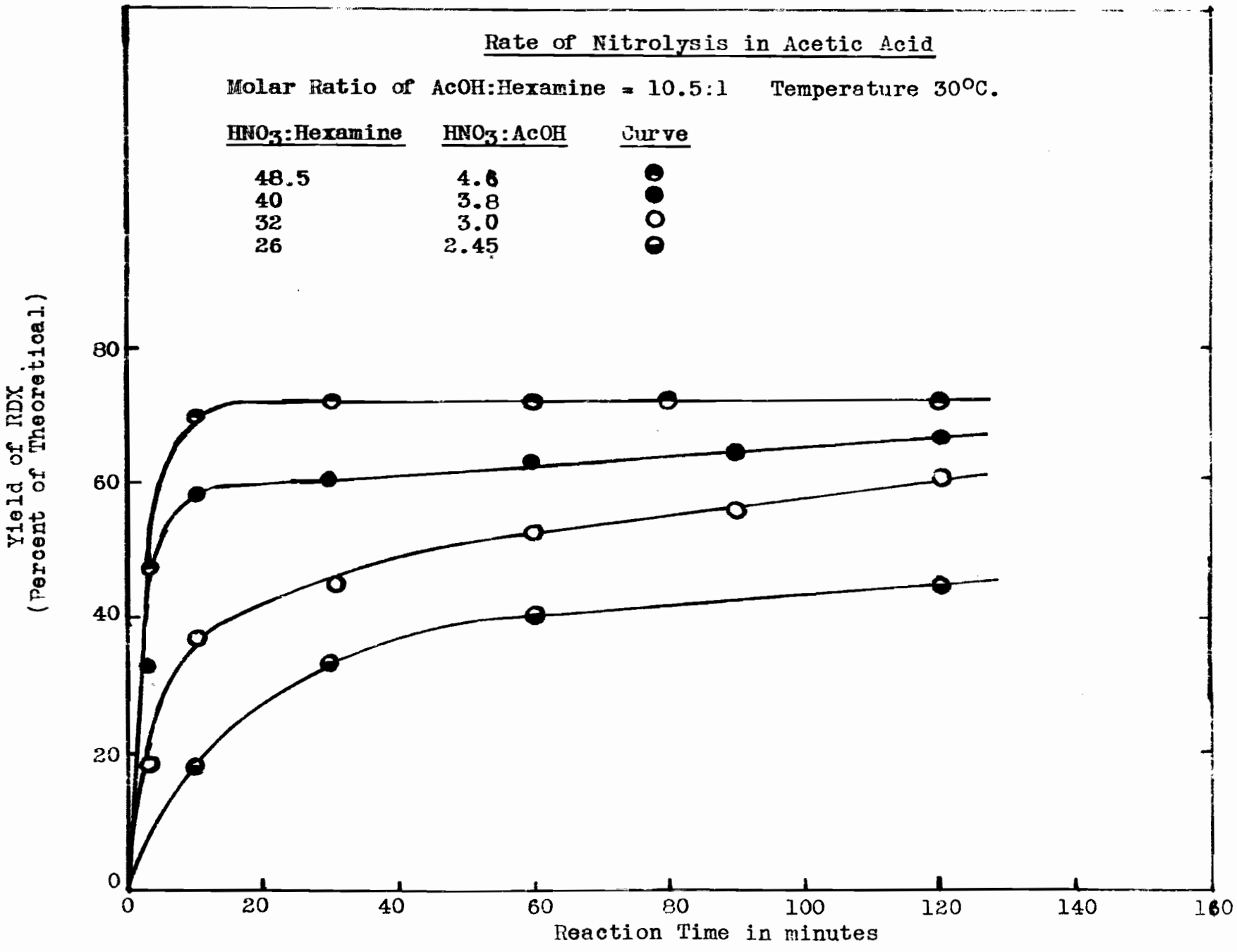
Rate of Nitrolysis in Acetic Acid
Molar Ratio of AcOH:Hexamine = 10.5:1 Temperature 30°C.
HNO3:Hexamine
HNO3:AcOH
Curve
48.5
4.6
40
3.8
32
3.0
26
2.45
Yield of RDX (Percent of Theoretical)
0
20
40
60
80
100
120
140
160
Reaction Time in minutes

FIGURE 7

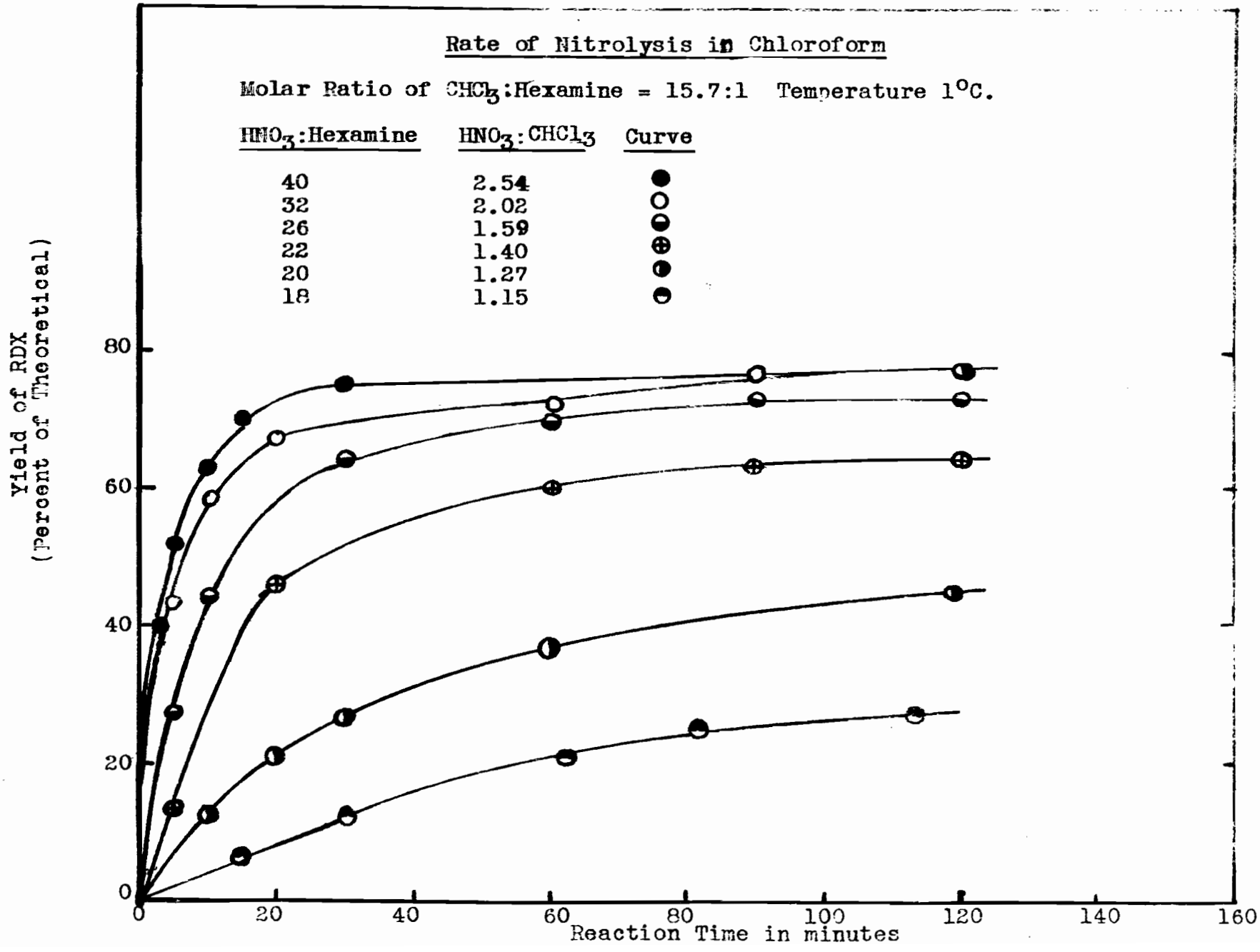
Rate of Nitrolysis in Chloroform
Molar Ratio of CHCl3:Hexamine = 15.7:1 Temperature 1°C.
HNO3:Hexamine
HNO3:CHCl3
Curve
40 2.54
32 2.02
26 1.59
22 1.40
20 1.27
18 1.15
Yield of RDX (Percent of Theoretical)
0
20
40
60
80
100
120
140
160
Reaction Time in minutes

FIGURE 8

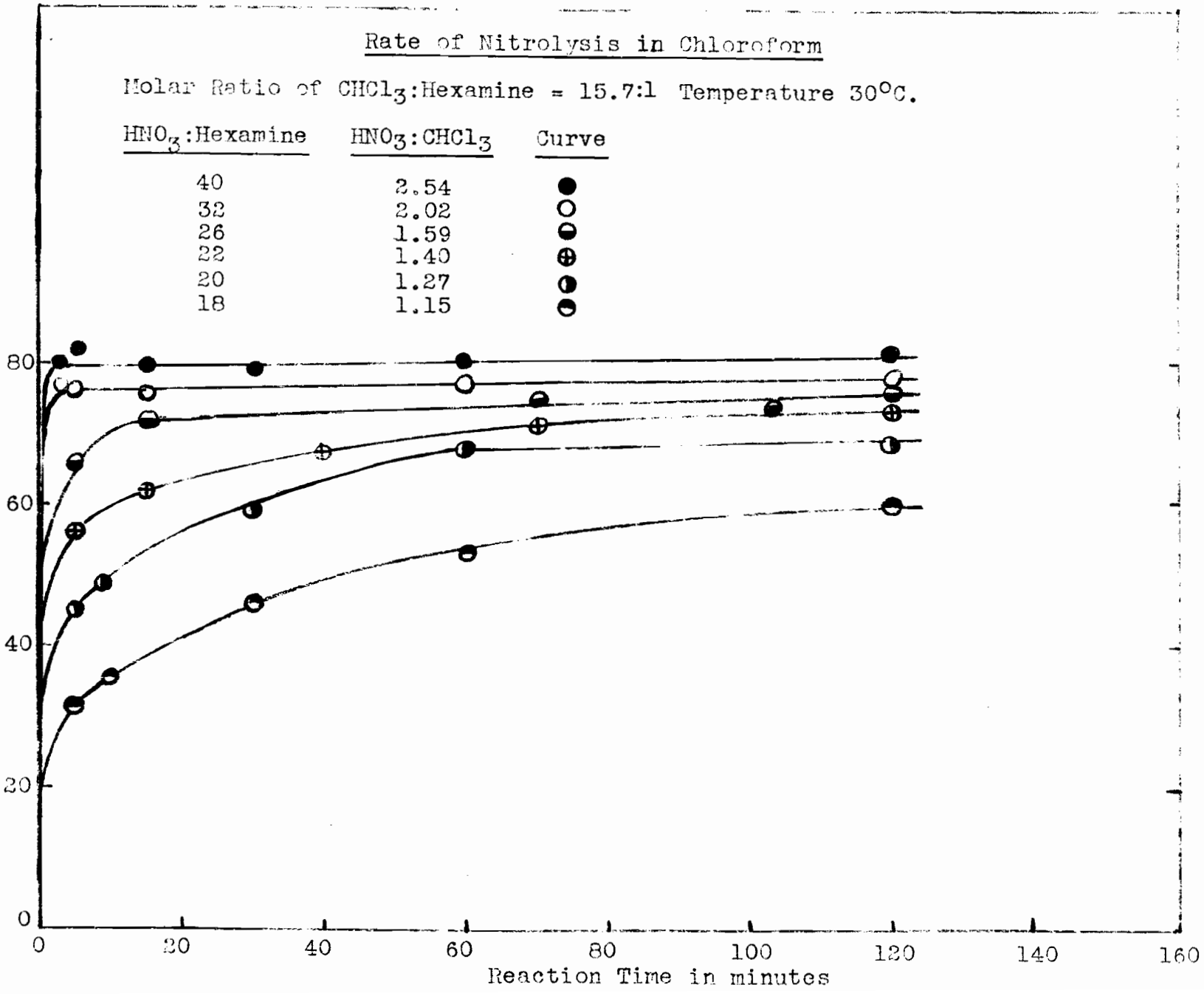
Rate of Nitrolysis in Chloroform
Molar Ratio of CHCl3:Hexamine = 15.7:1 Temperature 30°C.
HNO3:Hexamine
HNO3:CHCl3
Curve
40 2.54
32 2.02
26 1.59
22 1.40
20 1.27
18 1.15
Yield of RDX (Percent of Theoretical)
0
20
40
60
80
0
20
40
60
80
100
120
140
160
Reaction Time in minutes

FIGURE 9

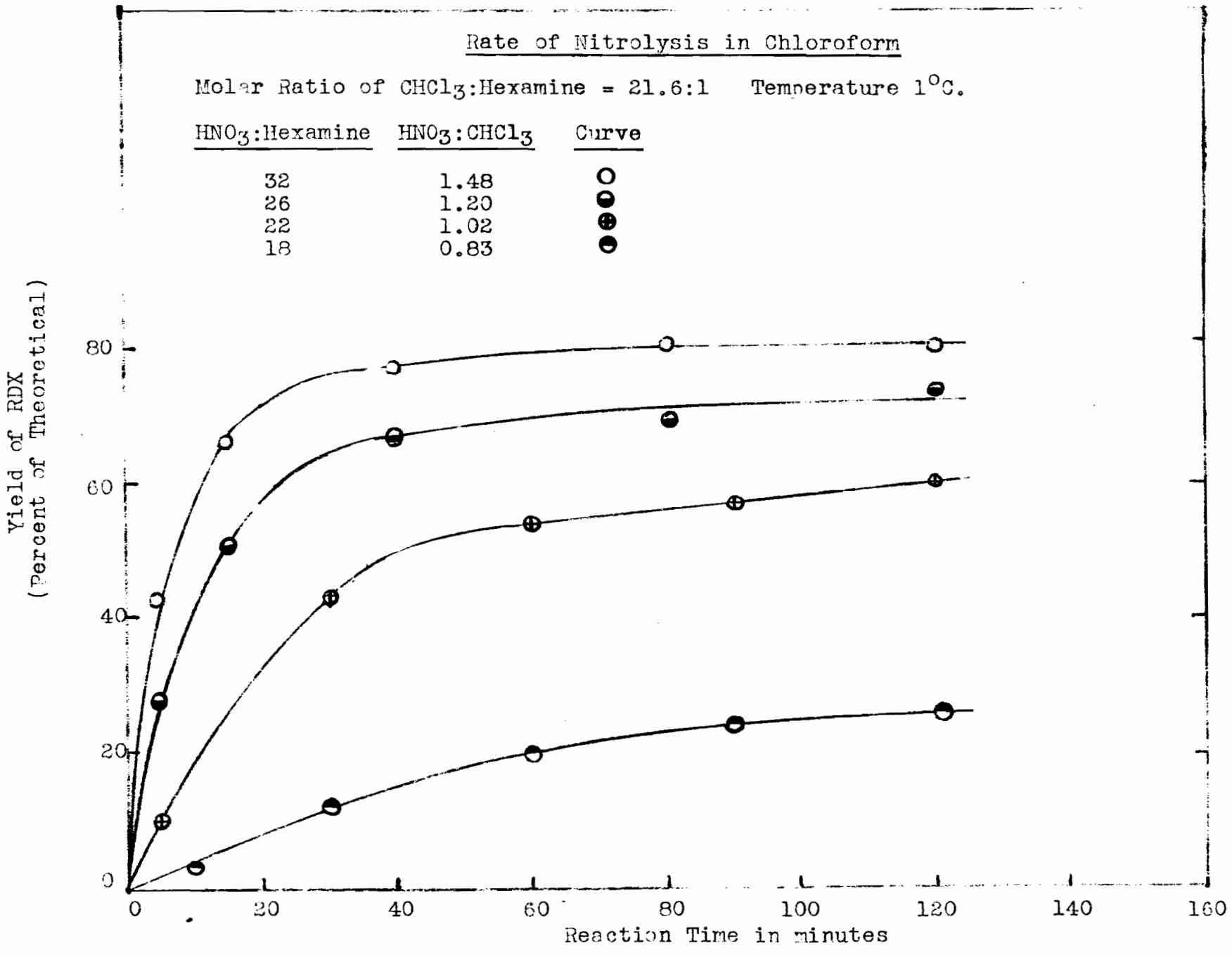
Rate of Nitrolysis in Chloroform
Molar Ratio of CHCl3:Hexamine = 21.6:1 Temperature 1°C.
HNO3:Hexamine HNO3:CHCl3 Curve
32 1.48
26 1.20
22 1.02
18 0.83
Yield of RDX (Percent of Theoretical)
0
20
40
60
80
0
20
40
60
80
100
120
140
160
Reaction Time in minutes

FIGURE 10

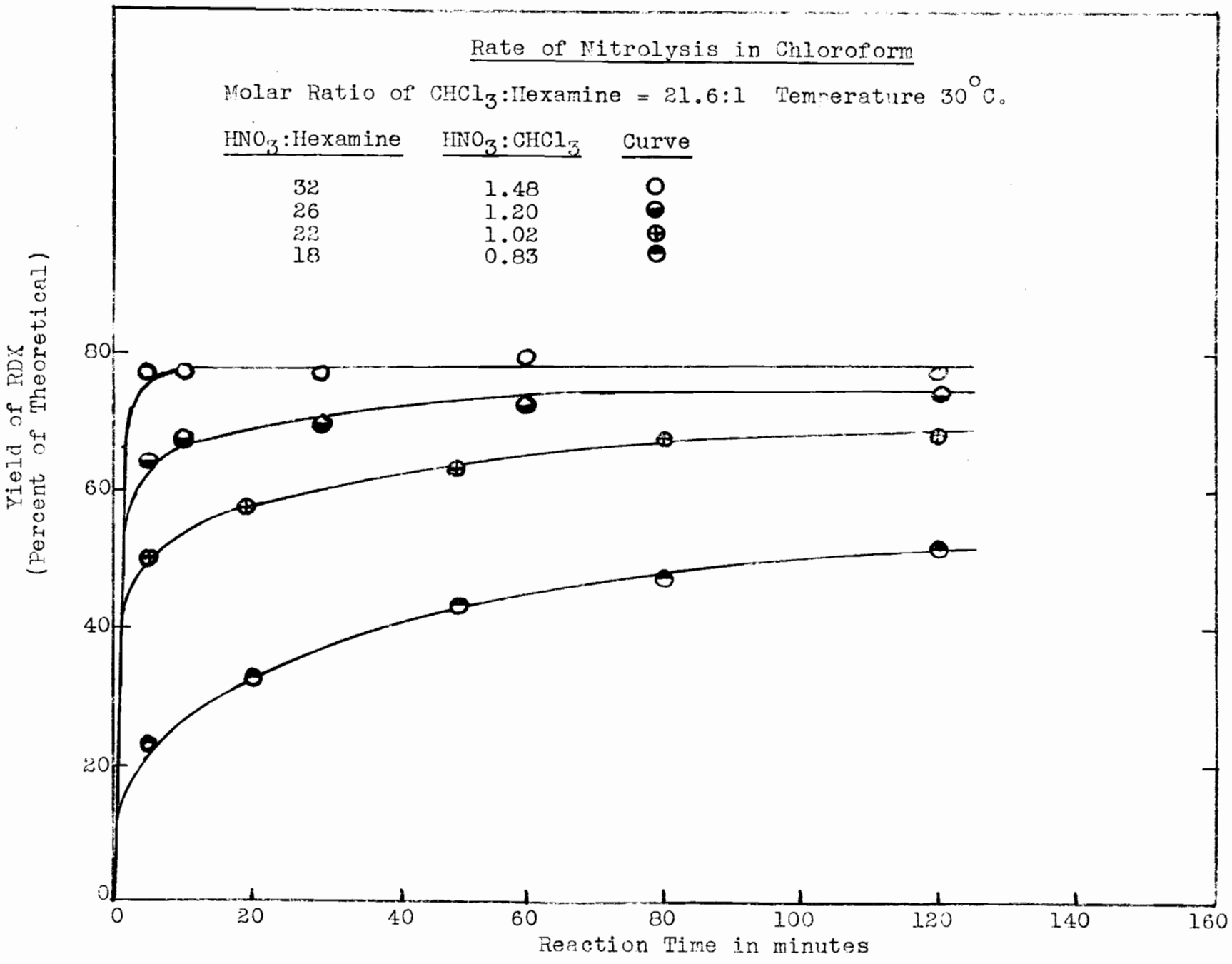
Rate of Nitrolysis in Chloroform
Molar Ratio of CHCl3:Hexamine = 21.6:1 Temperature 30°C.
HNO3:Hexamine
HNO3:CHCl3
Curve
32
1.48
26
1.20
22
1.02
18
0.83
Yield of RDX
(Percent of Theoretical)
0
20
40
60
80
0
20
40
60
80
100
120
140
160
Reaction Time in minutes

FIGURE 11

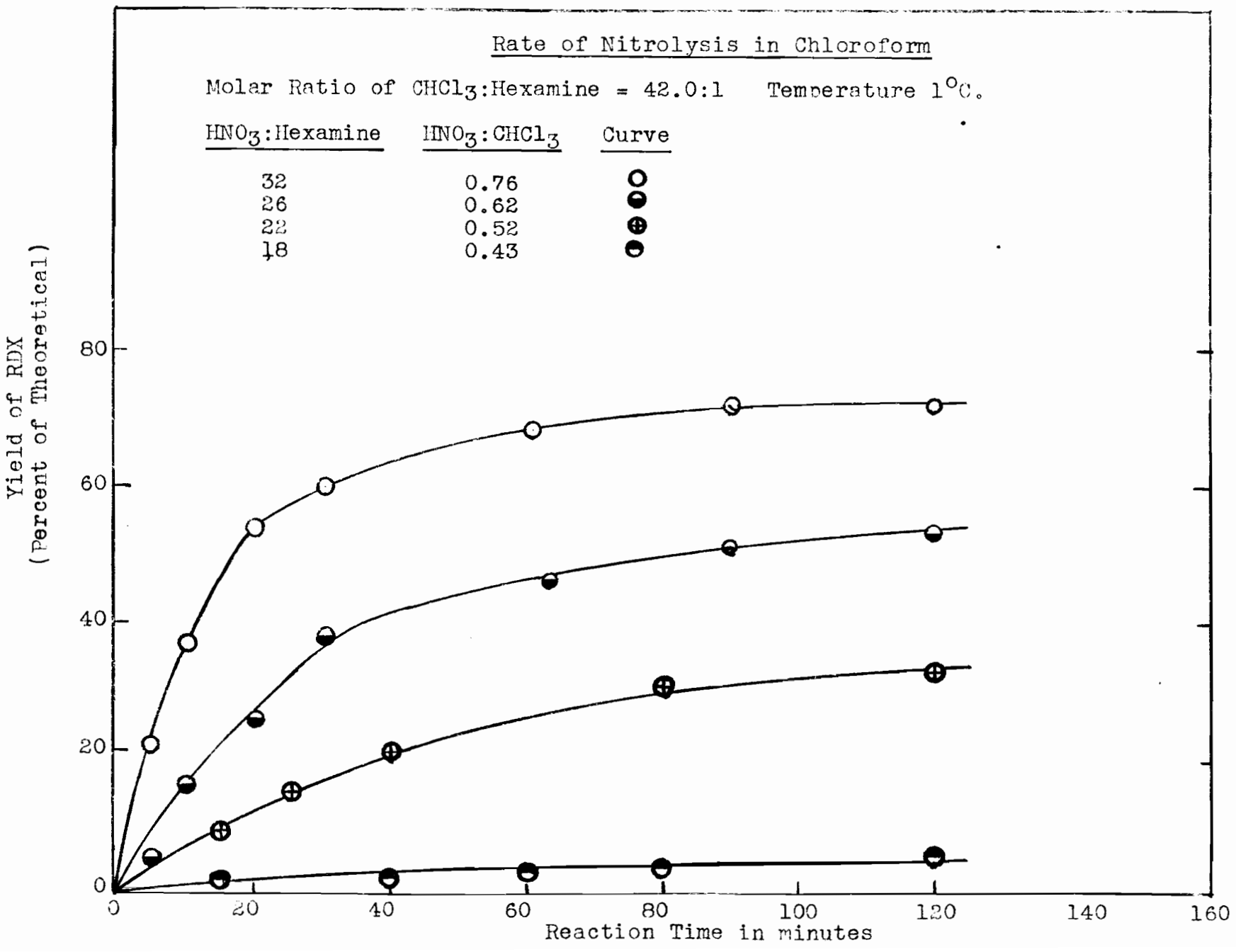
Rate of Nitrolysis in Chloroform
Molar Ratio of CHCl3:Hexamine = 42.0:1 Temperature 1°C.
HNO3:Hexamine
HNO3:CHCl3
Curve
32
0.76
26
0.62
22
0.52
18
0.43
Yield of RDX
(Percent of Theoretical)
0
20
40
60
80
0
20
40
60
80
100
120
140
160
Reaction Time in minutes

FIGURE 12

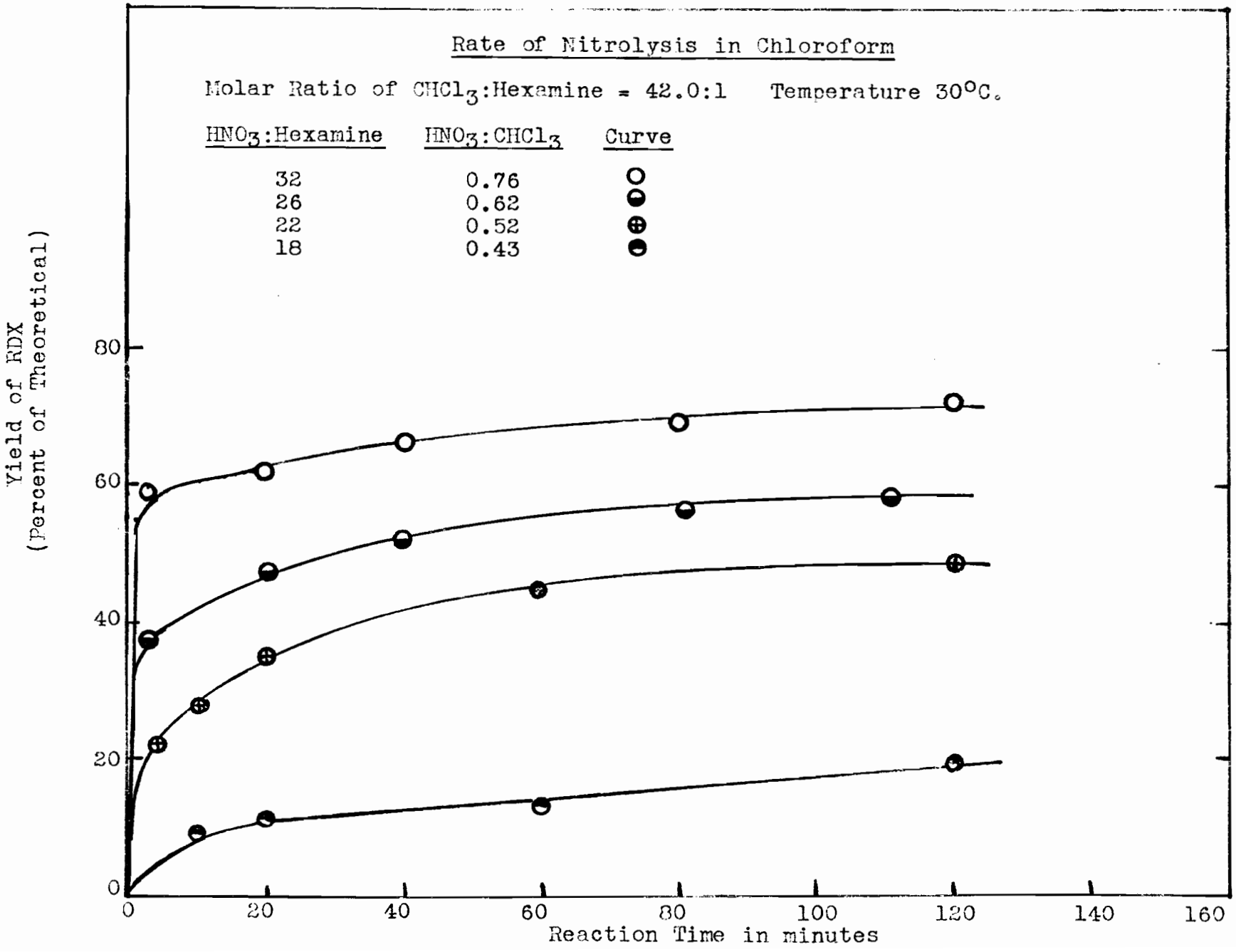
Rate of Nitrolysis in Chloroform
Molar Ratio of CHCl3:Hexamine = 42.0:1 Temperature 30°C.
HNO3:Hexamine HNO3:CHCl3 Curve
32 0.76
26 0.62
22 0.52
18 0.43
Yield of RDX (Percent of Theoretical)
0
20
40
60
80
0 20 40 60 80 100 120 140 160
Reaction Time in minutes

FIGURE 13

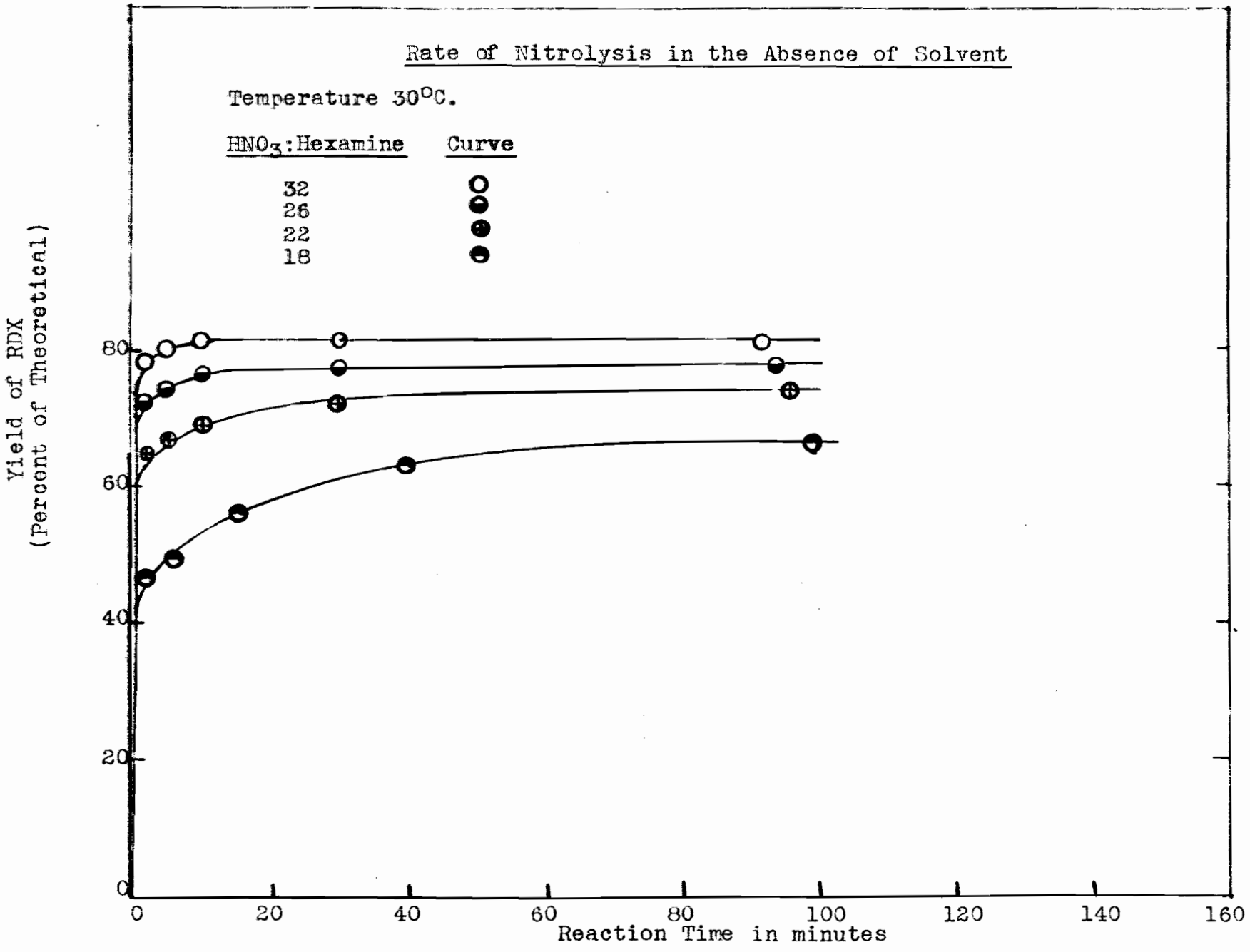
Rate of Nitrolysis in the Absence of Solvent
Temperature 30°C.
HNO3:Hexamine
Curve
32
26
22
18
Yield of RDX
(Percent of Theoretical)
0
20
40
60
80
0
20
40
60
80
100
120
140
160
Reaction Time in minutes

FIGURE 14

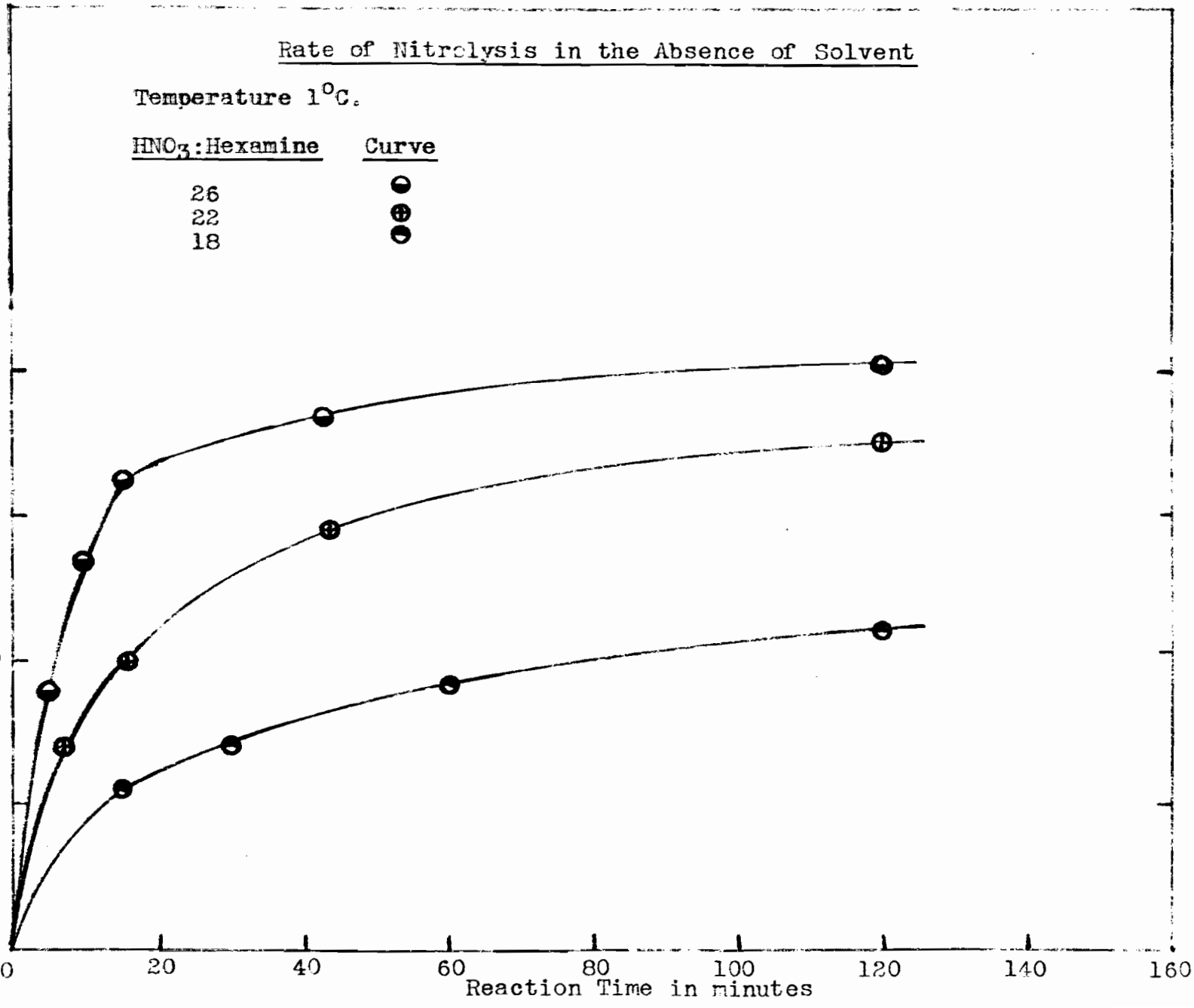
Rate of Nitrolysis in the Absence of Solvent
Temperature 1°C.
HNO3:Hexamine
Curve
26
22
18
Yield of RDX
(Percent of Theoretical)
0
20
40
60
80
0
20
40
60
80
100
120
140
160
Reaction Time in minutes

Effect of HNO_3:Hexamine Ratio on Final Yield

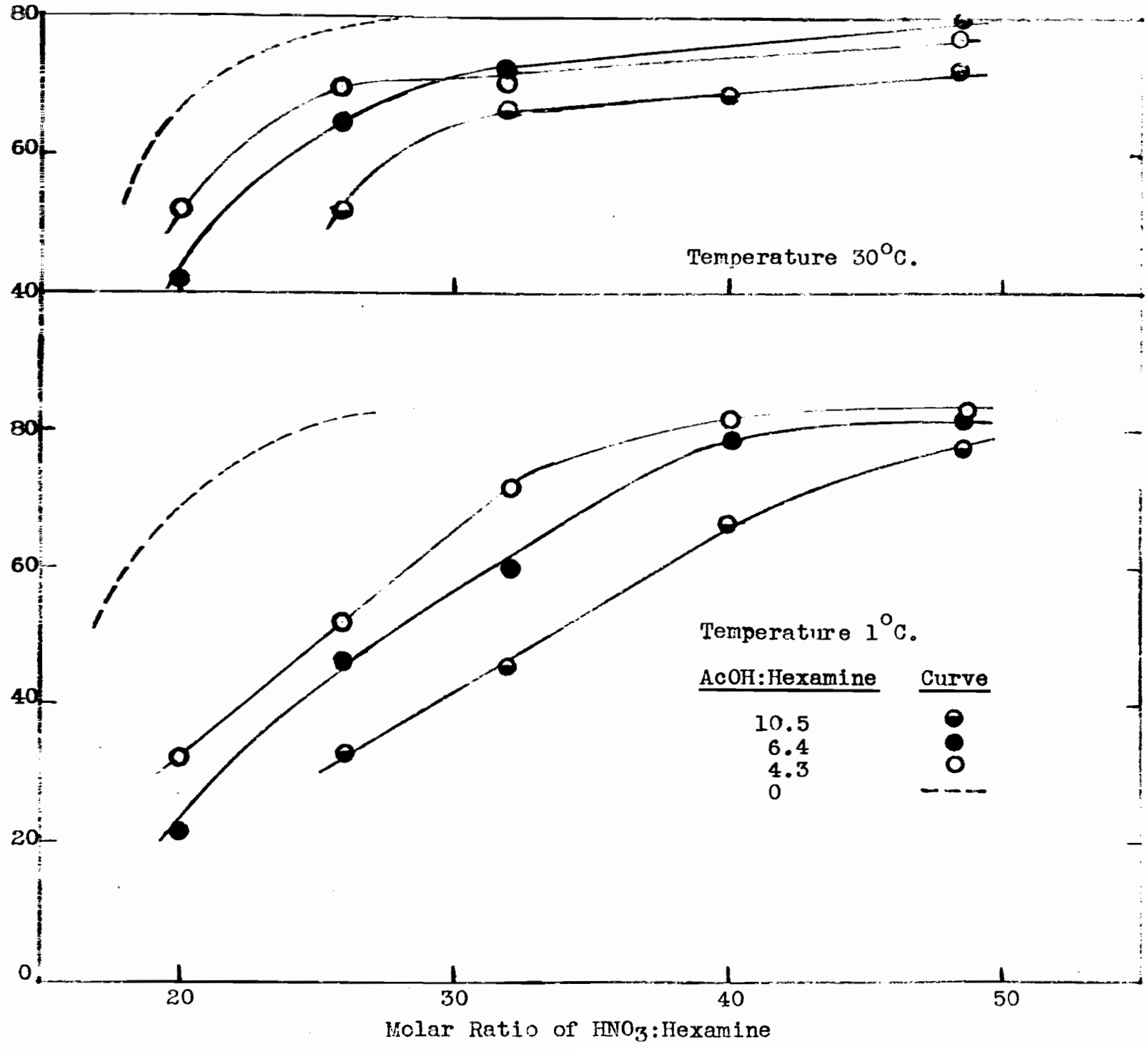

FIGURE 16

Effect of HNO_3:AcOH Ratio on Final Yield

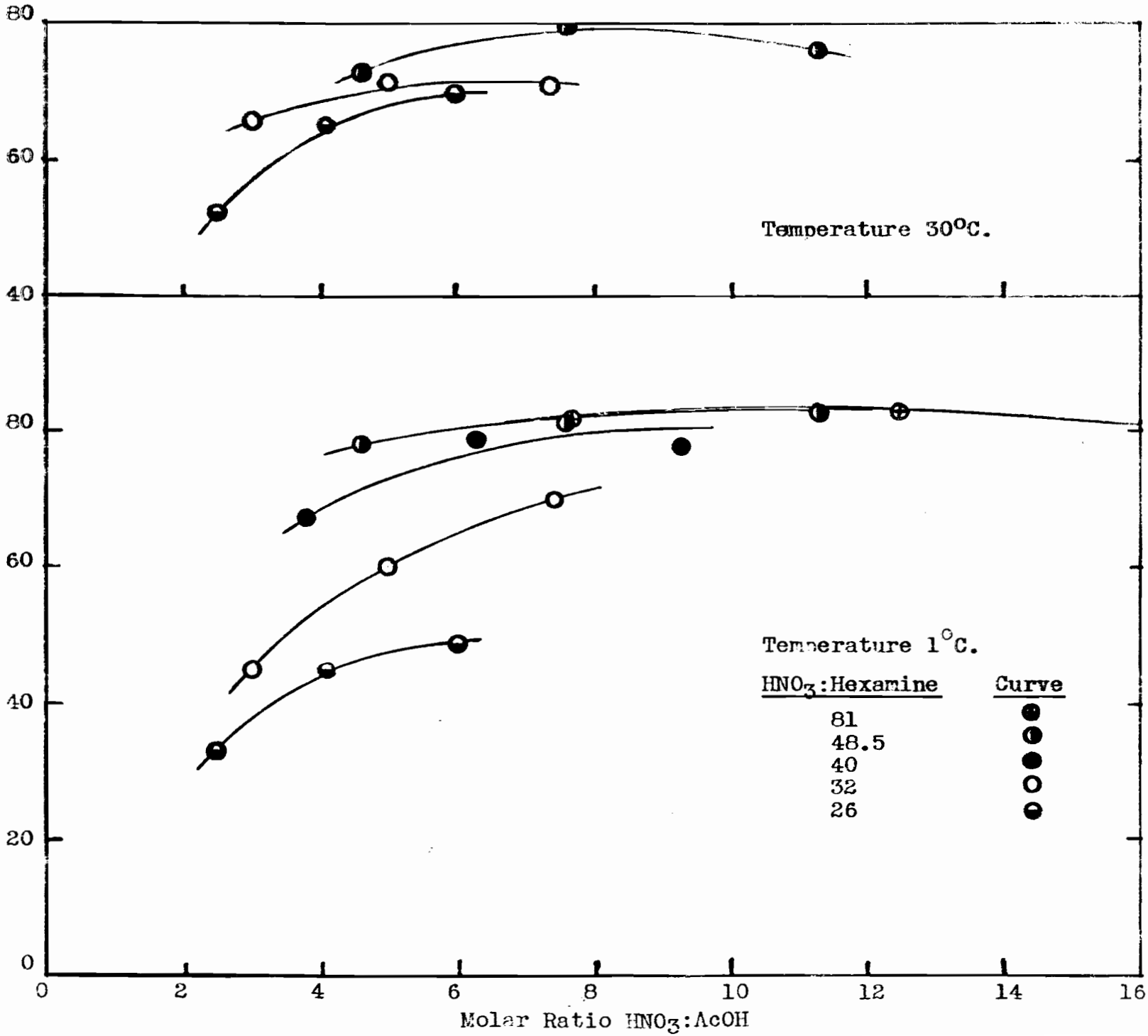

FIGURE 17

Effect of HNO_3:Hexamine Ratio on Final Yield

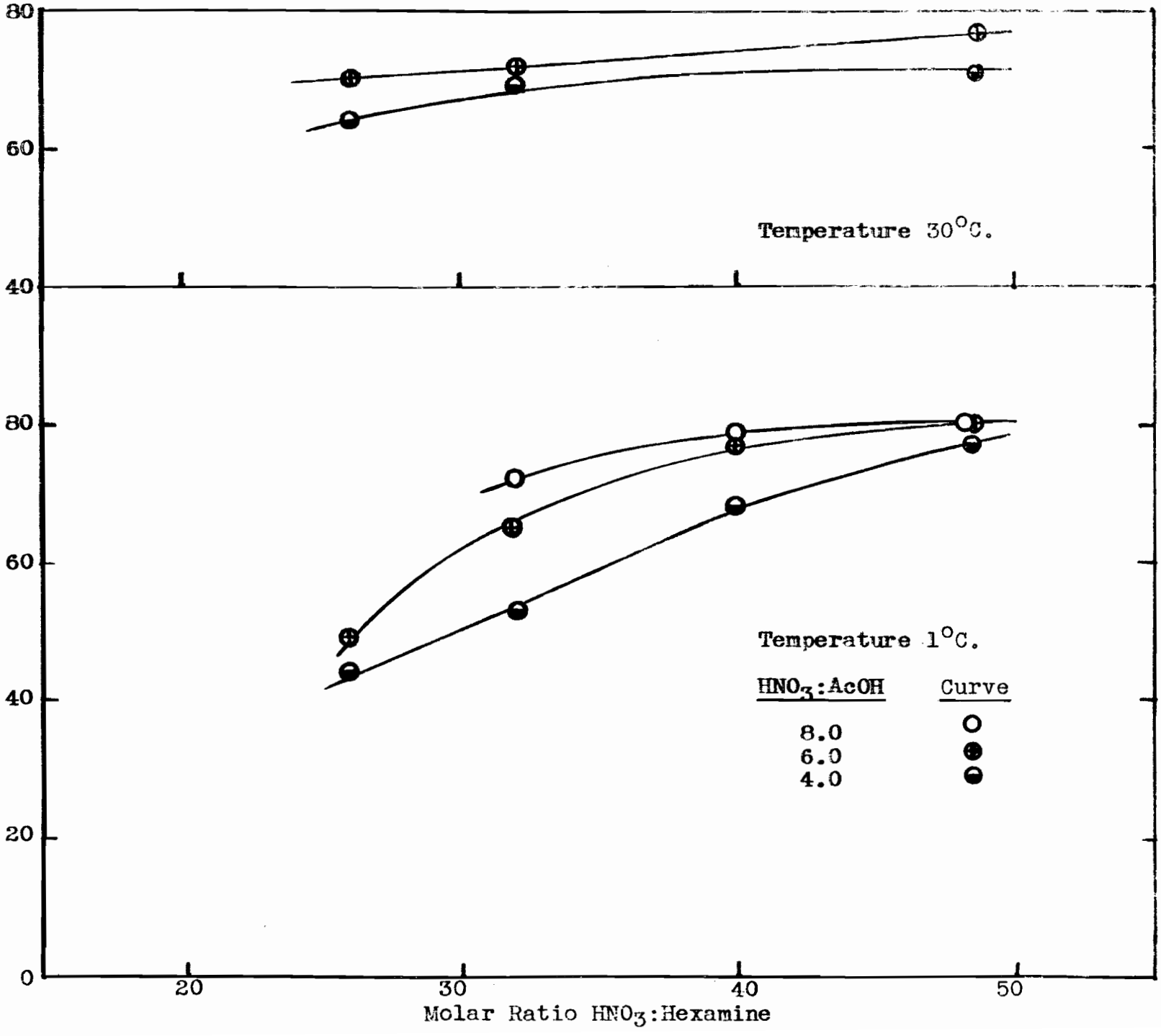

FIGURE 15

Effect of HNO_3:AcOH Ratio on Final Yield

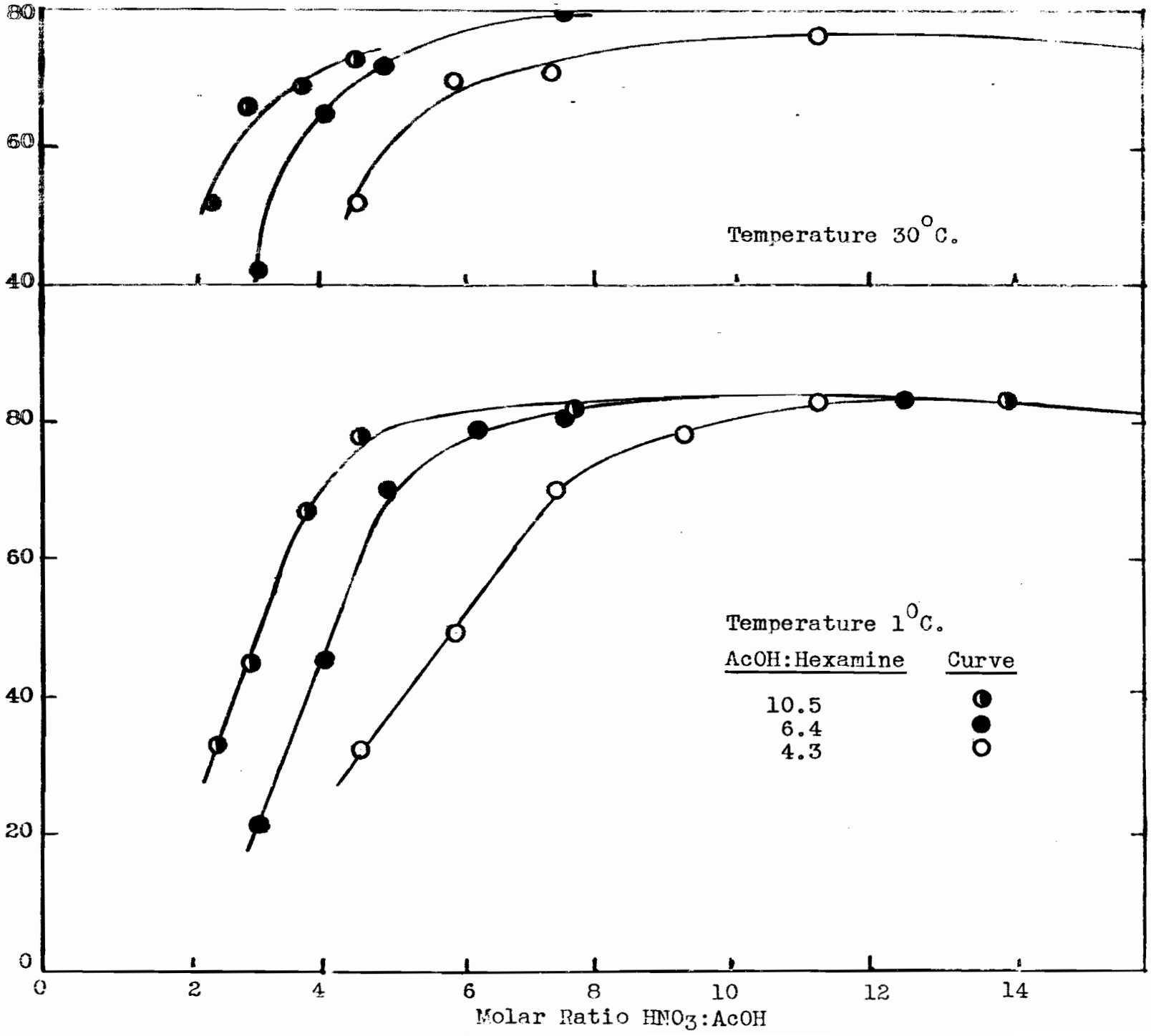

FIGURE 19

Effect of HNO_3:Hexamine Ratio on Final Yield

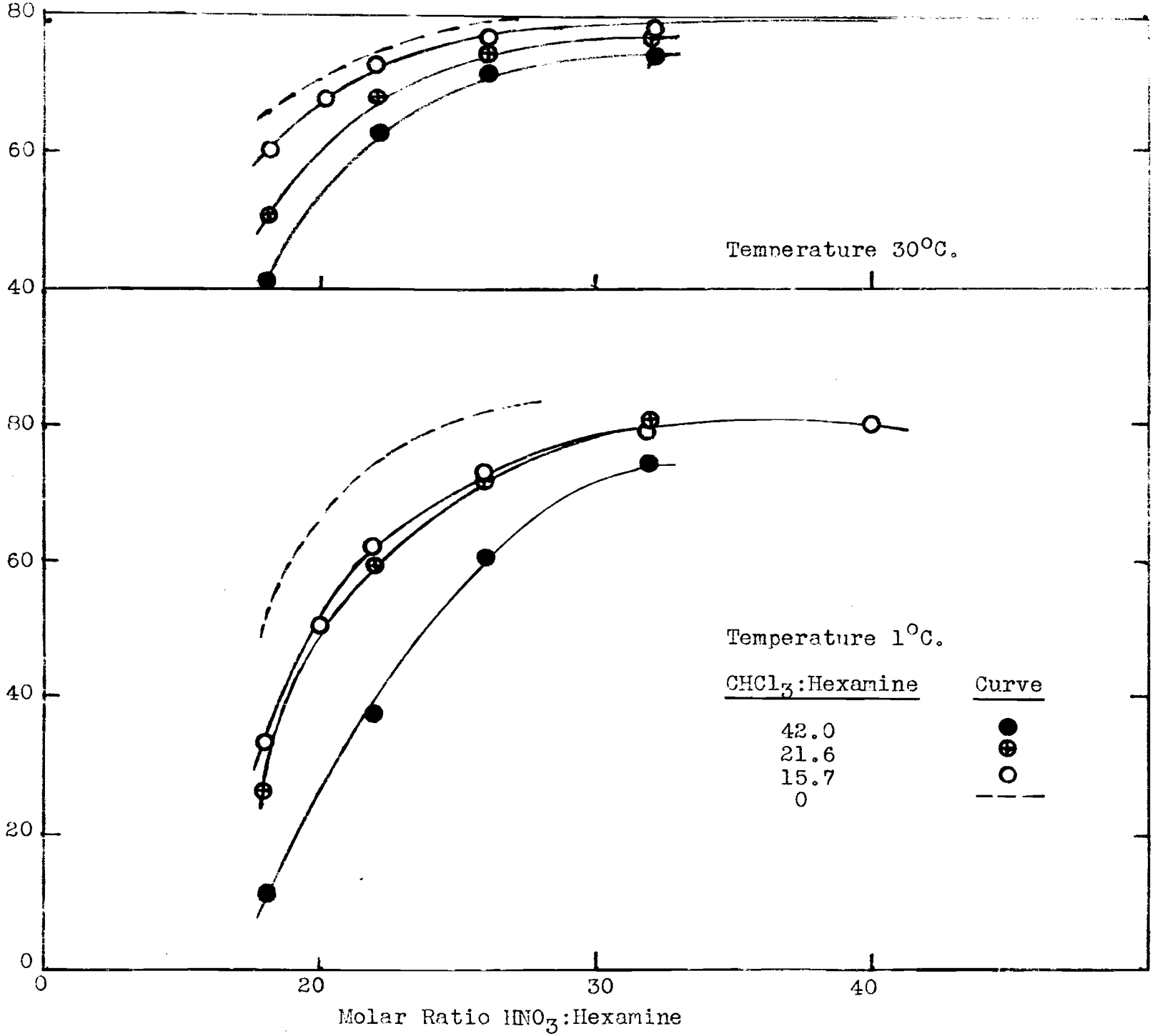

FIGURE 20

Effect of $HNO_3:CHCl_3$ Ratio on Final Yield

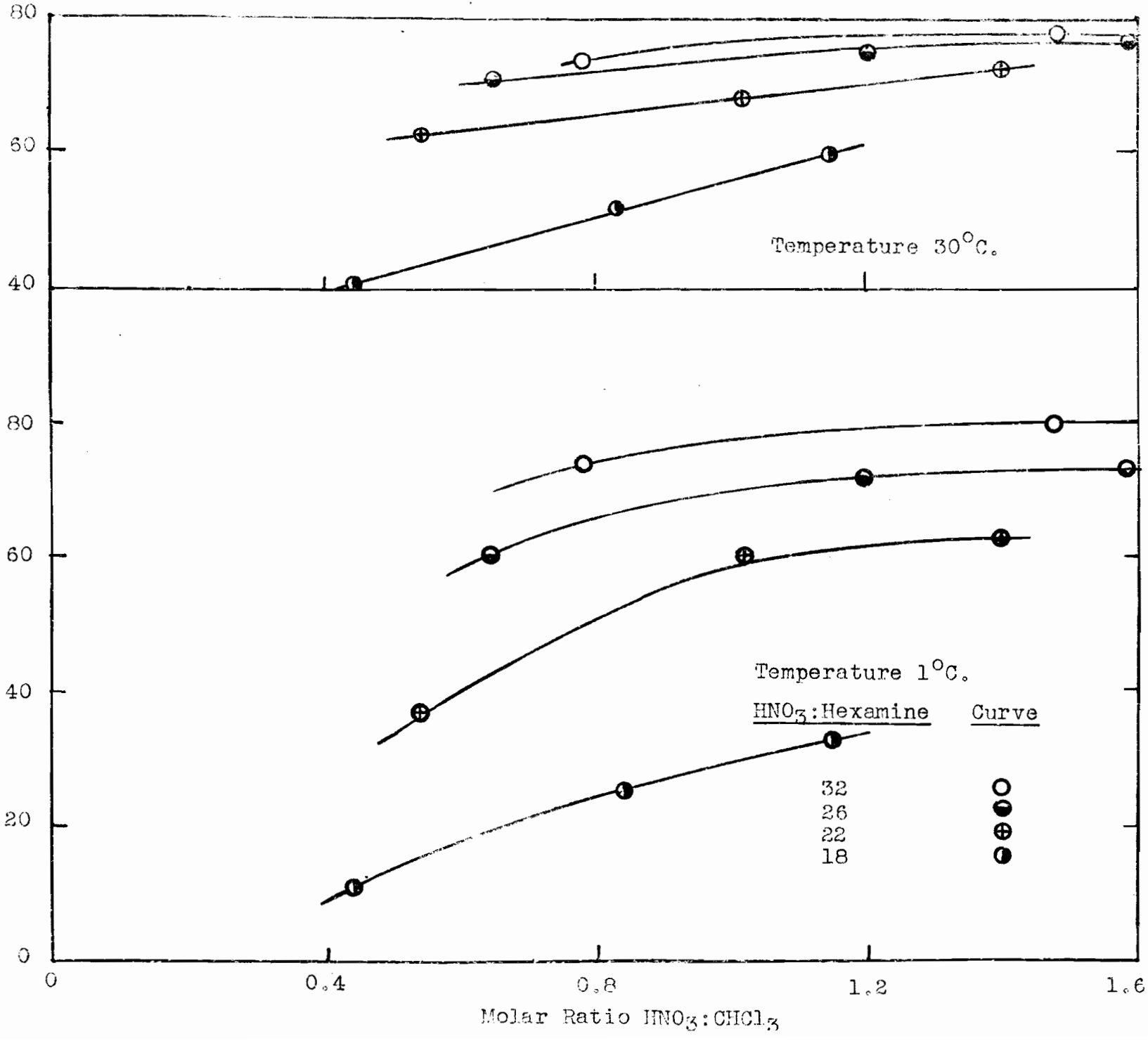

FIGURE 21

Effect of HNO_3:Hexamine Ratio on Final Yield

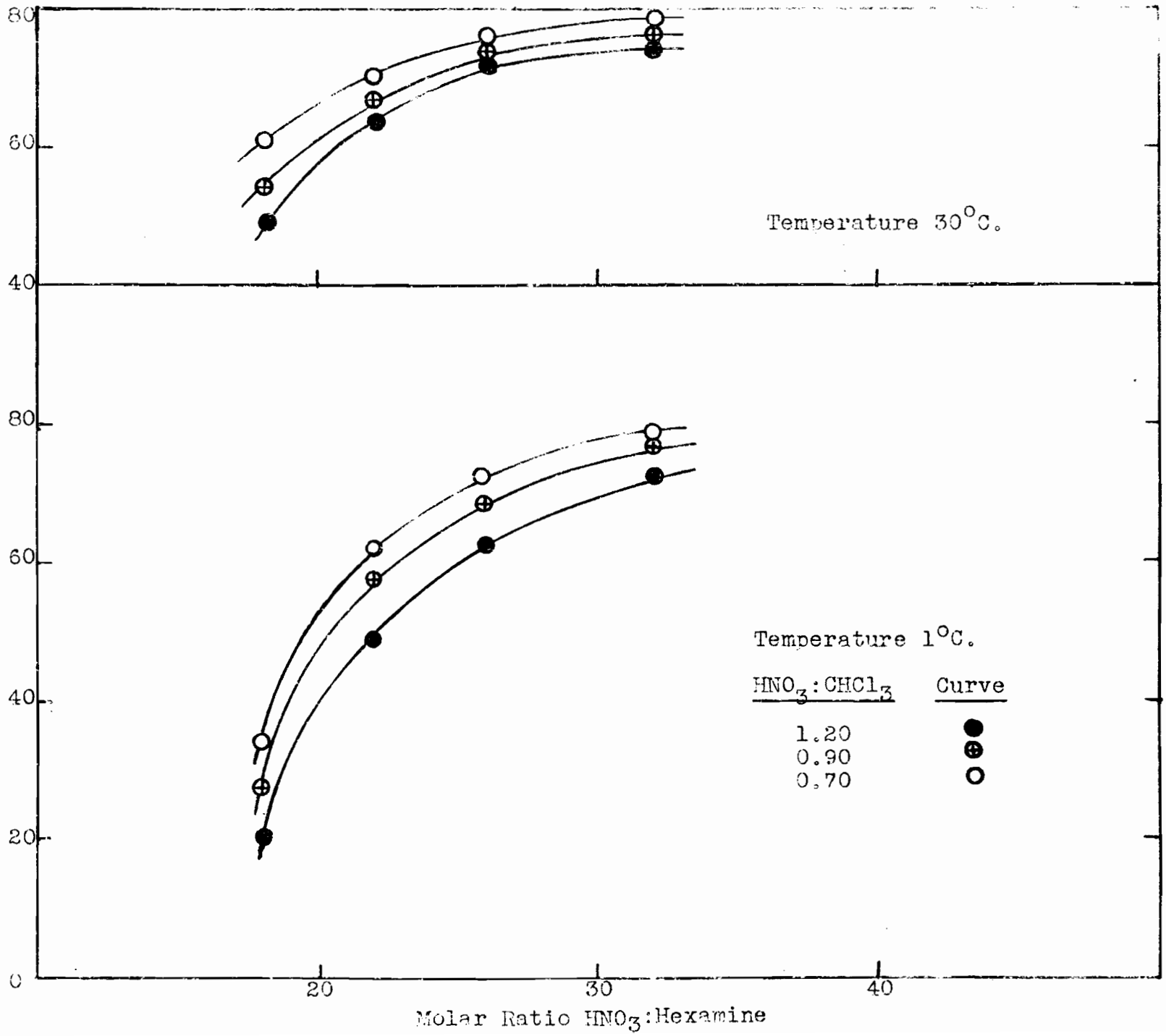

FIGURE 22

Effect of HNO_3:$CHCl_3$ Ratio on Final Yield

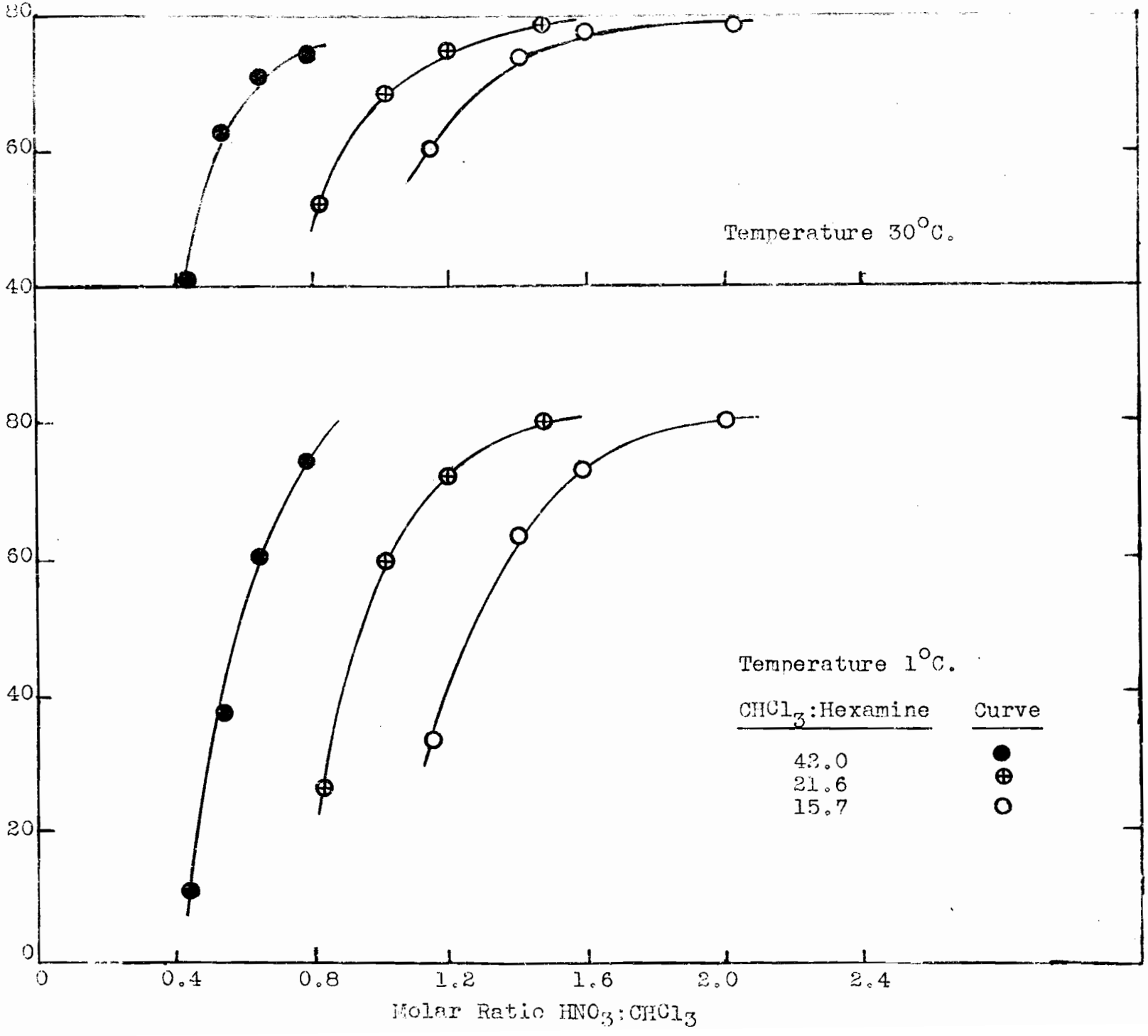

effect on both the rate of nitrolysis and on the final yield of RDX for a given molar ratio of nitric acid to hexamine. Where a decrease of yield is noted, the effect of acetic acid is evidently more pronounced than that of chloroform, but the difference in behaviour is much less marked the higher the temperature. Moreover, Figs. 15 and 19 indicate that if the molar ratio of nitric acid to hexamine is increased sufficiently in the presence of either acetic acid or chloroform, the maximum yield of 80% is approached regardless of temperature.

Effect of Acetic Acid on the Nitrolysis of Hexamine

Fig. 15 shows that even with the most dilute solution of hexamine in acetic acid (molar ratio 10.5:1) the final yield of RDX approaches the maximum of 80% at a molar ratio of nitric acid:hexamine of 50:1. In the absence of solvent, this yield is obtained when the molar ratio is only 26:1 (3, 5). It appears possible, therefore, that the acetic acid has in some way reacted with some of the nitric acid and made it unavailable for nitrolysis.

Since it seems that aromatic nitrations proceed by attack of positive nitracidium ion at nuclear carbon,

it is reasonable to assume that acetic acid exerts its harmful action on the rate of nitrolysis by decreasing somehow the available nitracidium ion concentration for a given nitric acid:hexamine ratio. This assumption finds support in the observation (20) that acetic acid acts as a base towards nitric acid. Moreover, Briner, Susz, and Favarger (21) found a maximum viscosity and a minimum melting point in an approximately equimolecular mixture of nitric and acetic acids. Their Raman data, however, revealed no lines other than those characteristic of the pure components, and they postulated, therefore, that the compound formed was a molecular complex:

$$CH_3COOH + HNO_3 \rightleftharpoons CH_3COOH.HNO_3 \quad \ldots\ldots\ldots (4)$$

This reaction should remove molecular nitric acid, thereby shifting the equilibrium (2) between nitracidium ion and pseudo-nitric acid to decrease the concentration of the former.

On this basis, it is possible to explain qualitatively the results obtained with acetic acid. It might be expected that with sufficient nitric acid, essentially all the acetic acid would be tied up as the nitric acid-acetic acid complex. If the amount of nitric acid is then further increased, the reaction mixture would behave essentially as

if no solvent were present. Fig. 18 shows that for a given hexamine:acetic acid ratio the yield does, in fact, increase to its maximum value (ca. 80%) as the nitric acid:acetic acid ratio is increased.

The effect of increased temperature is to decrease the harmful effect of the solvent, as shown by the two sets of rate curves in Fig. 15. This behaviour may be explained by assuming that the nitric acid-acetic acid complex is more dissociated at the higher temperature, thus giving rise to a greater nitracidium ion concentration than exists at 1°C in the same nitrolysis mixture.

The following assumptions, therefore, seem adequate to account for the nature of the results obtained for the nitrolysis of hexamine in acetic acid:

1. The active nitrolyzing agent is nitracidium ion, $NO(OH)_2^+$, formed according to the reaction,

$$2HNO_3 \rightleftharpoons NO(OH)_2^+ + NO_3^- \quad \ldots\ldots\ldots\ldots (2)$$

2. Acetic acid decreases the concentration of nitracidium ion by forming a complex with nitric acid:

$$CH_3COOH + HNO_3 \rightleftharpoons CH_3COOH.HNO_3 \quad \ldots\ldots (4)$$

3. This complex tends to dissociate as the temperature is raised.

Evidence for the first two assumptions has already been presented. Evidence for the last may be obtained from a more detailed examination of the kinetic data.

An attempt has been made to calculate the reaction order and the activation energy from the data obtained in the presence of acetic acid. The results are given in Table X. The initial rates, $\left(\frac{dx}{dt}\right)_{t=0}$ were determined from the slopes of the tangents to the rate curves at zero time. The half-time and three-quarter-time values, $t_{\frac{1}{2}}$ and $t_{\frac{3}{4}}$, were read off from the rate curves, Figs. 1-6. The activation energies, E, were calculated from the usual formula,

$$E = \frac{2.3\ R \log \frac{k_2}{k_1}}{\frac{1}{T_1} - \frac{1}{T_2}},$$

with rate constants replaced by the initial rates.

The relative values of $t_{\frac{1}{2}}$ and $t_{\frac{3}{4}}$ indicate that no simple order can be assigned to the reaction. In an attempt to determine the rate constant and reaction order, the rate expression was written

$$k = \left(\frac{dx}{dt}\right) \frac{1}{a.b^n}$$

where $\left(\frac{dx}{dt}\right)$ is the initial rate in moles per litre per sec.,

TABLE X

Initial Rates and Activation Energies in Acetic Acid.

AcOH:Hexamine	HNO_3:Hexamine	Initial Rate		$t_{\frac{1}{2}}$		$t_{\frac{3}{4}}$		E
Molar Ratio	Molar Ratio	%/min.		Minutes		Minutes		Kcal.
		1°C	30°C	1°C	30°C	1°C	30°C	
4.3	48.5	-	-	4	1	10	1½	-
	40	-	-	5	-	13	-	-
	32	7.5	23	7	1	25	2	6.2
	26	3.2	21	20	4	41	10	10
	20	0.4	10	90	7	-	26	18
6.4	48.5	-	-	7	2	20	3	-
	40	6	-	13	-	30	-	-
	32	2.0	40	22	3	40	7	16
	26	0.9	18	103	8	-	27	16
	20	0.25	2.9	-	33	-	141	13
10.5	48.5	8.7	-	10	2	32	4½	-
	40	1.8	12	23	3	71	7	10
	32	0.5	8	130	7	-	48	15
	26	0.1₂	3.0	-	17	-	53	18

a is the molar concentration of hexamine,

b is the molar concentration of nitric acid,

n is the reaction order with respect to nitric acid, to be determined from the fact that the k values must be the same for all reaction mixtures at a given temperature.

From the data of experiments 4 and 5 (Table I):

$$\frac{k_{26}}{k_{20}} = \frac{3.2}{0.4}\left(\frac{8.4}{0.147} \times \frac{0.113}{6.9}\right)^n$$

where the subscripts refer to the nitric acid:hexamine ratio. But $k_{26} = k_{20}$, and hence n can be calculated. Proceeding in this way values of the index, n, ranging from 1.5 to 34 are found by comparing different pairs of rate constants. It is evident, then, that no significant reaction order can be calculated by assuming that the rate of reaction depends directly on some power of the nitric acid concentration. Indeed this result is to be expected, since in the absence of solvent the rate of reaction increases considerably as the nitric acid:hexamine ratio is increased for a given acid strength (5).

If it is now assumed that the nitrolysis of hexamine follows a second order law, the relative concentrations of the nitrolyzing agent in various reaction mixtures may be

calculated from the expression

$$k = \left(\frac{dx}{dt}\right)\frac{1}{a.c}$$

where a is the molar concentration of hexamine, and

c is the molar concentration of the nitrolyzing agent, assumed to be nitracidium ion.

Taking the value of c as unity in the reaction mixture where hexamine:acetic acid is 1:10.5 and nitric acid:hexamine is 26:1, the relative values of c at 1°C and at 30°C for other hexamine:acetic acid and nitric acid:hexamine ratios are those shown in Table XI.

At best, the figures in the last two columns are only a rough approximation to the corresponding nitracidium ion concentrations, but the general trends are obvious. The nitracidium ion concentration increases rapidly as the amount of nitric acid is increased for a given hexamine: acetic acid ratio. Dilution of the nitric acid by water formed in the first stages of the nitrolysis, before any RDX is produced, is greatest when the amount of nitric acid is least; and since dilution with water reduces the nitracidium ion concentration very markedly (5), the relative concentration of nitracidium ion increases sharply with increase in the nitric acid:hexamine ratio.

Table XI also shows clearly that for a given

TABLE XI

Relative Nitracidium Ion Concentrations in Acetic Acid.

Molar Ratio			c	
AcOH:Hexamine	HNO_3:Hexamine	HNO_3:AcOH	1°C.	30°C.
4.3	40	9.3	95	-
	32	7.4	62	-
	26	6.0	28	7.0
	20	4.6	3.3	3.3
6.4	40	6.3	50	-
	32	5.0	17	13.3
	26	4.1	7.5	6.0
	20	3.1	2.1	1.0
10.5	48.5	4.6	72	-
	40	3.8	15	4.1
	32	3.0	4.2	2.7
	26	2.5	1.0	1.0

nitric acid:hexamine ratio, the nitracidium ion concentration decreases rapidly as the amount of acetic acid is increased. Thus, when the nitric acid:hexamine ratio is 32:1, the relative concentration falls from 62 to 4.2 as the nitric acid:acetic acid ratio falls from 7.4 to 3.0. This result is further evidence for the formation of a compound between nitric and acetic acids.

The effect of increased temperature on the values of c is noteworthy. At 30°C, c is much more constant than it is at 1°C. This behaviour might be expected if at 30°C the major factor influencing the nitracidium ion concentration is not the nitric acid:acetic acid ratio (as it is at 1°C), but dilution of the nitric acid by water formed in the reaction. This leads to the conclusion that the acetic acid-nitric acid complex is more highly dissociated at 30°C than at 1°C.

The activation energies listed in Table XI are apparent values only. They were calculated by assuming that the k values could be replaced legitimately by the initial rates. Actually this substitution is valid only when the concentrations of the reactants do not change with temperature. But Table XI shows clearly that the nitracidium ion concentration is not constant with temperature.

In this case, $\frac{k_2}{k_1} \neq \frac{\left(\frac{dx}{dt}\right)_2}{\left(\frac{dx}{dt}\right)_1}$,

but $\frac{k_2}{k_1} = \frac{\left(\frac{dx}{dt}\right)_2}{\left(\frac{dx}{dt}\right)_1} \frac{a_1}{a_2} \frac{c_1}{c_2}$

where a is the molar concentration of hexamine,

c is the molar concentration of nitracidium ion,

and the subscripts refer to different temperatures.

The concentration of hexamine is essentially independent of temperature, and therefore,

$$\frac{\left(\frac{dx}{dt}\right)_2}{\left(\frac{dx}{dt}\right)_1} = \frac{k_2}{k_1} \frac{c_2}{c_1}$$

The relative magnitudes of c_1 and c_2 (and, hence, the discrepancy between the apparent and true activation energies of the nitrolysis) will be determined by the effect of temperature on

1. The nitric acid-nitracidium ion equilibrium.
2. The dissociation of the acetic acid-nitric acid complex.
3. The interaction of these two effects on one another.

The activation energies calculated may be erratic because each of these factors influences the ratio c_2/c_1, in a different way for each of the nitric acid:hexamine and nitric acid:acetic acid ratios.

Effect of Chloroform on the Nitrolysis

A comparison of Figs. 18 and 22 shows that at a molar ratio of nitric acid:solvent of 2:1, all of the chloroform solutions give the maximum yield of RDX (or have passed their peak) at both temperatures investigated, whereas the yields in the presence of acetic acid (by extrapolation) are less than 40% at 30°C and less than 20% at 1°C. Hence, the effect of chloroform seems to be entirely different from that of acetic acid. Since Wright (22) found that 98% of the chloroform was recoverable by distillation, it is logical to assume that it is an inert diluent. Fig. 20 shows, moreover, that at small molar ratios of nitric acid: hexamine, there is a linear increase in the final yield of RDX with increasing nitric acid:chloroform ratio. The action of chloroform may be to decrease the rate of nitrolysis by decreasing the nitracidium ion concentration in two ways:

1. By increasing the volume of the reaction mixture;
2. The solvent may remove some of the nitric acid from the reaction (hexamine dinitrate being insoluble in chloroform), since nitric acid and chloroform are not completely miscible.

Owing to the heterogeneity of the system, detailed analysis of the data has not been attempted.

BIBLIOGRAPHY

1. Henning G. F.; German Patent 104,280 (June 14, 1899).
   von Herz E.; German Patent 298,539, 299,028 (1919), British Patent 145,791 (1920), Swiss Patent 88,759 (1921), U.S.A. Patent 1,402,693 (1922).
2. Linstead R.P.; The Chemistry of RDX, p. 4, Oct. 1, 1941.
3. Hale G.C.; J. A. C. S., 47, 2754, (1925).
4. Research Department, Woolwich; RDX 5, Isothermal Nitration of Hexamine.
5. Vroom A.H. and Winkler C.A.; C. E. Project XR-6, Feb. 20, 1943.
6. Wright G.F.; Toronto Progress Report, C.E. 12, Sept. 15-30, 1943.
7. Springall H.D. and Woodbury N.H.; A.C. 5725/HE.I. 267/RDX 99, Jan. 25, 1944.
8. Bennett and Williams; A.C. 2379/ORG/EX. 150.
9. Lauer and Oda; J. Prakt. Chem., 144, 176, (1936).
10. Usanovich et al.; J. Gen. Chem. (U.S.S.R.), 10, 223, (1940).
11. Hantzsch A.; Ber., 58, 941, (1925).
12. Chédin; Ann. Chim., 8, 243, (1937).
13. Hetherington and Masson; J. Chem. Soc., 105, (1933).
14. Bennett, Brand and Williams; A.C. 7259/HE.I. 396/TNT. 233.
15. Bennett et al.; A.C. 7258/HE.I. 395/TNT. 232.
16. Robinson; J. Chem. Soc., 238, (1941).
17. Cohen and Wibaut; Rec. Trav. Chim., 54, 409, (1935).

18. Benford and Ingold; J. Chem. Soc., 929, (1938).

19. Briner, Susz and Favarger; Helv. Chim. Acta, 18, 375, (1935).

20. Wright G.F.; Toronto Progress Report, C.E. 12, Jan. 15-Feb. 1, 1941.

SECTION II

THE DETONATION VELOCITY OF AXIALLY CAVITATED CYLINDERS OF CAST DINA

ACKNOWLEDGMENT

The author gratefully acknowledges the kind cooperation of Dr. J. S. Tapp, who designed and built the firing box and assembled the equipment of the front plate for the drum camera. Acknowledgments are also due to Mr. M. C. Fletcher, whose cooperation throughout the investigation was greatly appreciated, and to Mr. G. Papineau-Couture, in collaboration with whom the studies described in this section were made.

INTRODUCTION

An explosive has been defined (1) as a pure substance or a mixture of substances which is capable of producing an explosion by means of its own intrinsic energy. The concept of an explosion is so familiar as to require no definition. It involves almost invariably a sudden expansion of gas, a sharp noise and a great disturbance of material in the neighbourhood. Explosives require various stimuli to set them off, depending on the class to which they belong. Primary explosives, or initiators, such as lead azide or mercury fulminate are easily detonated by a light blow, while high explosives usually may be detonated only by the shock of a detonating initiator in contact with them.

Several methods of estimating the destructive power of an explosive have been devised. The Trauzl block test measures the increase in volume caused by the detonation of a 10-gm. sample of explosive placed in a cylindrical well in a lead block 8" in diameter and 8" high. The ballistic mortar compares the power of different explosives by measuring the recoil of a 600-lb. pendulum brought about by the explosion of a 10-gm. charge. Both methods suffer from the disadvantages that the loading density of the solid explosive under test is difficult to control, and that the time factor is

neglected entirely.

The distinguishing feature of a detonation is the rapid rise in pressure and temperature, and their maximum values will determine, in part, the ability of an explosive to cause destruction. The detonation velocity, being the rate at which the chemical reaction proceeds through a decomposing stick, affects the pressure and temperature behind the reaction zone, and, in fact, has been used to calculate the magnitude of these quantities for many explosives (2, 3, 4). Various means of measuring the detonation velocity have been used. The earliest workers, Berthelot and Vieille (5), strung two wires through opposite ends of the explosive stick, and connected them to a Boulengé chronograph. Since this instrument can detect time intervals no smaller than 1/10,000th of a second, the train of explosive had to be approximately thirty-five meters long to lend some accuracy to the measurements. The Mettegang recorder (6) is able to differentiate events that occur one microsecond apart. A spark is set up between platinum points and the surface of a smoked steel drum, as wires at two points in the detonating explosive a known distance apart are broken. The writing speed may be as great as 100 meters per second, so that a short stick of explosive suffices for the determination.

Dautriche (7) developed a method for comparing the

detonation velocity of a new explosive with that of Cordeau Bickford, a detonating fuse with accurately known uniform detonation velocity. The method is based on the enhanced effect on a lead plate where two detonation waves meet. The arrangement for the test is illustrated in Fig. 23.

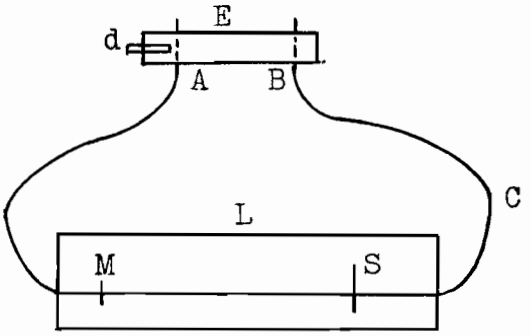

Figure 23

The ends of a long column of Cordeau, C, are threaded through the ends, A and B, of a stick of the explosive, E, under test, the middle portion of the Cordeau being firmly fixed to a lead plate, L. As the detonation, initiated at d, travels through the explosive, the Cordeau is initiated at both ends but at different times. The detonation wave in the Cordeau starting from A will, therefore, travel further than that from B before the two waves meet at S, where there is a marked indentation in the lead. If M is the mid-point of the Cordeau, the detonation from A travels a distance 2MS greater than that from B, and in this time the detonation in the explosive has proceeded a distance AB. The unknown detonation velocity, D, of the explosive is given in terms of that of

Cordeau, U, by

$$D = U \times \frac{AB}{2MS}$$

Other recently developed techniques (8, 9, 10) depend upon breaking electrical circuits as the detonation wave passes two points in the explosive column a known distance apart. One distinct disadvantage to all these methods, however, is that they all measure only the average rate at which the explosive is decomposing with no possibility of ascertaining if the detonation velocity is constant in the region over which the determination is made. Since this constancy is dependent upon several factors, such as the confinement, the strength of the initiation and the physical state of the explosive, it is important that changes in the velocity be detectable. The photographic method makes this possible. In principle, it consists of photographing on a rapidly moving film the progress of the luminosity in a detonation. In the picture obtained, fluctuations from constancy are recorded as deviations from the straight line trace characteristic of the steady state. The method of photographic recording was first used for gaseous explosives (11, 12), but was later (13) extended to solid explosives. The sharpness of the image was greatly improved by interposition of a narrow slit between the lens of the camera and the explosive charge (14). The greatest advance in the

photographic technique has occurred recently, however, with the installation of a modern, high-speed rotating drum camera at Bruceton, Pa. (15).

Theoretical discussion of detonation velocity dates from Chapman (16) and Jouguet (17). Their treatment has recently been developed and enlarged by various investigators, notably by Kistiakowsky and Wilson (18). The theory is essentially hydrodynamic and thermodynamic, and permits calculation of the detonation velocity, and the pressure and temperature in the narrow reaction zone, from a knowledge of the equation of state and of the heat capacities of the gaseous products of detonation (2, 3, 4). The results of the theory are obtained by consideration of the steady state conditions on both sides of the detonation wave without regard for the chemical process involved in the change from solid explosive to gaseous products. This treatment implies that the detonation front is an absolute discontinuity, but it has been shown (19) that the reaction zone length is of the order of 5 mm. It has been observed, moreover, that the Chapman-Jouguet theory might be expected to be successful for those solid explosives in which the reaction zone length is small compared with the charge diameter (20).

A theory for the explosion of a long cylindrical bomb detonated at one end has been developed independent of

the Chapman-Jouguet condition (21, 22). Taylor's analysis (21) for the explosion of a solid or liquid charge in a long cylindrical case several times heavier than itself gives the shape of the case at any time after the detonation has passed, while Jones (22) relates the observed detonation velocity to several factors by the equation:

$$\frac{U_\infty - U}{U_\infty} = \frac{fU^2\tau^2\Delta}{4R_o\sigma} \quad \ldots\ldots\ldots\ldots\ldots (1).$$

where U_∞ is the detonation velocity under infinite confinement,

U is the observed detonation velocity,

f is a factor which can be expressed in terms of the ratio of the exploded to unexploded densities,

τ is the reaction time,

Δ is the loading density,

σ is the mass per unit area of the encasing tube,

R_o is the charge radius.

A perfectly general relation between detonation velocity and density has been derived (20):

$$\left(\frac{U_o}{U}\right)^2 = 1 + c(r_1^4 - 1) \quad \ldots\ldots\ldots\ldots\ldots\ldots (2).$$

where $$c \doteq \frac{1}{(\mu - 1)^2}\left(1 - \frac{\Delta}{\rho_o}\right)$$

where μ is the compression ratio,

Δ is the loading density,

ρ_o is the density of the gaseous products,

r_1 is the stream tube in units of its initial radius.

Wilkinson (23) applied this general relation to lightly cased charges. Plotting $\frac{U}{U_o}$ vs. $\frac{\sigma}{R\Delta}$ shows that the detonation velocity varies only slowly with case thickness, but variation with charge diameter is much more marked. Results of Copp and Ubbelohde (24) indicate a more abrupt initial rise than theory predicts, which may be due to the reaction time itself being greater for unconfined charges.

Eyring (19) observed that many different methods of estimating the length of the reaction zone, a_1, all agree within one or two orders of magnitude. These methods, mostly indirect, depend on vastly different experimental data, and any agreement among them is, therefore, highly satisfactory. They include:

1. Direct observation. A picture is taken with the film moving parallel to the direction of propagation of the detonation. The width of the trace is a direct measure of the reaction time, τ_1. For liquid nitroglycerine, this turns out to be 0.5 microseconds, and is larger for the slower

explosives. This sets an upper limit to the reaction time as the gaseous products may themselves be luminous.

2. Extrapolation of low temperature data of the decomposition of various explosives to the temperature in the detonation wave, (3000-5000°C) by assuming that

   Rate of decomposition = $Ze^{-\Delta H/RT}$.

   Although this is admittedly a bold extrapolation, values of τ_1 obtained are of the right order of magnitude.

3. Rate of build-up of the stable detonation velocity. This phenomenon has been subjected to analysis assuming that deviation from the steady state hydrodynamic equations is small.

These and several other independent methods give a reaction time for TNT of approximately one microsecond. Because of this short reaction time, Eyring is led to the conclusion that the decomposition occurs in the detonation wave as a surface reation, since

1. If the reaction begins on the surface, thermal conduction is inadequate to heat the interior of a grain in one microsecond; and the reaction will, therefore, continue on the surface, and

2. The work done by a shock front is calculated to be insufficient to raise all of the explosive to the temperature at which reaction would be complete in a microsecond. The energy is, therefore, non-uniformly distributed, being concentrated near contact points of grains.

Eyring shows that for a grain of 100 microns radius, it would take at least one millisecond to heat its interior to the temperature at which it could detonate. If the reaction towards the middle of the grain proceeds 1/m as fast as it is propagated along the stick, the reaction will be over when the detonation wave has moved forward m times the grain radius. When reactions require no activation energy they move forward with the velocity of sound; this is also approximately the detonation velocity. Thus, m would be about unity. But for known explosives the decomposition does require an activation energy, and the reaction will go more slowly by the factor

$$m = e^{\Delta F^*/RT}, \text{ or,}$$

$$\text{Rate of decomposition} = \text{Grain radius} \times e^{\Delta F^*/RT}.$$

Assuming that ΔS^* is zero, $\Delta F^*_{TNT} = \Delta H^*_{TNT} = 25$ kcal., and at 3000°K, m = 66. For grains of 50 microns radius this makes the reaction zone length, $a_1 = 0.33$ cm., and the reaction time, $\tau_1 = 0.7$ sec. These values agree extremely well with those found from hydrodynamic theory. The essential

point of the Eyring theory, then, is that the chemical reaction starts at isolated points. At low detonation velocities (corresponding to shock waves of small amplitude) it is to be expected that the reaction would be initiated only at gross inhomogeneities, such as contact points between grains. Then at higher detonation velocities, additional points of initiation could occur at inhomogeneities within the grain. Since the detonation temperature falls only slightly with decreasing detonation velocity, it may well be that the major cause of the lengthening of the reaction zone with falling detonation velocity is the reduction in the number of points of initiation (25).

The theory may be easily extended to initiation in liquid explosives, in which case it is assumed that the initiation occurs at the surface of gas bubbles within the liquid (25). It is proposed that the detonation wave heats each bubble by compression to a high enough temperature to start the decomposition, the temperature subsequently being maintained by the heat of decomposition.

The detonation wave, the region in which the chemical reaction accompanying the explosion occurs, gives rise to a shock wave, the front of which is of molecular dimensions (19). It is in this very narrow region that the temperature and pressure rise to approximately their values

in the reaction zone. Pictures obtained with charges surrounded by a spaced wrapper, indicate (27) that the luminosity of the explosion of a confined charge is mainly due to the shock wave impinging on the confining wrapper.

The velocity of the product gases has been measured by firing various explosives in evacuated glass tubes (28). It was found that the gas velocity for a number of explosives was approximately 1.75 times the detonation velocity.

The velocities of the shock wave and of the luminous gases have been found to be identical in the vicinity of a column of detonating tetryl (29), and greater than the detonation velocity in the explosive. The velocity of the gas beyond the charge decreased more rapidly than that of the shock wave, the two waves separating at a distance from the charge that increased with increasing packing density of the explosive.

There are, therefore, at least three different luminous effects to be distinguished in a photograph of a detonating stick of explosive: the faintly luminous trace of the detonation wave, the intensely luminous shock wave, and the bright self-luminous gaseous products of the detonation. It is not always an easy matter to distinguish these three effects, but it has been possible to obtain (30) a record in

one rotating drum picture of both the shock wave front and that of the product gases by using an Argon flash and firing the charge in profile, i.e., by having the detonation wave travel parallel to the moving ilm instead of perpendicular to it.

Recently attempts have been made in various ways to increase the detonation velocity of an explosive, and hence, its destructiveness. Investigation of the behaviour of two explosives of widely differing detonation velocities (CE/TNT 40/60 and Rounkol; 7125 and 2000 m./sec. respectively) in contact with each other either end-to-end or concentrically (31) indicates the existence of interesting phenomena in composite charges. When two cylindrical charges are placed end-to-end axially and fired from the CE/TNT end the detonation velocity in the Rounkol falls only gradually (over 4 in.) to its normal low value. But when initiated at the Rounkol, the velocity rises much more rapidly once the detonation reaches the CE/TNT. A series of cartridges of Rounkol and of RDX/TNT (60/40) (rate of detonation: 7790 m./sec.) was arranged alternately end-to-end. Each section detonated, almost as soon as the wave in the preceding section reached the contact surface. The slight delay in pick-up in the faster explosive when initiated by the slower and the enhanced initial speed of the latter when initiated by the former were equivalent, since the time of detonation of the

whole composite charge was approximately that calculated by assuming that each detonated at its normal rate. With concentric charges, those in which the inner axial core has the higher detonation velocity are the most interesting. These give rise to an almost conical wave in which the centre is well in advance of the periphery. The detonation in the Rounkol apparently travels along the side of the cartridge at the same speed as the detonation velocity in the inner core. This, of course, does not represent the true detonation velocity of Rounkol, but its normal velocity has been augmented by the detonation in its core of the faster explosive.

Cybulski and Woodhead (32) studied photographically the effect of an axial cavity on the detonation of a cylindrical charge. They found that the detonation wave travelled down such a charge at a greater rate than that at which it moves along a solid charge. The detonation velocity of charges of CE/TNT (40/60) with axial cavities increased with decreasing diameter of cavity. The same effect was observed in pure TNT, but with a 0.1" cavity the rate of detonation was below the maximum, although still above that for a solid charge. The charges of CE/TNT (40/60) and of pure TNT were translucent enough to give a record of the luminosity in the cavity, which may be due to

1. Confinement of the hot gases projected through the cavity, or

2. A Munroe effect.

If the top of the cavity was filled with plasticine, it was found that the detonation velocity was the same as that of a solid stick of explosive. This presumably eliminated the first possibility, and it was necessary to accept the second. The increase in detonation velocity, owing to the cavity, could not be due to a continuous inner initiation because

1. When the speed of the internal luminosity decreased, the detonation velocity was maintained.
2. Substitution of one of the holed pellets by a solid pellet sometimes caused the detonation to die out, instead of the explosion being re-initiated.
3. It was shown that the detonation is propagated via the solid portion of the charge by inserting a cardboard washer between adjacent annular pellets, thus forming a barrier to the detonation wave but not to the luminous effect in the cavity.

Continuing the investigation on pressed CE, the same workers found (33) that if the cartridge were closed at the far end with a solid pellet of CE, the arrival of the disturbance in the cavity at this end would result in detonation. Two new waves were initiated at the end of the cavity, and travelled in opposite directions through the remainder of the charge. A Dautriche effect occurred at the point where the wave which travelled backward through the charge collided

with the original detonation wave moving down. The overall decomposition time of a cartridge of CE could, therefore, be considerably decreased by means of a succession of cavities. The actual magnitude of the reduction depends on the arrangement and relative lengths of the holed (h) and solid (s) pellets, as shown in Table XII, reproduced from the report (33) of Cybulski and Woodhead.

TABLE XII

Decrease in Decomposition Time in Cavitated Charges.

Density of pressed CE = 1.45 gm./cc.
Diameter of charge = 7/8".
Diameter of cavity = 1/4".

Initiation	Length of Construction Unit	No. of Units in Charge	Length of Solid End Pellet	% Reduction in Decomposition Time
Terminal	1"s 2"h	10	1"	20.0
"	1"s 3"h	7	2"	23.6
"	1"s 5"h	5	1"	29.3
"	½"s 8"h	2	1¼"	31.6
"	½"s 12"h	2	1½"	31.2
Central	18¼"s	2	-	50.0
"	½"s 8"h	2	2 x 1¼"	65.2

The central initiation obviously would cause the total decomposition of the explosive in a much smaller time than terminal initiation, but the 30% decrease in the decomposition time caused by the holed pellets is noteworthy.

In view of the impetus the war has given explosives research in general, and because of the absence in Canada of specialized equipment necessary for a thorough study of the properties of explosives, the author and Mr. G. Papineau-Couture, in collaboration with whom the investigation here described was made, were requested to supervise the installation of the required apparatus at the Explosives Laboratory of the National Research Council, Ottawa. Considerable time was involved in modification of the rotating drum camera and perfection of the manipulative details. After development of the technique, the investigation of cavitated DINA charges was begun in an attempt to elucidate the effect on detonation velocity of an axial cavity in a cylindrical stick of explosive.

EXPERIMENTAL

Equipment and Operation

The equipment consisted essentially of a high speed rotating drum camera and of an ordinary long focal length still camera housed in a thunder-hut of two chambers, in one of which, the camera house, were the recording instruments and accessories, while the explosive charge was fired in the adjoining bomb-proof.

The bomb-proof was 8 feet high, 10 feet wide, and 20 feet long, with 2 feet thick concrete walls, reinforced by 1-inch diameter iron rods at 8-inch centers. This construction permitted the safe firing of a high explosive charge as large as fifteen pounds. The inner walls and ceiling of the bomb-proof were lined with fireproofed wood baffles which deadened the sound of the explosion. A penthouse on the roof contained a $\frac{3}{4}$-h.p. motor which operated a fan to clear the bomb-proof of fumes after an explosion. The motor and fan were protected by a 5/8" steel damper that was raised and lowered by a winch in the camera house. Since the drum camera was loaded from the bomb-proof, access to it was through four right-angle turns which effectively eliminated all daylight.

A terminal block on the outside wall of the bomb-proof permitted electrical connections to the blasting cap, used to initiate the detonation, to be made in an open circuit, and only after all other operations had been made was the connection completed to the firing point, a hundred feet away.

The wall between the camera house and the bomb-proof contained a 31" square aperture, flanked on both sides by smaller 8" square holes that expanded to 15" x 10" on the camera house side. The rotating drum camera rested on a pier which was the extension into the camera house of the bottom or central opening. One of the side holes housed the still camera used in the present investigation; the other was designed to accommodate either a spectograph or a rotating mirror camera (34). The openings were so arranged that all the recording instruments could be focussed on a charge 6 to 18 feet away.

The equipment in the camera house was protected from the explosion by a 1-inch steel plate bolted through the wall. A hinged door in the middle of the plate allowed easy access to the drum camera. The explosion-proof glass windows in front of the cameras consisted of three different types of one-quarter inch thick glass plates held together by a vinylite resin.

The high speed camera, built by Northern Tool and Gauge, Ottawa, from blueprints supplied by Picatinny Arsenal, was essentially the same as that described by Messerly (15). It consisted of an aluminum drum (Plate I) which carried the film, and was rotated at high speed by a 2-h.p. 1800 r.p.m. induction motor through a two step 8:1 speed increaser. The motor and speed increaser were mounted on a base plate fastened to the camera housing, which was a 45" long steel pipe, 22" in diameter and 5/16" thick, flanged at both ends to support the front and back plates which enclosed the moving parts. Electrical connections to the camera were made at a terminal box on the back plate, through which was screwed a short length of 1/4" pipe, connected to a vacuum pump, shown in Plate II.

The front plate of the camera was provided with a small hand hole through which the film was loaded into the drum, a small viewing window fitted with a screwcap through which the drum surface could be seen for focussing when the camera was otherwise closed, and a lens - prism arrangement. Light from the detonating explosive charge entered the camera through a super-Cinephor lens, was totally reflected downward through a 45° prism, and passed through a narrow slit to the film carried on the inside surface of the drum. The lens was held in a snugly fitting brass sleeve, so that its distance

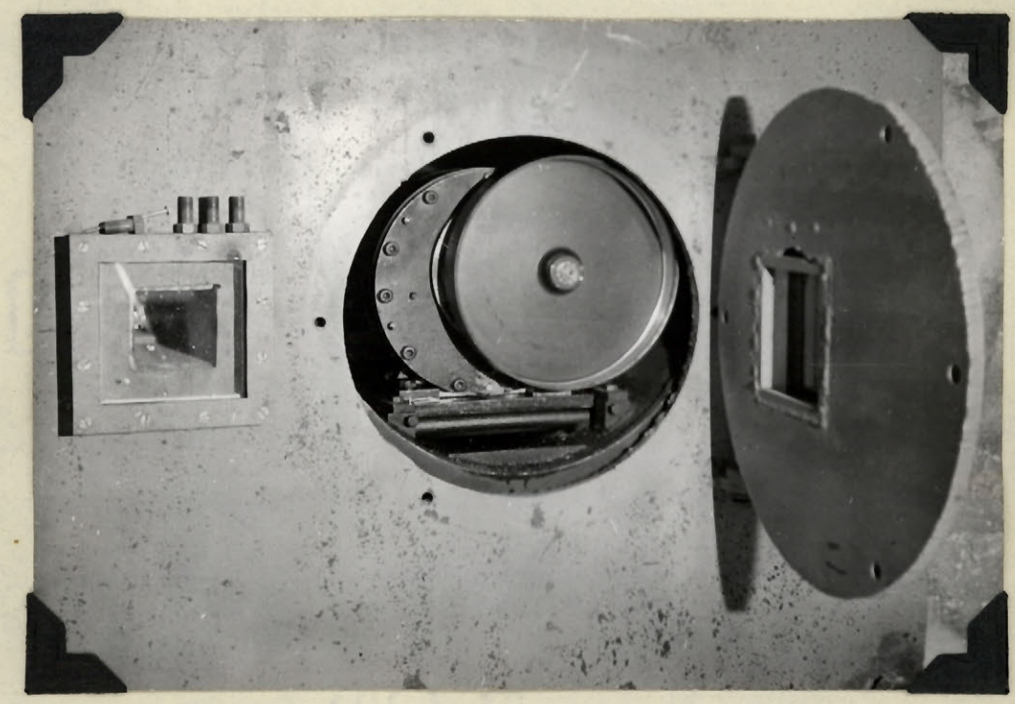

PLATE I

High Speed Camera Showing Aluminum Drum
Hinged Door and Window for Still Camera.

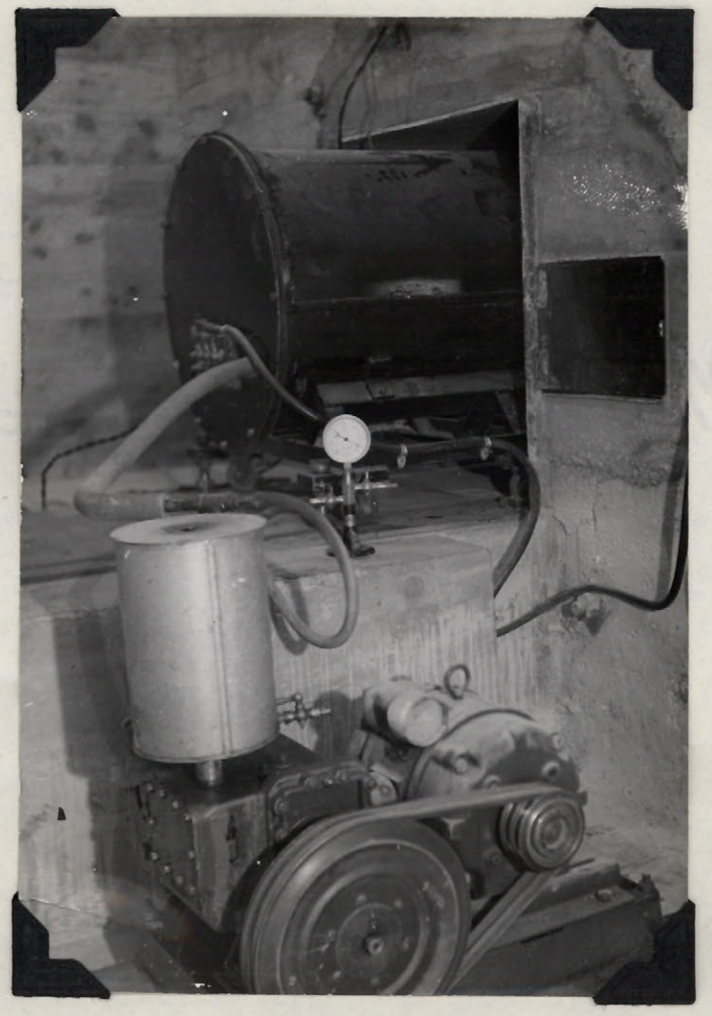

PLATE II

Back of Drum Camera showing Vacuum Pump and Aperture for Still Camera.

from the film could be varied to focus the camera. Between the lens and the prism there was a 1/4" glass plate, which was held on the front plate by the same frame to which was attached a thin sheet brass holder for the prism. The inside of the front plate indicating the position of the slit and prism, is shown in Plate III, while Plate IV shows the appearance of the front of the drum camera with the front plate in place.

The slit, 0.003" wide, consisting of two razor blades held in a brass frame, was interposed between the prism and the film. Its purpose was to exclude all light but that which came from a very narrow section of the charge. The clearance between the slit and the drum was normally about 1/4", so that the film could readily be put into position without interference from the slit. After the drum had reached speed, however, the slit was brought down to within 1/64" of the film by a magnetically-operated arm, shown in Plate IV, controlled from the firing point. Centrifugal force at this speed held the film tightly against the drum, and there was no danger of its catching on the blades of the slit.

Since the purpose of the high speed camera was to differentiate between events which occurred within a very short time of each other, it was essential to operate the drum at the maximum possible speed, which could be accomplished

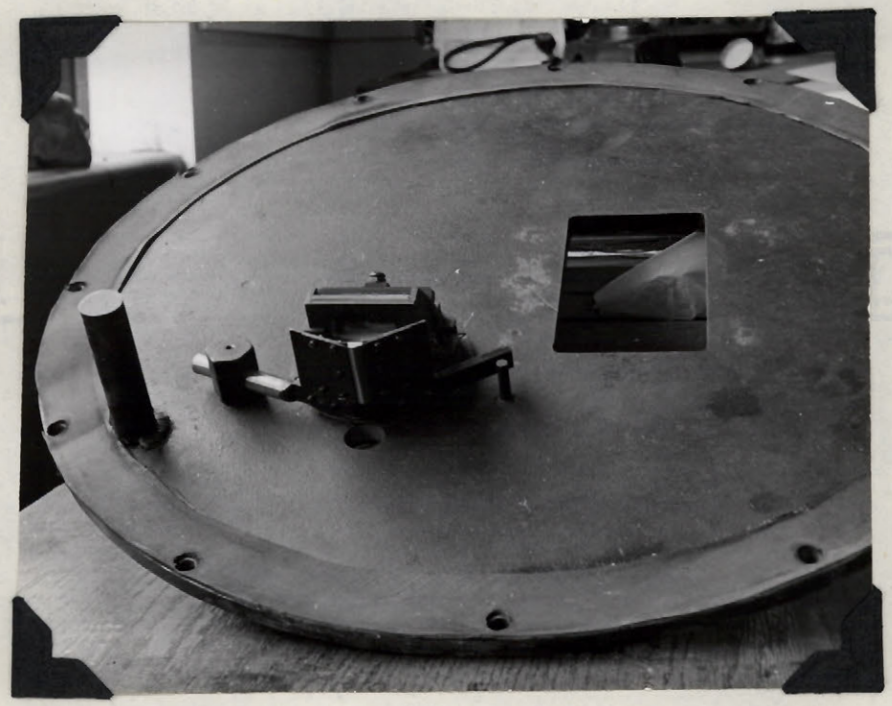

PLATE III

Inside of Front Plate showing

Hand Hole Slit and Prism.

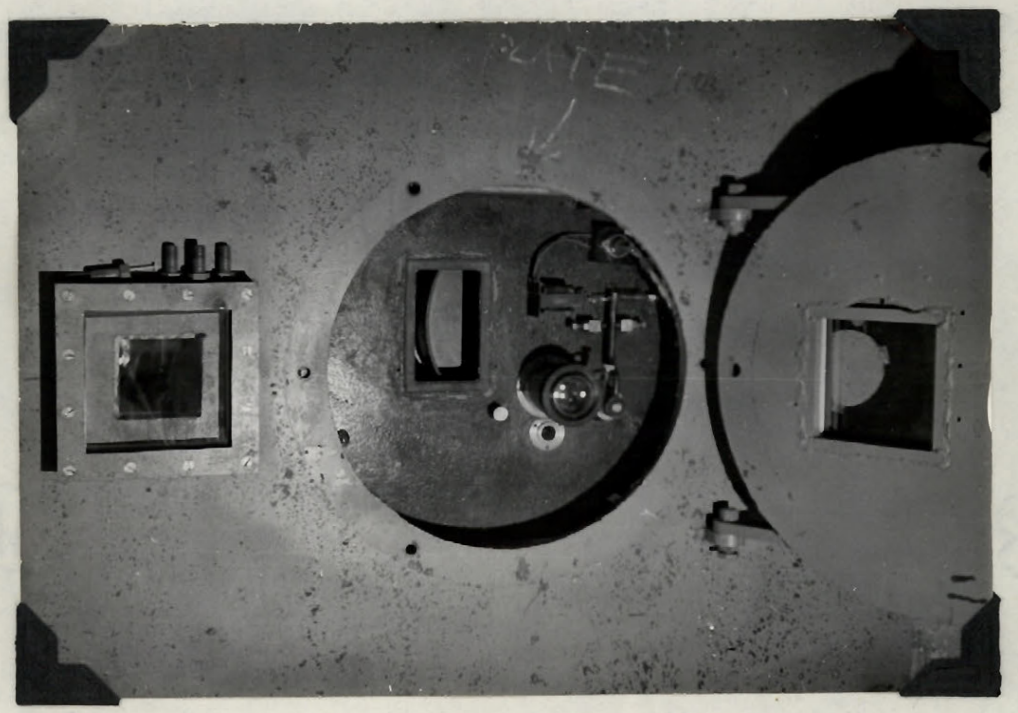

PLATE IV

Drum Camera with Front Plate in Place showing Rim of Aluminum Drum through Hand Hole.

only by running the entire camera under reduced pressure. Accordingly, all the camera doors were heavily gasketed with rubber to ensure a vacuum-tight fit. The vacuum pump, connected to the back plate of the camera as shown in Plate II, was operated by a 1-h.p. motor and reduced the pressure in the camera to 3 to 5 cm. of mercury in about 5 minutes, at which pressure the maximum speed of the drum was obtained, and there was no danger of overheating the motor.

The speed of the drum was measured with a split commutator on the slow (motor) shaft, connected to a Frahm vibrating reed frequency meter at the firing point 100 feet from the thunder-hut. The meter was activated by a source of 12 volts D.C. and had a range of 53 to 67 cycles per second. Since the commutator gave two impulses per revolution of the motor shaft, the speed of the drum was four times the frequency meter reading.

Controls for the high speed camera motor and the detonation of the charge were also at the firing point. To fire a charge, three keys had to be inserted into a firing box, specially designed and built for maximum safety by Dr. J. S. Tapp of the National Research Council. The electromagnet which operated the slit of the drum camera was activated by pressing a push button in the box, while another push button, in series with the limit switches on all the

doors of the equipment in the thunder-hut, completed a circuit if the doors were closed, and released the firing pin.

It was realized early that considerable time could be saved in firing a series of shots if both of the collaborators involved in the present investigation worked together, and a procedure was followed throughout which was least time-consuming consistent with maximum safety. Each investigator carried at all times at least one of the three keys required to fire the charge. While one operator loaded the rate camera, the other made the final attachment of the booster to the series of charges to be fired, and started the vacuum pump when the camera was loaded, and the hand hole cover had been replaced and sealed tightly with plasticine. The drum camera lens was then covered to permit further operations in the bomb-proof in the light. The charge was hung by a string from an eye-screw in the ceiling, the position of this screw having been previously determined to make the image of the charge fall on the slit of the drum camera. The detonator was then connected to the leads from the terminal block outside the bomb-proof and inserted into the charge which was finally adjusted to hang in the desired orientation. As one of the investigators left the bomb-proof to re-enter the camera house, the light in the bomb-proof was extinguished,

the drum camera lens cover removed and the protecting hinged steel door bolted into place. In the meantime, the damper protecting the fan was raised, and the still camera loaded with Kodak Contrast Process Ortho cut film and its shutter opened in the camera house. After both investigators had left the thunder-hut, the firing leads were connected on the outside, and both proceeded to the firing point. There the three keys required to fire the shot were inserted into the firing box, and the drum camera motor switch was closed, its speed being watched on the frequency meter. When a reading of 58.5 was reached, the slit was lowered, and if all the protecting doors were closed, the firing pin was pressed to detonate the charge. Immediately after the shot was fired, the slit was allowed to resume its normal position, and the motor switch was opened. The damper was then lowered, the fan started, and the still camera closed. After the leads were disconnected at the terminal block, and the bomb-proof had been cleared of fumes, the cover was replaced on the drum camera lens and another charge could then be hung in position.

Several rate pictures taken on the same strip of film were distinguished from each other by placing friction tapes at different positions along the various charges.

With a charge hanging vertically and initiated at the top, the luminosity moves down the stick as the film

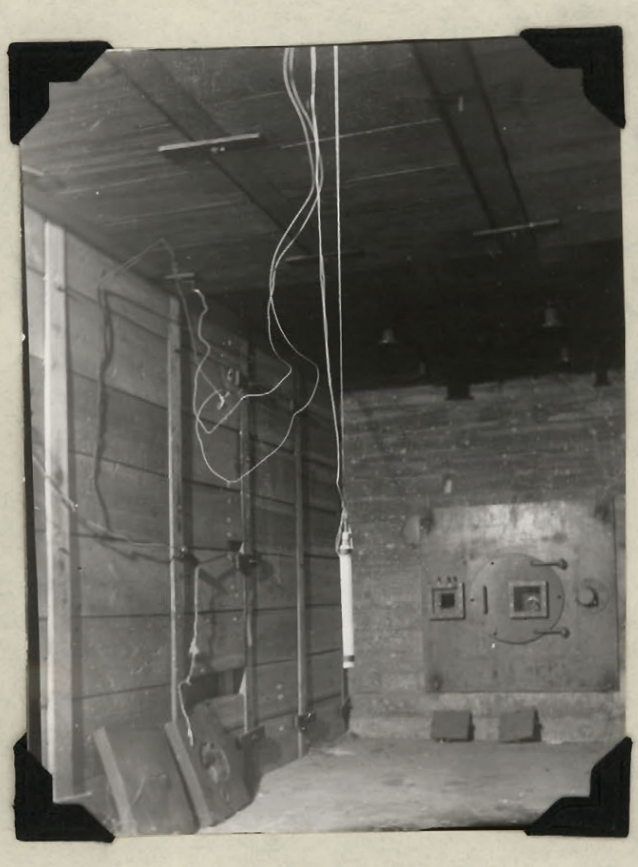

PLATE V

Bomb-Proof Showing Charge

Ready to be Fired.

moves across the slit. The photograph obtained was, therefore, a line slanted across the film. In the region where the rate of detonation is constant, this line was perfectly straight. Knowledge of the angle which this line made with the edge of the film, the magnification factor for the lens, and the linear speed of the film permitted calculation of the rate of progress of the luminosity. A correction was necessary for the deviation of the slit image from perpendicularity to the edge of the film.

The magnification factor, M, was measured by photographing (with the slit removed from the rate camera) a scale consisting of several black tapes on a white background, placed in the same position as that in which the charge was hung. The actual distance between successive tapes was accurately known, and the distance between them on the image was easily measured by projecting an enlarged image on a scale. The ratio image/object was thus determined.

The linear speed of the film, calculated from the diameter of the drum (12.47 inches) and the usual frequency meter reading of 58.5 cycles per second, was 233.5 m./sec.

Since the image of the slit was not necessarily perfectly perpendicular to the edge of the film, and since the inclination of the detonation trace to the vertical

obviously depends on the slit angle, a "slit constant" was determined by lowering the slit and exposing a strip of film with the drum at rest. The angle between the slit image and the edge of the film was then determined in the same way as that of a detonation trace described below.

Measurement of angles was made with a Jones and Lamson Comparator, Plate VI, which consists of a large ground glass disc on which was projected a magnified image of the film. The disc face is crossed diametrically by two perpendicular scratches, and could be rotated by a rack and pinion arrangement. A scale on its periphery read directly in minutes of arc. In making a measurement, the film was held between two glass plates in a small vise that rested on the movable table of the instrument. With the cross-lines set at zero, the film was adjusted until its edge was parallel to the horizontal line. The disc was then rotated until the vertical line on it coincided with the edge of the trace on the film. The velocity of the luminosity was then given by

$$V = \frac{d}{M(\tan\theta - \tan A)}$$

where $\underline{V}$ = the velocity of the luminosity in m./sec.,

$\underline{d}$ = the drum velocity in m./sec.,

$\underline{M}$ = the magnification factor for the drum camera

$= \frac{\text{image}}{\text{object}}$,

PLATE VI

The Jones and Lamson

Comparator

$\underline{\theta}$ = the angle which the straight line detonation trace makes with the vertical,

$\underline{A}$ = the angle which the slit image makes with the vertical.

In practice, six independent readings of the angle (three each by two different observers) were taken, on the principle that the average was likely to be closer to the true value than any individual reading.

For charges before No. 152, which were fired 8 feet from the camera, the magnification factor, $\underline{M}$, was 0.1031, while for all later charges, fired 14 feet away, its value was 0.05345.

The value of the "slit constant" was 48 minutes of arc for shots below No. 152, between 152 and 167 it was -27 minutes, while for all later shots, its value was 7 minutes.

Significance of the Photographs

The appearance of the photographic record obtained on the rapidly moving film of the drum camera depends in part on the orientation of the charge and on the type of initiation. Thus central initiation would obviously give a symmetrical photograph, while the nature of the picture obtained with a

cylindrical charge depends on whether the charge is hanging vertically or horizontally. The appearance of the drum photographs, obtained by initiating charges of different shapes in different places, and by orienting them differently, may be predicted on the assumption of a spherical propagation of the detonation wave from the detonator considered as a point source (14). The luminosity from a disc of explosive initiated at its centre, should reach all of the periphery at the same time, so that if the edge of the charge were facing the camera, a line perpendicular to the edge of the film should represent the simultaneous arrival of the detonation wave at all points on the edge of the disc, while if a diameter of the disc faced the camera, with the same type of initiation, the photograph should be symmetrical about the centre and might be used to calculate the rate of detonation. It is clear, then, that the type of picture obtained from such charges can readily be predicted, and a study of them may lead to information useful in the interpretation of other photographs, particularly in forming a unified and coherent idea of the significance of the rate and still photographs and the correlation between them.

With this end in view, experiments were made with cast NENO charges of various shapes fired in different positions relative to the slit. Square slabs and discs of NENO

were prepared by pouring the molten NENO into heavy paper molds of the desired shape, and after crystallizing at 40°C, the paper covering was removed. A disc, hanging vertically, was fired with the thin edge facing the drum, and initiated at the end of the horizontal diameter furthest removed from the camera, while a square slab in which one corner faced the camera, was initiated at the diagonally opposite corner. The photographs obtained, shown in Plates VII and VIII, although blurred, are exactly what might be expected on the basis of a spherical propagation. The direction of motion of the film in these, as in all the rate pictures, is from left to right, so that the earliest regions of luminosity appear farthest to the right in the photographs. Thus, in both the square slab and disc, the luminosity reached the top and bottom edges of the charge before the region directly opposite the detonator. Since the charges were in line with the drum camera, they were slightly inclined to the still camera so that one of their broad faces was visible, and the still photographs (taken at f-40, and developed in Eastman D-11, which was used for all of them), shown to the right in the Plates, indicated an opaque region a short distance beyond the charges, which may be due to the shock wave.

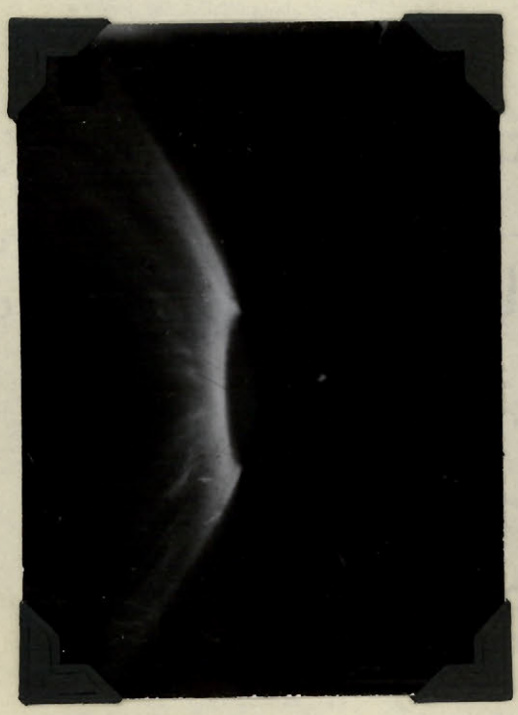

(a) Rate Picture

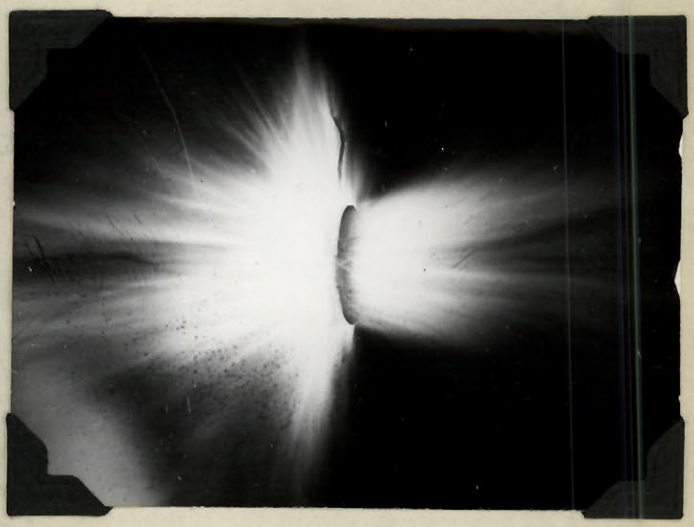

(b) Still Picture

PLATE VII

Detonation of Cast NENO Disc.

(a) Rate Picture

(b) Still Picture

PLATE VIII

Detonation of Square Slab of Cast NENO.

Modification of Procedure

Since the present investigation was concerned primarily with determining the effects of cavitation of a cylindrical charge on detonation velocity, it was essential that small changes of detonation velocity be readily detectable. In the early rate experiments, made with the drum camera lens fully open at f-3.5 and the charge 8 feet away, the 35 mm. Super XX Panchromatic film used was developed in Eastman D-11, and the typical blurred photograph, shown in Plate IX, indicates that the drum film was badly overexposed. Velocity measurements on the fuzzy image were difficult to make, and hence inaccurate. To improve the definition of the image by decreasing the exposure, the lens was diaphragmed to f-16, and to increase the contrast and density of the negative, the film was developed for three minutes in a highly alkaline developer, Eastman D-8 diluted with one part water for two parts developer. In this way a much sharper image of the detonation was obtained, and the angle could be measured more accurately.

With the charge fired only 8 feet from the drum camera, the detonation trace, inclined to the vertical by about 17°, corresponds to a detonation velocity of about 7800 m./sec. Since the calculation of detonation velocity from the photographic record involved the tangent of this

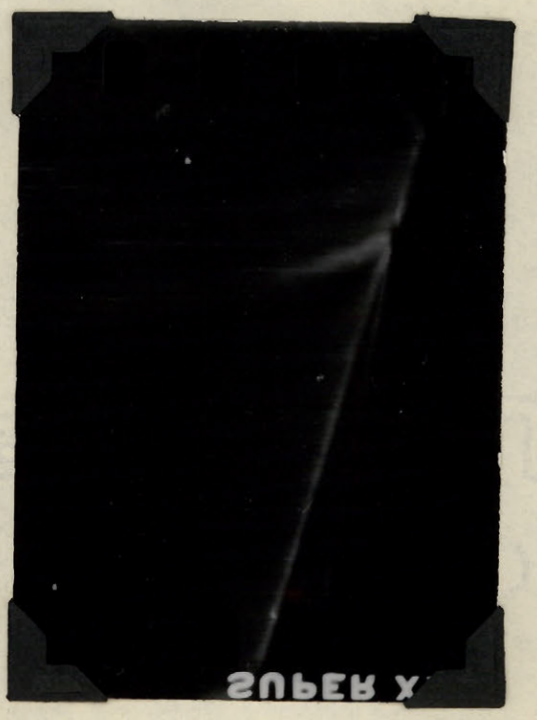

PLATE IX

Early Drum Photograph of

Unconfined Cavitated Charge.

angle, and since in this region a small error in the angle results in a relatively large percentage error in the tangent, the angle was increased to about 29° (and the relative error in the tangent thus decreased) by moving the charge back to 14 feet from the camera. All but the fuzziest lines could be read easily within 3 minutes of arc, corresponding to a reading error in the measurements of about 0.2%, which was of the same order of magnitude as the reproducibility.

Preparation of Cavitated Charges

DINA (Bis (β-nitroxyethyl) nitramine) was chosen for the investigation of cavitated charges because it was easily cast free of inner cracks, and its translucence facilitated the examination of the luminous effect in the cavity.

To prepare a cavitated charge, the crystalline DINA was melted in a steam-bath and allowed to cool to 70°C before casting. The mold consisted simply of a 10" long glass tube of appropriate diameter in which fitted a smaller tube held in a concentric position at both ends with two carefully bored stoppers. With one of the stoppers removed, the annular space between the two glass tubes was almost filled with liquid DINA, and the stopper replaced to ensure that the inner and outer tubes were concentric. The charge was half-

immersed in running water at about 10°C, the other half being cooled in air. The crystallization caused considerable decrease in volume, and when the solidification of the DINA had proceeded far enough to fix the inner tube in position, but before the top of the DINA had crystallized, the tube was refilled with the liquid DINA. This process was continued until the tube was completely filled with explosive, care being taken always to pour the DINA before the melt had crystallized completely. In this way irregularities within the charge were minimized.

When the entire charge had crystallized, it was clamped vertically, and hot water (at ca. 60°C) was run down the inner tube to melt a thin film of the DINA (m.p. 52°C) so that the inner tube could be removed (steam was used to remove the inner tube when its diameter was 3.2 mm.). A bare charge was prepared from a charge confined in glass as above by rotating it under hot running water to loosen the outer glass tube and permit its removal.

It is important that the packing density of the explosive be closely controlled in a detonation velocity study involving the effect of other variables, since theory predicts (18, 19, 21) and experiment indicates (35) that the detonation velocity increases almost proportionally with increasing packing density. The density of all the DINA

charges used in the present investigation, determined simply by measuring the volume of water displaced by the charge of known weight, was found to be constant at 1.60 gm./cc. Moreover, since the detonation velocities of the full charges were reproducible within 0.2%, which was of the same order of magnitude as the error in reading the angle of the detonation trace, the packing density was apparently sufficiently constant not to effect the detonation velocity.

In preparing a water-filled charge, one end of the cavity was plugged with DINA, a long fine jet was inserted to the bottom of the cavity, and water poured through it into the hole until several drops of water overflowed at the top of the charge to eliminate all air bubbles. Charges filled with solid rods were prepared by casting the explosive around the rod in the usual way.

All the charges were boosted with plastic explosive and a 10 gm. or 25 gm. tetryl pellet. A thin layer of PE was placed between the DINA and the tetryl pellet to improve the contact between them and the No. 8 electric blasting cap fitted into a hole in another wad of PE placed above the tetryl, the whole booster being attached to the charge with cellulose tape.

RESULTS

Effect of Polymorphism on Detonation Velocity

One apparent disadvantage to the use of DINA in a study of detonation velocity is its polymorphism (36). Immediately after casting, the charges were distinctly yellow in colour, but after standing at room temperature for several days, they changed to almost pure white. The method of casting was such as to favour the initial formation of the β-polymorph, and the solid-solid transformation to the room temperature stable α-form was then characteristically slow. Since the γ-form is extremely labile, and the δ- and ϵ-polymorphs crystallize only in a region of high pressure, none of these forms of DINA can be present in the charges fired. A series of experiments indicated that the detonation velocity was the same for both of the DINA polymorphs likely to crystallize under the casting conditions, the results being given in Table XIII.

TABLE XIII

Effect of Polymorphism on Detonation Velocity

22 mm. diameter bare cast DINA

Charge No.	Crystal Form	Angle θ	Detonation Velocity m./sec.
206	α-	$29^{\circ}26'$	7770
207	Mixture α- and β-	$29^{\circ}22'$	7790
208	β-	$29^{\circ}24'$	7779
209	β-	$29^{\circ}32'$	7738

Since the density of the charges was constant, and the polymorphism apparently did not complicate the characteristic detonation velocity of DINA, no special precautions were necessary in the preparation of charges for the investigation of the effect of cavitation on the rate of detonation.

Confined Cavitated Charges.

Experiments with cylindrical charges of cast DINA, with axial cavities of various diameters, confined in glass tubes of two different diameters indicate the variation of detonation velocity with cavity size. The results are given in Table XIV for charges of 16 mm. outside diameter and in Table XV for 22 mm. The photographs of the 16 mm. charges are typical, the corresponding rotating drum pictures being given in Plates X and XI and the still pictures in Plates XII and XIII. The data show clearly the poor reproducibility of the detonation velocity of those charges with the smallest cavity compared with that when solid charges were used, but the increase in the rate of detonation with decreasing hole diameter is of a considerably larger magnitude than the variability of the results for a given hole size. A similar increase in detonation velocity with decreasing cavity diameter has been found with cast TNT and with pressed tetryl (29, 30). It is to be noted, further, that the detonation velocity is

TABLE XIV

Cavitated DINA Confined in Glass

Charge Diameter = 16 mm.

Diameter of Cavity (mms.)	Charge No.	Angle θ	Detonation Velocity (m./sec.)	Mean Detonation Velocity (m./sec.)	Average Deviation (m./sec.)
0	210 211 212 213	29°22' 29°23' 29°22' 29°15'	7790 7785 7790 7827	7798	14
3.2	252 253 293	28°32' 28°33' 28°29'	8061 8056 8078	8065	9
4.2	223 254 255	28°41' 28°43' 28°35'	8010 8001 8047	8019	18
7.5	224 248 249 251	29°34' 29°58' 29°50' 29°30'	7724 7657[1] 7701 7746	7707	28
9.9	225 256 257	29°25' 29°31' 29°46'	7774 7740 7658	7724	44

[1] Frequency meter read 59.0 instead of the usual 58.5

TABLE XV

Cavitated DINA Confined in Glass

Charge Diameter = 22 mm.

Diameter of Cavity (mms.)	Charge No.	Angle θ	Detonation Velocity (m./sec.)	Mean Detonation Velocity (m./sec.)	Average Deviation (m./sec.)
0	130 148 226 308 332	$16^{\circ}53'$ $16^{\circ}53'$ $29^{\circ}11'$ $29^{\circ}13'$ $29^{\circ}10'$	7840[1] 7840[1] 7850 7837 7855	7844	6
3.2	309 314 323	$27^{\circ}34'$ $27^{\circ}37'$ $28^{\circ}\ 3'$	8400 8380 8230	8337	71
7.5	230 310 315	$28^{\circ}23'$ $28^{\circ}30'$ $28^{\circ}26'$	8113 8073 8093	8093	13
12.6	311 316 328	$28^{\circ}58'$ $28^{\circ}43'$ $28^{\circ}44'$	7920 8001 7994	7972	33
15.2	312 317	$29^{\circ}24'$ $29^{\circ}10'$	7782 7855	7818	37

[1] Charges fired 8 feet from camera, $\underline{M}$ = 0.1031

(a) Full Charge

(b) Cavity Diameter: 3.2 mm.

(c) Cavity Diameter: 4.2 mm.

PLATE X

Rate Photographs of Confined 16 mm. Diameter Charges with Axial Cavities of Various Diameters.

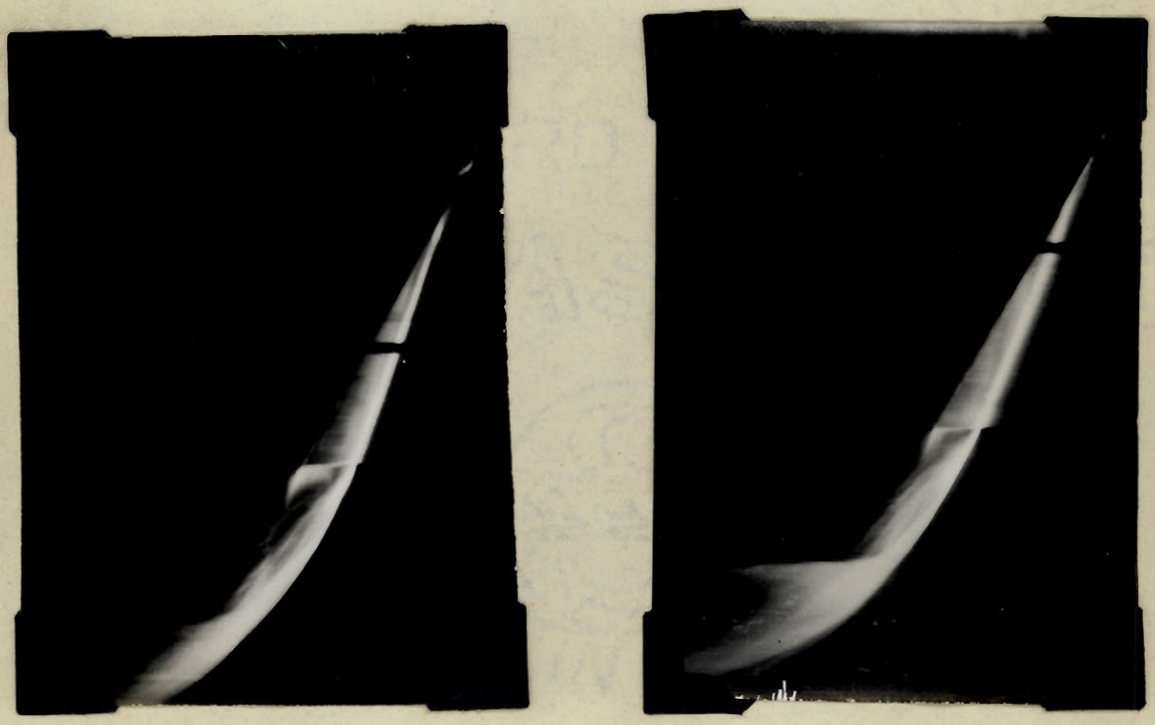

(a) Cavity Diameter: 7.5 mm. (b) Cavity Diameter: 9.9 mm.

PLATE XI

Rate Photographs of Confined 16 mm. Diameter Charges with Axial Cavities of Various Diameters.

(a) Full Charge

(b) Cavity Diameter: 3.2 mm.

(c) Cavity Diameter: 4.2 mm.

PLATE XII

Still Photographs of Confined 16 mm. Diameter Charges with Axial Cavities of Various Diameters.

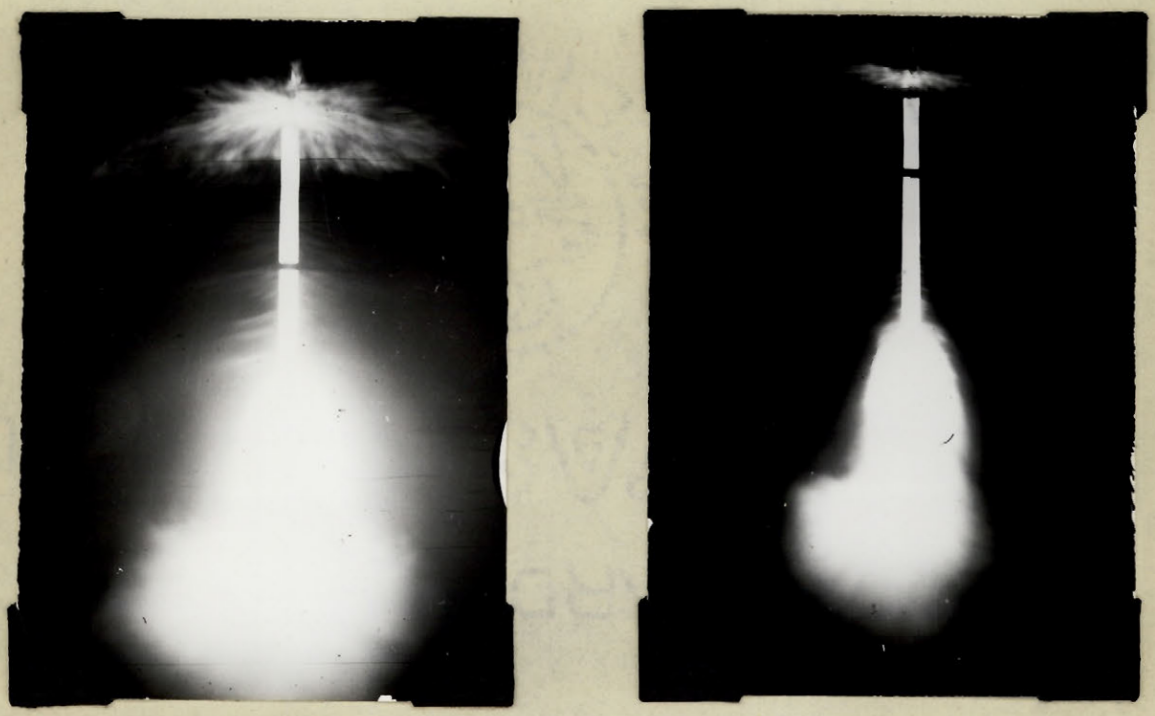

(a) Cavity Diameter: 7.5 mm. (b) Cavity Diameter: 9.9 mm.

PLATE XIII

Still Photographs of Confined 16 mm. Diameter Charges with Axial Cavities of Various Diameters.

greater with the larger outside diameter charges for all the cavity sizes investigated.

The most noticeable feature of the still pictures is the sharp side boundaries to the luminosity, which correspond to the outside wall of the confining glass tube. The large, broad, diffuse region at the top of the column of the explosive is due to the detonator and tetryl pellet booster. The distinct breaks, which occur in some of the photographs, are caused by strips of friction tape that are wrapped around the charges to distinguish different shots on the rate camera film. The luminosity from the end of the charges extends for a greater distance the larger the diameter of the cavity. A rate camera picture of a detonating solid column of explosive is simply a sharp, bright straight line slanted across the film (Plate X(a)). The rate pictures of cavitated charges are qualitatively different from those of the solid charges with the appearance in the former of a luminous effect which is much faster than the detonation velocity, and is apparently caused by the presence in the charge of the axial cavity. It is this luminosity, observable in cast TNT as well as DINA, which has been ascribed to a Munroe effect within the cavity (29), visible because of the translucence of the explosive. Beyond the end of the charge, the luminous effect from the cavity is retarded more rapidly the smaller the cavity, in accord with the effect found by Cybulski and Woodhead (29).

Unconfined Cavitated Charges

The measured detonation velocities of unconfined charges are given in Tables XVI and XVII, and the corresponding photographs in Plates XIV - XVII. The same qualitative variation in the rate of detonation is observed in the bare as in the confined charges, but the appearance of the photographs is considerably different. The luminosity is no longer confined to the region of the charge itself, but tapers off gradually at the sides in feathery streaks of light as shown in both the still and rate pictures. The cavitated charges give a much sharper outline of the explosive column than the full charge because the luminous effect within the cavity is confined by the annular ring of explosive, and as the thickness of the wall of explosive decreases (i.e., with increasing diameter of the cavity), the intensity of the luminosity from the cavity transmitted is increased. Hence, the outline of the charge is brightest with the largest hole size. The speed characteristics of the luminous effect from the cavity and of the blast from the end of the charge vary in the same way with bare as with confined charges. The detonation trace in bare charges does not appear as a sharp bright line, but rather as the limit of the blast from the sides of the explosive column. At the points where the distinguishing tapes are placed on the charge, there appear enhanced blasts in both the still and rate pictures.

TABLE XVI

Unconfined Cavitated DINA

Charge Diameter = 16 mm.

Diameter of Cavity (mms.)	Charge No.	Angle θ	Detonation Velocity (m./sec.)	Mean Detonation Velocity (m./sec.)	Average Deviation (m./sec.)
0	118	17° 1'	7768[1]	7753	15
	258	29°33'	7732		
	259	29°28'	7760		
3.2	260	29° 1'	7908	8021	82
	261	28°35'	8057		
	274	28°16'	8149		
	275	28°50'	7970		
4.2	143	16°38'	7954[1]	7993	47
	162	28° 9'	8045[2]		
	279	28°56'	7937		
	280	28°39'	8035		
7.5	163	28°50'	7823[2]	7886	32
	177	28°55'	7936		
	265	29° 5'	7887		
	277	29° 3'	7898		
9.9	282	29°25'	7776	7757	19
	283	29°32'	7738		

[1] Charges fired 8 feet from camera

[2] "Slit constant" = -27 minutes of arc

TABLE XVII

Unconfined Cavitated DINA

Charge Diameter = 22 mm.

Diameter of Cavity (mms.)	Charge No.	Angle θ	Detonation Velocity (m./sec.)	Mean Detonation Velocity (m./sec.)	Average Deviation (m./sec.)
0	164	29°28'	7801[2]	7776	17
	206	29°26'	7770		
	207	29°22'	7790		
	208	29°24'	7779		
	209	29°32'	7738		
3.2	330	29°43'	8000	8190	190
	332	29°10'	8380		
7.5	167	28°13'	8023[2]	7989	22
	335	28°49'	7967		
	336	28°47'	7978		
12.6	138	16°59'	7782[1]	7797	10
	337	29°21'	7797		
	338	29°18'	7813		
15.2	329	30° 0'	7594	7593	13
	339	30° 4'	7573		
	340	29°56'	7612		

[1] Charge fired 8 feet from camera

[2] "Slit constant" = -27 minutes of arc

(a) Full Charge

(b) Cavity Diameter: 3.2 mm.

(c) Cavity Diameter: 4.2 mm.

PLATE XIV

Rate Photographs of Unconfined 16 mm. Diameter Charges with Axial Cavities of Various Diameters.

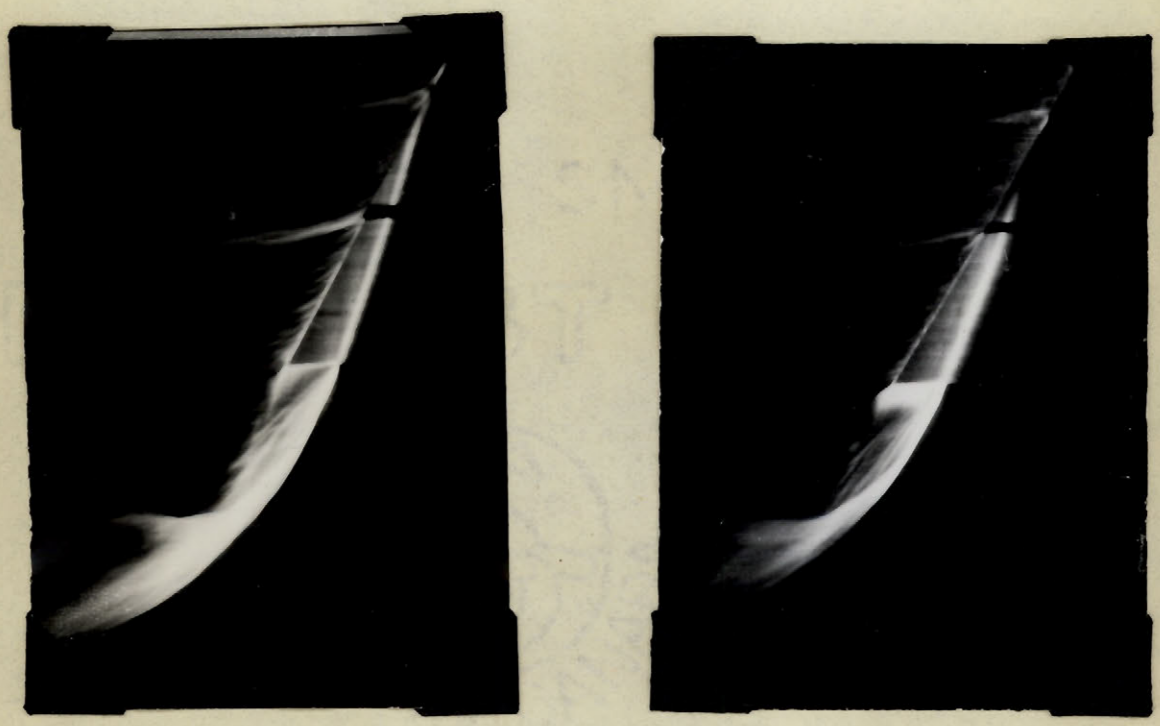

(a) Cavity Diameter: 7.5 mm. (b) Cavity Diameter: 9.9 mm.

PLATE XV

Rate Photographs of Unconfined 16 mm. Diameter Charges with Axial Cavities of Various Diameters.

(a) Full Charge

(b) Cavity Diameter: 3.2 mm.

(c) Cavity Diameter: 4.2 mm.

PLATE XVI

Still Photographs of Unconfined 16 mm. Diameter Charges with Axial Cavities of Various Diameters.

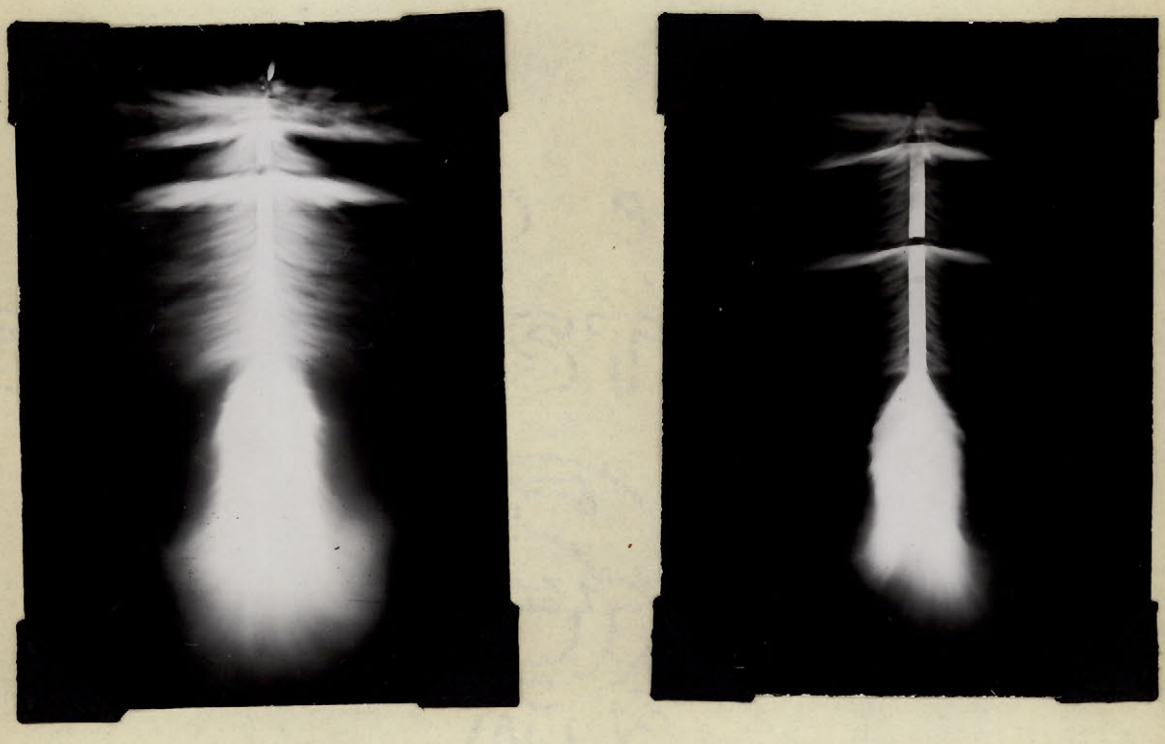

(a) Cavity Diameter: 7.5 mm. (b) Cavity Diameter: 9.9 mm.

PLATE XVII

Still Photographs of Unconfined 16 mm. Diameter Charges with Axial Cavities of Various Diameters.

Water-filled Charges

Charges in which the cavities were filled with water were fired immediately after preparation to minimize the loss of liquid by seepage through the walls of the explosive. The measured detonation velocities are given in Tables XVIII and XIX, and typical photographs are shown in Plates XVIII - XX. The still pictures were taken at f-20 instead of the customary f-40, since the detonations were far less luminous than those obtained from solid or air-filled charges. The results indicate that the water apparently reduces or eliminates entirely the increase in detonation velocity caused by an air-filled cavity, and the photographs show that the luminous effect within the cavity disappears when water is present.

Miscellaneous Shots

To clarify the mechanism of the increase in detonation velocity brought about by a cavity, charges containing various axial fillings were fired. The results with glass rods 10.2 mm. in diameter fitting loosely into the cavities in confined 22 mm. charges are given in Table XX.

TABLE XVIII

Water-Filled Cavitated DINA confined in Glass

Charge Diameter = 16 mm.

Diameter of Cavity (mms.)	Charge No.	Angle θ	Detonation Velocity (m./sec.)	Mean Detonation Velocity (m./sec.)	Average Deviation (m./sec.)
3.2	266 313 318	29° 5' 29°14' 29° 6'	7887 7832 7876	7865	22
4.2	268 269 302	29°21' 29°20' 29°26'	7798 7804 7773	7792	12
7.5	270 303 304	29°24' 29°16' 29°15'	7782 7823 7830	7812	20
9.9	305 306	29°22' 29°30'	7795 7749	7772	23

TABLE XIX

Water-Filled Cavitated DINA Confined in Glass

Charge Diameter = 22 mm.

Diameter of Cavity (mms.)	Charge No.	Angle θ	Detonation Velocity (m./sec.)	Mean Detonation Velocity (m./sec.)	Average Deviation (m./sec.)
3.2	341 342	$28^{\circ}55'$ $29^{\circ}\ 4'$	7935 7887	7911	24
7.5	343 344	$29^{\circ}15'$ $29^{\circ}15'$	7828 7828	7828	0
12.6	345 346	$29^{\circ}10'$ $29^{\circ}\ 4'$	7855 7887	7871	16
15.2	347 348	$29^{\circ}36'$ $29^{\circ}11'$	7716 7818	7767	51

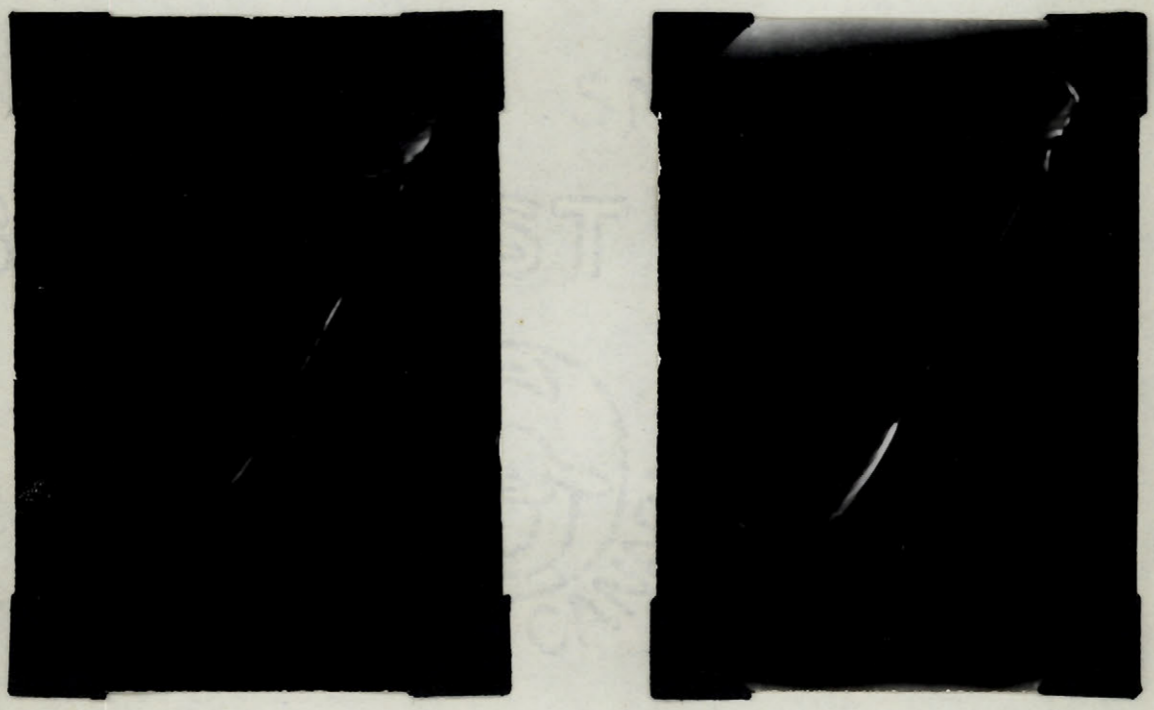

(a) Cavity Diameter: 3.2 mm. (b) Cavity Diameter: 4.2 mm.

PLATE XVIII

Rate Photographs of Confined 16 mm. Diameter Charges

with Water-Filled Cavities of Various Diameters.

(a) Cavity Diameter: 7.5 mm. (b) Cavity Diameter: 9.9 mm.

PLATE XIX

Rate Photographs of Confined 16 mm. Diameter Charges with Water-Filled Cavities of Various Diameters.

(a) Cavity Diameter: 3.2 mm.

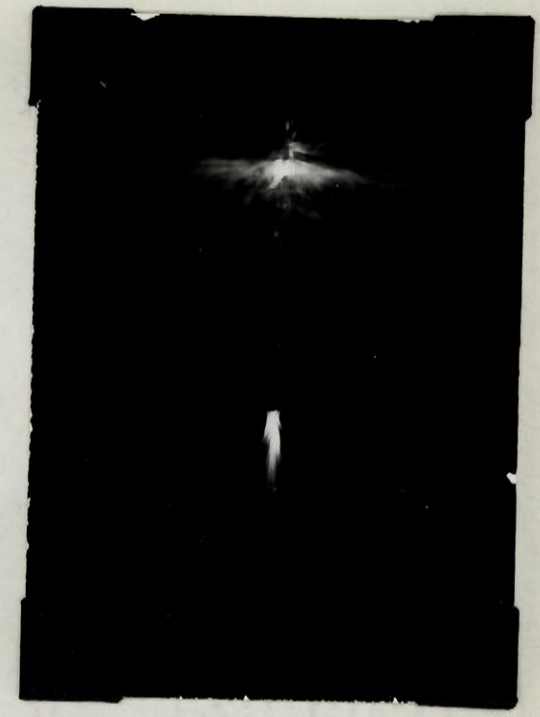

(b) Cavity Diameter: 7.5 mm.

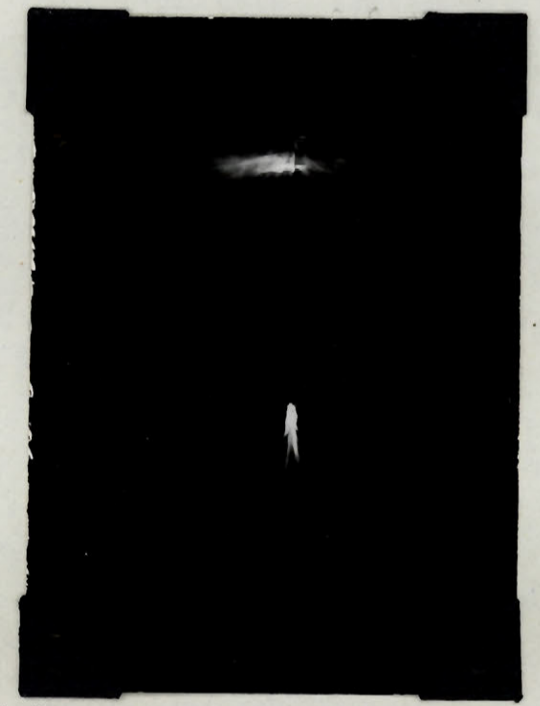

(c) Cavity Diameter: 9.9 mm.

PLATE XX

Still Photographs of Confined 16 mm. Diameter Charges with Water-Filled Cavities of Various Diameters.

TABLE XX

Detonation Velocity of Cavitated Confined Charges with Loosely Fitting Glass Rods

Diameter of Charge = 22 mm.
Diameter of Glass Rod = 10.2 mm.

Diameter of Cavity (mms.)	Charge No.	Angle θ	Detonation Velocity (m./sec.)	Mean Detonation Velocity (m./sec.)	Average Deviation (m./sec.)
15.2	349 350	$29^{\circ}31'$ $29^{\circ}28'$	7744 7760	7752	8
12.6	351 352	$28^{\circ}57'$ $29^{\circ}\ 3'$	7923 7892	7907	16

These velocities are approximately 70 m./sec. less than those obtained by omitting the inner glass tube.

More interesting still are the results obtained with 12.8 mm. diameter copper rods fitting both loosely and snugly in confined cavitated 22 mm. charges, the numerical results being given in Table XXI, and the corresponding rate photographs in Plate XXI.

TABLE XXI

Effect of Copper Rod on Detonation Velocity

Charge Diameter = 22 mm.
Diameter of Copper Rod = 12.8 mm.

Diameter of Cavity (mms.)	Charge No.	Angle θ	Detonation Velocity (m./sec.)	Mean Detonation Velocity (m./sec.)	Average Deviation (m./sec.)
15.2	358 359	29°22' 29°29'	7792 7765	7779	14
12.8	367 371 372	29°33' 29°29' 29°27'	7733 7765 7754	7751	11

The first set of figures corresponds to loosely fitting rods, while the second represents charges in which the DINA was cast around the copper rod. The detonation velocities are considerably below those characteristic of air cavities of the same

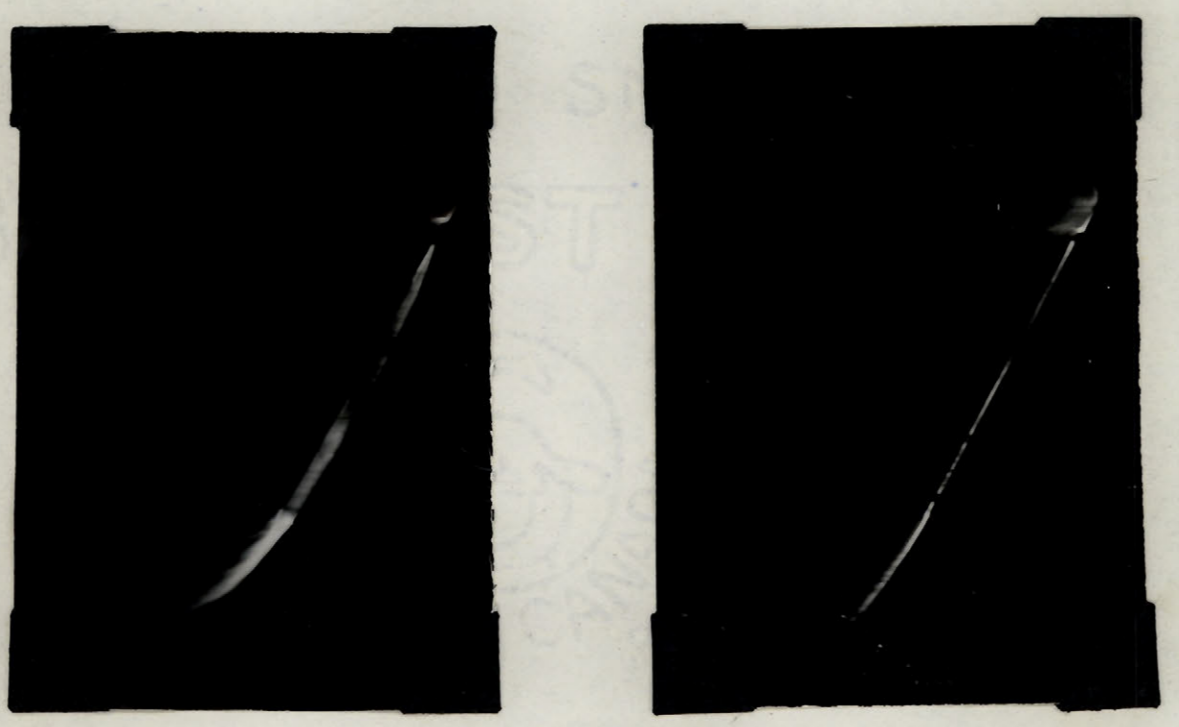

(a) Loosely Fitting Copper Rod (b) Tightly Fitting Copper Rod

PLATE XXI

Rate Photographs of 22 mm. Diameter Charges with Copper Rods in the Axial Cavities.

dimensions given in Table XV. The effect of the detonation on the metal rod depended on whether it fitted tightly or loosely into the cavity. In the latter case, the metal surface was badly gouged and the rod diameter increased by about a millimeter, but the rod was not shattered, while the tightly fitting rod was completely fragmented longitudinally, the greatest damage being done along its axis, not to the surface of the metal.

Photographs of profile and end-on shots, of confined and bare charges (Plates XXII and XXIII) show exactly what might be expected from a careful examination of the rate pictures. The confined profile shows a luminous effect preceding the detonation, with no luminosity outside the narrow boundaries of the charge. The original negative indicated a very faint luminosity occurring much later than the detonation wave with a time-lag of about twenty microseconds, presumably the time required to break the confining glass tube. The bare profile shows the progress of the faint, feathery blast from the sides of the charge, with the luminosity in the cavity again ahead of the detonation wave. The end-on shots, initiated at the end removed from the camera, are the only ones in which the photographs record the luminous effect within the cavity directly, not through the translucent DINA.

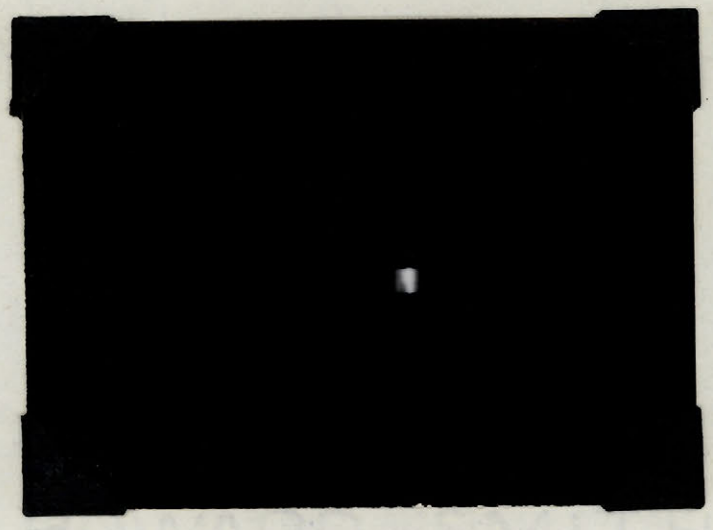

(a) Confined

(b) Unconfined

PLATE XXII

Profile Drum Photographs of 22 mm. Diameter Charges with 12.6 mm. Diameter Cavities.

(a) Confined

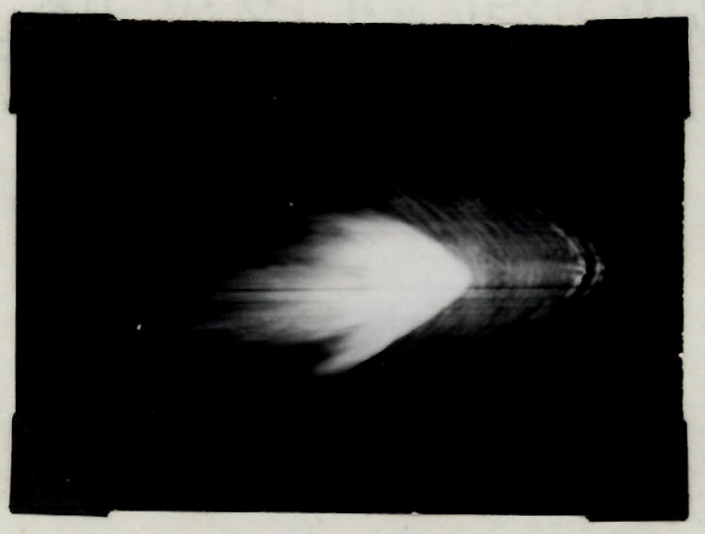

(b) Unconfined

PLATE XXIII

End-On Drum Photographs of 22 mm. Diameter Charges with 12.6 mm. Diameter Cavities.

DISCUSSION

The difference in appearance in the photographs obtained with confined and unconfined charges is essentially the same whether the charge be solid or cavitated. In a detonating unconfined charge the luminous product gases are free to expand to the sides of the column of explosive, as shown in the still pictures (Plates XVI and XVII), while the glass tube of a cased charge confines the gases, so that the luminosity is concentrated over a smaller region (Plates XII and XIII). In particular, the product gases of a detonating bare charge move continuously towards the rate camera as the detonation wave proceeds down the explosive stick. Hence, the luminosity of the gases is recorded over a wide region of the moving film, bounded on one side by the trace of the detonation wave (Plate XIVa). If the charge is confined, however, the product gases do not expand beyond the confining tube before they are cooled too much to be luminous, as shown in the profile photograph (Plate XXIIa). The rate picture of a detonating confined solid charge is, therefore, an integration over a relatively narrow region of all the luminous effects recorded for the bare explosive, and appears as a very sharp, bright line (Plate Xa).

Rate photographs of detonating cavitated air-filled

charges differ from those of solid charges in the appearance in the former of a diffuse, intense luminosity which is very much faster than that due to the detonation wave itself, and is apparently caused by some disturbance within the cavity. Photographs of detonating cavitated charges in which one end was directed towards the drum camera (Plate XXIII) show an intense luminosity bounded on both sides by the walls of explosive and preceding the expanding luminous front which appears at the end of the explosive column. In the rate photographs, the trace of the cavity luminosity is blurred (Plates X, XI, XIV, XV) because, although the luminous front may be narrow, its intensity is so great that it is scattered by the annulus of explosive, and a faint light is transmitted by a given horizontal section of the charge both before and after the main luminous front passes it.

The results to be explained may be divided logically into two main groups only indirectly related to each other:

1. The appearance of the photographs obtained with cavitated charges, and in particular, the source of the extremely rapid cavity luminosity, and
2. The effect of cavitation on the observed detonation velocity.

The possible source of the luminosity in the cavity has already been discussed (32). It has long been known that

the intensity of the shock from the end of an explosive charge is greatly increased by hollowing out the end (37), to produce a Munroe effect. Of this enhanced blast, Marshall wrote (38):

> "In the axis of the hollow of one of the bored-out charges the waves of highly compressed air come together with tremendous violence and necessarily produce a blast in the same direction as the original wave of detonation. This is not only much more intense than the original wave, because it is more concentrated, but it also lasts longer."

The exact nature of the blast is not discussed, but Cybulski and Woodhead (32) attributed the cavity luminosity in pressed CE/TNT to a Munroe effect. Since the detonation of the explosive along the walls of the cavity results in a shock wave front, it is logical to assume that the various shock waves originating from the walls interact in such a way that a resultant intensely luminous front is formed which moves down the cavity at high speed ahead of the detonation wave. Spark photographs indicate (39) that under certain conditions a shock wave may be reflected from an obstacle before it actually impinges upon it, giving rise to a so-called Mach wave, and that when two shock wave fronts intersect no obstacle is required to produce the Mach wave.

It is reasonable, therefore, to postulate the formation of a Mach wave in cavitated charges as resulting from the interaction of shock waves arising from the detonation of diametrically opposite portions of explosive along the walls of the cavity, and the luminous effect within the cavity may be ascribed to this Mach wave.

The shock wave in the cavity (whatever may be its exact nature) is maintained by the continuous production of highly compressed gas resulting from the detonation behind the shock front. Since these gases are at a high temperature, they are probably luminous, and part of the faint light which appears in the rate pictures (Plates X, XI, XIV, XV) following the brilliantly luminous front in the cavity may be attributed to them. The hot luminous product gases, then, follow behind the shock front which is the source of the intense line that appears in the drum photographs of detonating air-filled cavitated charges.

Although accurate measurement of the speed of the cavity luminosity was not possible, it was estimated as about 1.65 times the detonation velocity. This value agrees fairly well with that found (28) for the speed of the product gases in vacuo. Since the shock wave is acoustic in nature, it too might be expected to have a velocity of the order of that

actually found for the cavity luminosity at the high temperatures and pressures existing.

At the end of the charge, the photographs (Plates Xb, Xc, XIa, XIb, XIVb, XIVc, XVa, XVb) show that the luminosity from the cavity is retarded more rapidly the smaller the diameter of the cavity. With the smallest cavity it might be expected that the pressure maintaining the shock front would be greatest, although the absolute volume of gas causing the pressure is least. As soon as the gases are free to expand, the pressure behind the shock front is no longer maintained, and the speed of the shock wave falls sharply. However, the shock front projected from the cavity eventually intersects that from the annular ring of explosive, which travels at a higher velocity, and after meeting, the two waves continue with increased velocity.

The hypothesis that the cavity luminosity is caused mainly by a shock front which is followed by hot gases may explain satisfactorily the quantitative results previously described.

The detonation velocities of the axially cavitated charges investigated are greater (except for the largest cavity diameters) than those of similar full charges, and since the increase disappears when the luminosity is eliminated by filling

the charges (Tables XVIII - XXI and Plates XVIII, XIX, XXIb) it appears that the increase in detonation velocity is attributable to the same source as cavity luminosity. It may therefore be assumed that the increase in detonation velocity is associated with the presence of the shock wave in the cavity which may sensitize the explosive by impinging upon it and raising its temperature ahead of the detonation wave.

It is well known that explosives may be sensitized by heating, and lead azide has been sensitized (40) by heating it for a shorter time than that required to detonate it at a given temperature. Furthermore, sudden shock may produce detonation of an explosive, and it has been postulated (41) from impact sensitivity measurements that shock energy is more effective than heat energy in producing detonation, since it was found that the minimum height from which a weight falling on a sample of explosive produced a detonation was always less than that calculated from the specific heat and ignition temperature of the explosive. However, Eyring's hot-spot hypothesis (19) attributes the apparent efficiency of shock energy to its non-uniform dissipation to heat upon the surface of the solid explosive. Thus, the shock waves from diametrically opposite portions of the explosive on the walls of the cavity are reflected when they meet (39), and the front of the reflected wave, striking the walls of the explosive

ahead of the detonation front, may therefore heat the explosive and so sensitize it. The objection (32) that there is insufficient time for a temperature sensitization of the explosive seems to be invalidated since it has been found (33) that the disturbance in the cavity may cause an instantaneous initiation when it reaches a solid portion of the explosive column in a tetryl charge. Since with tetryl there is no detectable time lag between the arrival of the disturbance at the solid portion of the charge and the initiation there of detonation, it is conceivable that with a less sensitive explosive, such as DINA, the shock wave may sensitize the explosive along the walls of the cavity. When the detonation front reaches this sensitized region, it need not raise its temperature to such a great extent as would normally be the case, and the reaction time may therefore be decreased and the detonation velocity increased.

Sensitization by the hot product gases is equally possible, since they are in contact with the walls of the cavity, and may easily be the cause of the same type of temperature sensitization as has been postulated for the reflected shock front. The fact that either or both the shock wave and hot gases do not bring about continuous initiation along the cavity walls may possibly be due to the very short time available for their attack of the explosive, since the

detonation was never more than twenty microseconds behind the cavity luminosity.

Whatever the actual cause of the sensitization, it can occur only on the walls of the cavity in the short time available, and therefore the detonation wave would presumably tend to move through the explosive along the walls of the cavity at a greater rate than it does on the outside of the annulus. Hence, the detonation wave in the explosive is probably conical, similar to that found (31) in composite charges in which the inner core of explosive had a much higher detonation velocity than that in the annular cylinder.

The observed constancy of the detonation velocity in cavitated charges indicates that a steady state is set up, although both the shock front and the hot gases in the cavity get further ahead of the detonation wave as it proceeds down the stick of explosive. In the 10-inch long charges used, the luminous effect never passed a given point on the charge more than about twenty microseconds before the detonation wave reached it, and in this short time it is inconceivable that heat conduction would be sufficient to cause any loss of the energy gained by the explosive from the disturbance, before the detonation wave reached the sensitized region. It might, however, be expected that with a sufficiently long column of explosive the luminous effect might get far enough ahead of

the detonation wave so that loss through heat conduction would be appreciable, although the magnitude of this loss would probably be too small to be detected in measurements of detonation velocity using techniques already developed.

The size of the cavity probably affects the increase in detonation velocity simply because of a "volume effect", since the surface/volume ratio decreases with increasing diameter. It might therefore be expected that as the cavity diameter is increased, the shock wave front, being dispersed over a larger cross-sectional area, would not heat the explosive along the walls of the cavity to as great an extent, so that the detonation velocity would fall below the optimum observed with the smallest diameter of cavity.

Similarly if the hot gases are responsible for the sensitization, they have a relatively greater surface of explosive on which to act as the cavity diameter is decreased. Furthermore, since the surface/volume ratio increases with decreasing diameter and the gases in the cavity presumably originate in the surface layer of the explosive, there will be a larger quantity of gas per unit volume the smaller the diameter of the cavity, so that sensitization by hot gases might be expected to be more effective as the size of the cavity is decreased.

Conversely, unless the amplitude of the shock wave were built up to its maximum value instantaneously, it might be expected that with sufficiently small diameter of cavity a point would be reached below which sensitization by the reflected shock wave would not be so efficient as with larger cavities, and the detonation velocity would fall below the maximum. It has indeed been found that with a 0.1 inch cavity in cast TNT the detonation velocity fell below the optimum (32), and this behaviour may be a manifestation of a delay in the attainment by the shock wave of its greatest effect. For a shock wave travelling at 12,000 metres per second, this critical diameter indicates that the shock wave, which travels approximately 1 mm. before being reflected from the opposite wave, is not completely built up in somewhat less than one-tenth of a microsecond, which is not an unreasonable value for the time required for a shock wave to attain its maximum amplitude.

Unless the assumption be made that frictional forces acting on the gases might slow them enough to preclude sensitization of the explosive along the walls of an extremely small cavity, the hypothesis of sensitization by hot gases cannot predict a decrease in detonation velocity with sufficiently small cavities. It appears that the assumption of shock wave sensitization is superior to that of hot gases in meeting this problem rather nicely.

The sensitization should be greatly affected by the physical state of the surface of the walls. A rough surface, exposing a greater area to either the reflected shock front or to the hot gases, should lead to a greater sensitization than a perfectly smooth one, and the effect of surface irregularities of the cavity on detonation velocity might be expected to be greatest when the cavity diameter were least, since it is in this case that the surface/volume ratio is greatest. The relatively poor reproducibility of the results with the smallest cavity (Tables XV, XVI, XVII) may thus be explained since the method of casting never left a perfectly smooth surface.

When the cavity is filled with either liquid or solid the luminous effect disappears and the detonation velocity is that characteristic of a full column of explosive. This behaviour is easily explained on the basis of a sensitization caused by a reflected shock front, since the acoustic wave is now travelling in media in which the velocity of sound is less than the detonation velocity so that there is no possibility of a sensitization occurring.

On the other hand, when the cavity is filled with relatively incompressible liquids or solids there is no possibility for the hot gases to enter the cavity, so that they

too would be unable to sensitize the explosive, and the detonation velocity therefore would revert to that of a full charge.

The effect of a loosely fitting copper rod on both the velocity of detonation and the appearance of the rate photograph is significant. Table XXI indicates that the detonation velocity of a charge containing a loosely fitting copper rod is essentially the same as one in which the rod is in close contact with the explosive along the entire length of the cavity. Plate XXIa shows that with the former arrangement, the luminosity is much slower than in an air-filled cavity (Plate Xb, Xc), while it disappears completely when the rod fits tightly. The absence of sensitization with the loosely fitting rod may be explained (not very satisfactorily) on the basis of the hot gases by assuming that they might heat the rod sufficiently to be cooled below a temperature at which they can sensitize the explosive appreciably. The shock wave, on the other hand, obviously did considerable work on the rod in increasing its radius by about a millimetre, and being thereby dissipated, it could not sensitize the explosive. Furthermore, the residual diameter of the annular air space in the cavity was about 0.1" in which distance it might be impossible for the shock wave to attain the amplitude most effective for sensitizing the explosive.

The radial and longitudinal fragmentation of the tightly fitting rod may obviously be explained only by the action of shock waves meeting on the axis of the rod, since when the rod fits closely the hot gases cannot enter the cavity.

It appears, therefore, that the results may generally be explained by assuming that the luminosity in the cavity of air-filled charges is caused by a shock wave which is followed by the hot luminous products of detonation. The hypotheses that sensitization of the explosive along the walls may be brought about by either the reflected shock wave or by the hot gases lead, with few exceptions, to equally satisfactory explanations of the observed phenomena, and the experimental data cannot as yet decide conclusively in favor of either one or the other.

BIBLIOGRAPHY

1. Davis T.L.; Chemistry of Powder and Explosives, Chap. I, (New York) 1943.
2. Brinkley S.R. Jr. and Wilson E.B. Jr.; O.S.R.D. 905, B-374.
3. Brinkley S.R. Jr. and Wilson E.B. Jr.; O.S.R.D. 1231, 8.1-7.
4. Brinkley S.R. Jr. and Wilson E.B. Jr.; O.S.R.D. 1707, 8.1-27.
5. Berthelot and Vieille; Sur la force des matières explosives, Vol. I, p. 133, Paris, 1883, 3rd edition.
6. Marshall A.; Explosives, Vol. II, p. 477, (London) 1917, 2nd edition.
7. Dautriche M.; Mém. poudres, 14, 216, (1907).
8. Jones E.; Safety in Mines Research Board, Paper No. 22, (1926).
9. Rumpff H.; Z. ges. Schiess.-Sprengstoffw., 24, 55-7, 99-100, (1929).
10. Roth J.F.; ibid, 28, 42-6, (1933).
11. Dixon; Trans. Roy. Soc., 200A, 315, (1903).
12. Bone, Towend and Wheeler; ibid, 228A, 197, (1921).
13. Lafitte P.; Compt. Rend., 178, 1277, 2176, (1924).
14. Jones E.; Proc. Roy. Soc., A120, 603, (1928).
15. Messerly G.H.; A Rotating Drum Camera, O.S.R.D. 682, B-285.

16. Chapman; Phil. Mag., 47, 90, (1898).

17. Jouguet; Mécanique des Explosifs, Paris, 1917.

18. Kistiakowsky and Wilson; Hydrodynamic Thermodynamic Theory of Detonation, NDRC Report, Serial No. B-52.

19. Eyring H.; The Chemical Reaction in the Detonation Wave, O.S.R.D. 3796, 8.1-71.

20. Jones H.; A.C. 4499, Phys/EX. 463.

21. Taylor G.I.; R. C. 193.

22. Jones H.; R. C. 247.

23. Wilkinson J.H.; A. R. D. Theoretical Research Report, No. 30/44.

24. Copp and Ubbelohde; Phys/EX. 570.

25. Eyring H.; NDRC Report, 8-219, DF-13.

26. Eyring H.; NDRC Report, 8-212, DF-12.

27. Messerly and Hall; O.S.R.D. 1413.

28. Jahresber. Chem.-Techn. Reichan., 6 , 97, (1927).

29. Lafitte P. and Patry M.; Compt. Rend., 192, 744, (1931).

30. MacDougall, Messerly and Boggs; NDRC Report, 8-173, DFA-9.

31. Woodhead and Wilson; A.C. 5519, Phys/EX. 507.

32. Cybulski and Woodhead; A.C. 5520, Phys/EX. 508.

33. Cybulski and Woodhead; A.C. 6999, Phys/EX. 589.

34. Payman, Woodhead and Titman; Proc. Roy. Soc.; A148, 604, (1935).

Cairns R.W.; Ind. Eng. Chem., 36, 79, (1944).

35. Messerly et al.; NDRC Report, DFA-4, DFA-6, DFA-7, (1944).

36. Blömquist A.; O.S.R.D. 3014, (1944).

37. Munroe C.E.; Amer. J. Sci., 36, (1888).

38. Marshall A.; Explosives, Vol. III, p. 169, (London) 1932, 2nd edition.

39. Libessart P.; A.C. 6569, Phys/EX. 509.

40. Hawkes A.S.; The Thermal Detonation of Lead Azide, Ph. D. Thesis, McGill University, (1944).

41. Henkel H.; Z. ges. Schiess.-Sprengstoffw., 23, 266, (1928).

SUMMARY AND CONTRIBUTION TO KNOWLEDGE

Kinetic studies of the nitrolysis of hexamine in chloroform and in acetic acid have been made at 1°C and 30°C with various molar ratios of solvent:hexamine and of nitric acid:hexamine. The results indicate that both solvents exert a harmful effect on both the rate of reaction and on the final yield of RDX produced for a given nitric acid:hexamine ratio below a certain optimum value. At the optimum, however, (which is larger with acetic acid than with chloroform) the maximum yield of about 80% is obtained with both solvents at both temperatures.

By assuming that the nitrolysis is second order, calculations from the initial rates in acetic acid indicate that the concentration of the active nitrolyzing agent increases rapidly with increasing nitric acid:hexamine ratio and with increasing nitric acid:acetic acid ratio. The concentration of the active nitrolyzing agent (assumed to be nitracidium ion) appears to be more constant in the various nitrolysis mixtures at the higher temperature.

The results obtained with acetic acid may readily be explained by assuming that acetic and nitric acids form a molecular complex, which is more highly dissociated the higher the temperature.

APPENDIX

A NOTE ON THE TRAUZL BLOCK TEST

APPENDIX

A Note on the Trauzl Block Test

During the supervision of the construction of the equipment necessary for a fundamental study of the luminous effects accompanying the detonation process, the Associate Committee on Explosives requested that investigation be made of the reproducibility of results of the Trauzl block test. This test classically involves the measurement of the expansion in volume caused by the detonation of a 10 gm. sample of explosive placed in a cylindrical well in a lead block 8 inches in diameter and 8 inches high. The sample of explosive is normally weighed into a tin-foil cup, a detonator inserted into the charge which is then placed into a well in the lead block and stemmed with sand. After detonation, the cavity produced is cleaned and its volume measured. The expansion has been considered to be a measure of the power of the explosive. It has long been known that the test is not entirely satisfactory as an indication of the power of an explosive but no mention has apparently been made of the necessity of a firm support for the block, or of controlling the packing density of the explosive to obtain consistent results.

Experiments were made to ascertain the possible

effect of the nature of the support on which the lead block rested during the detonation of the charge. During this investigation, the explosive samples were tamped to a density of 0.92 gm./cc. directly in the well of the block. A 10-gm. charge of NENO caused an expansion of 413 cc. when the block was supported on a 1-inch steel plate, while the same charge gave a 460 cc. expansion when the block rested on a plate that was only one-eighth inch thick. Similar results were obtained with DINA. On the other hand, when the blocks rested on the heavy plate, successive tests with identical 7-gm. samples of DINA gave expansions of 256 cc., 258 cc. and 246 cc., indicating an average deviation from the mean of 2%. By firing on a 6-inch thick concrete slab specially poured for the purpose, consistent results were obtained similar to those on the heavy steel plate.

Another factor which is not universally recognized as of importance in the test is the packing density of the explosive. The expansions obtained with 10.0-gm. samples of picrite of various packing densities, given in Table XXII, indicate that the test is sensitive to the loading density of the explosive.

TABLE XXII

Effect of Loading Density on Expansion

Weight of Picrite = 10.0 gm.

Density (gm./cc.)	Expansion (cc.)
0.24	228
0.32	273
0.55	282
0.67	275
0.86	268

The results in Table XXII are qualitatively typical of the observed variation of expansion with packing density for several different explosives.

The data indicate that to obtain reproducible expansions in the Trauzl test it is essential that successive tests be made at the same loading density of the explosive. Furthermore, to use the Trauzl block expansion to compare the relative powers of different explosives, it appears that the densities at which the various explosives are fired must be standardized.